Spring 1-1-2012

Thermal Performance and Design Guidelines of Thermo-Active Foundations

Byung Chang Kwag
University of Colorado at Boulder, byung-chang.kwag@colorado.edu

THERMAL PERFORMANCE AND DESIGN GUIDELINES OF THERMO-ACTIVE FOUNDATIONS

By

BYUNG CHANG KWAG

B.S. Hanyang University, 2009

Seoul, South Korea

A thesis submitted to the

Faculty of the Graduate School of the

University of Colorado in partial fulfillment

Of the requirement for the degree of

Master of Science

Department of Civil, Environment, and Architectural Engineering

2012

This thesis entitled:

THERMAL PERFORMANCE AND DESIGN GUIDELINES OF THERMO-ACTIVE FOUNDATION SYSTEMS

Written by Byung Chang Kwag

has been approved for the Department of Civil Engineering

by

Moncef Krarti

Michael J. Brandemuehl

John Z. Zhai

Date

The final copy of this thesis has been examined by the signatories, and we find that both the content and the form meet acceptable presentation standards of scholarly work in the above mentioned discipline.

Kwag, Byung Chang (M.S., Civil Engineering)

THERMAL PERFORMANCE AND DESIGN GUIDELINES OF THERMO-ACTIVE FOUNDATION SYSTEMS

Thesis directed by Professor Moncef Krarti

A thermo-active foundation system can be a cost-effective technology to utilize ground thermal energy to heat and cool buildings. Indeed, thermo-active foundations, also known as thermal piles, integrate heat exchangers with the foundation elements and thus eliminate the need of drilling deep boreholes typically required by the conventional ground source heat pumps. In order to properly design thermo-active foundation systems, their thermal performance under various operating and climatic conditions are evaluated as part of this study using detailed modeling and simulation analyses. In particular, a transient three-dimensional finite difference numerical model has been developed and validated to analyze thermal performances of thermo-active foundations. The numerical model is then used to assess the impact of design parameters such as foundation depth, shank space, fluid flow rate, and the number of loops on the effectiveness of thermal piles to exchange heat between the building and the ground. Moreover, thermal response factors have been developed to integrate the performance of thermo-active foundations within detailed whole-building simulation programs. In this study, response factors specific to thermo-active foundations are implemented into EnergyPlus to investigate the impact of various design and operating conditions. The results from the detailed simulation analysis are then used to develop a set of guidelines to properly design thermo-active foundation to meet heating and cooling loads of commercial buildings.

The design guidelines define the required number of thermal piles needed heating and cooling loads for prototypical office buildings in selected US climatic zones. In particular, charts have been developed to help determine the number of thermal piles needed depending on heating and cooling loads, heat pump size, foundation depth, and climate.

TABLE OF CONTENTS

TABLES

FIGURES

CHAPTER 1. INTRODUCTION

1.1. Introduction

The global energy crisis and the increasing interest in environmental impact of greenhouse emissions have led to the need to explore alternatives of low-cost and clean energy sources. While distribution generation technologies such as applications of solar energy, wind power, and biomass have been considered and integrated with the built environment, geothermal energy provides a proven source to heat and cool buildings. In particular, using heat exchangers embedded in boreholes. Ground source heat pump systems (GSHPs) allow heat to be extracted and rejected into the soil medium depending on the building thermal loads without a significant reliance on any external energy source. GSHPs take advantage of the uniform deep ground temperature, which is in most climates higher than outside air temperature during winter and lower than outside air temperature during summer. According to U.S. Department of Energy (DOE, 2011), ground temperatures at 10 ft. or higher depth range between 10 and 16℃ (50 and 60°F) throughout the US climates.

In general, ground acts as a heat source or heat sink for GSHP systems. Heat is extracted from the ground to heat exchanger pipes during the heating season, and ground removes heat from the heat exchanger pipes during the cooling season. GSHPs are categorized by type of heat source and by ground heat exchanger pipe design. Types of ground heat sources are ground, groundwater, and surface water. In terms of the types of ground heat sources, GSHPs are subdivided to ground-coupled heat pumps, groundwater heat pumps, and surface water heat pumps, respectively. In addition, GSHPs are subdivided into horizontal systems and vertical systems in terms of ground heat exchanger pipe design.

Horizontal GSHP systems (Figure 1-1) uses horizontal heat exchanger pipes embedded large ground area at relatively shallow deep, generally 4ft deep. The advantage of this system is less expensive because of the low-installation costs. Disadvantage of this system is obviously that large ground area is required for the horizontal heat exchanger pipes. This may important because it may be hard to obtain 100% thermal performance of the system for commercial buildings and residential buildings where have not large enough space enough to install the horizontal heat exchanger pipes. In addition, since the depth which pipes are buried is also not much deep for the mild ground temperature, so that the ground temperature is easily affected by varying outside air temperature, sunlight, rainfall, snowfall, etc. (ASHRAE, 2007)

Vertical GSHP systems (Figure 1-2) utilize deep boreholes where heat exchanger pipes are placed. The depth of these boreholes ranges from 50 ft. to 600 ft. Compared to horizontal GSHPs, vertical GSHPs do not require an extended area to install pipes. In addition, the deep heat exchanger pipes are contact with the ground medium with mild, steady, and uniform temperatures. However, the vertical GSHPs require high initial costs due to expensive digging costs. (ASHRAE, 2007)

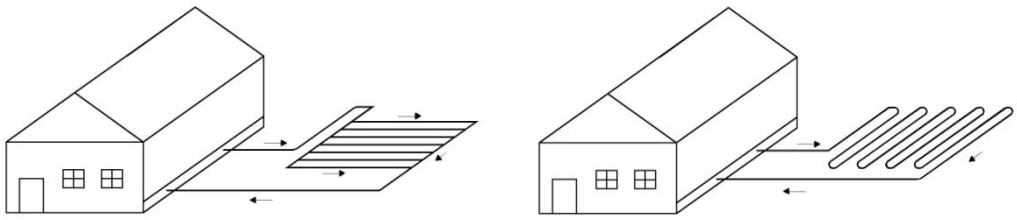

Figure 1-1: Horizontal GSHP systems with parallel pipes (left) and with series pipes (right)

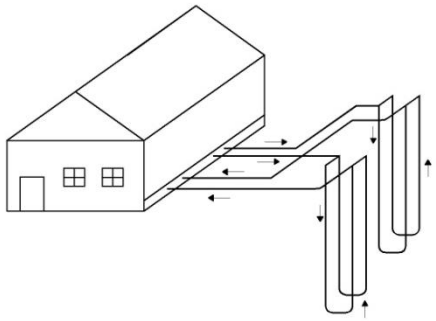

Figure 1-2: Typical configuration for vertical GSHP systems

It is the important to pinpoint that vertical ground source heat pump (GSHP) systems can have high installation costs due to the drilling work needed for the boreholes. Even though GSHP systems can take advantage of the mild ground temperature, the high installation costs would make these system less cost-effective compared to other more conventional systems. In fact, even GSHPs, horizontal systems have been more widely installed more than the vertical systems. Alternative systems or methods are desired to reduce the high installation costs of GSHP vertical systems. Thermo-active foundation (TAF) systems represent a viable solution to reduce the installation costs related drilling work associated with deep boreholes of vertical GSHPs.

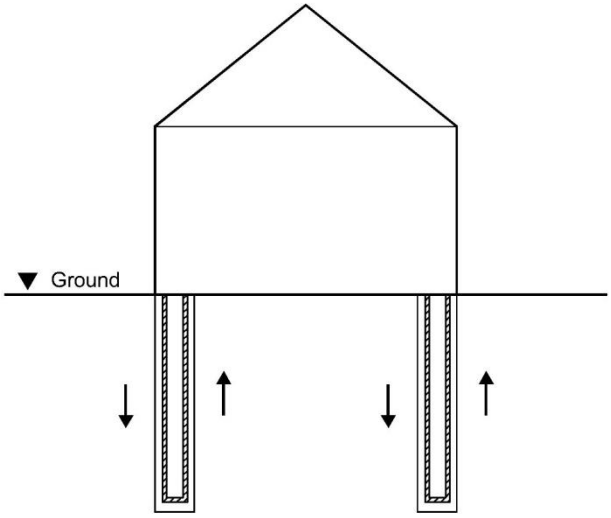

Figure 1-3: Schematic configuration for a TAF system

A thermo-active foundation (TAF) system (Figure 1-3) provides an option to integrate vertical ground heat exchanger pipes into building foundations. Since TAF systems take advantage of the deep building foundations, they eliminate the need for any digging work required for deep boreholes. Therefore, the installation costs associated with TAF systems can be significantly reduced compared to those of vertical GSHPs.

1.2. Definition of the Problem and Objectives

Compared to GCHP systems, only limited analyses and research studies have been reported for TAF systems especially for the US. In addition, these research studies have been mostly focused on the evaluation of the thermal and structural analysis of single thermal pile independently of its impact on building energy use. Indeed, there have been no detailed studies to evaluate TAF systems performance using whole-building building energy simulation programs as well as no design guidelines for TAF systems to ensure their proper sizing and operation. Therefore,

a detailed analysis of the TAF systems integrated with other building components is needed in order to optimize their design and their performance especially in US climates.

There are several types of building foundations including but not limited to spread footing as a shallow foundation which is usually about a meter deep, drilled shafts, caissons, helical piles, and earth stabilized columns as deep foundations. To utilize the constant temperature of the deep ground, pile foundations is the ideal types for TAF systems. Thus, the scope of the study presented in this thesis is to evaluate the thermal performance of TAF systems integrated as part of cast-in-place concrete pile foundations.

- One of the objectives of this research study is to estimate thermal performance of a thermo-active foundation pile as part of a commercial building. For this analysis, a transient three-dimensional numerical model is first developed to analyze heat transfer rate between the ground and the heat exchanger pipes.

- The second objective is to develop set of thermal response factors associated to thermo-active foundations, based on three-dimensional numerical model and the thermal response factor technique for vertical ground heat exchanger systems. Using the thermal response factors, the impact of design and operating parameters on the thermo-active foundations is evaluated.

- The third objective is to integrate thermal models of TAF systems in a detailed building energy simulation program, EnergyPlus, in order to assess their impact on building energy consumption.

- The fourth objective is to investigate the climate impact on the performance and design of thermo-active foundation piles.

- The last objective is to establish general design guidelines to select proper heat pump sizes and proper minimum number of thermo-active foundation piles.

The results from the research study presented in this thesis will be useful for thermo-active foundation designers or installers to ensure optimal design and operation of TAF systems. In addition, the integration of thermal models of TAF systems into EnergyPlus allows designers and modelers to assess the potential energy savings and the cost-effectiveness associated with these novel heating and cooling systems.

CHAPTER 2. BACKGROUND AND LITERATURE REVIEW

2.1. Ground Coupled Heat Exchanger

Ground coupled heat exchanger is the mean to transfer heat between ground and buildings for GSHP systems. During the cooling season, ground absorbs heat from the fluid circulating in the heat exchanger pipes, and during the heating season, the reverse heat flow occurs with heat extracted from the ground. Heat pumps and air conditioners are mechanical devices that facilitate heat transfer from low temperature mediums to high temperature mediums. This heat transfer mechanism which is against the natural flow energy (from hot to cold medium) requires energy (in the form of electrical work) to be used by the heat pump systems and air conditioners. The principles for these two devices are the same, but the purposes are different: an air conditioner is a cooling system, and a heat pump system can provide both heating and cooling. Both air conditioner and heat pump systems have basically four components; condenser, compressor, evaporator, and expansion device. These components are connected within a closed loop (Figure 2-1 (a)). The cycle used by air conditioners and heat pumps is vapor compression cycle. Ideally, it is assumed that there are no heat losses and no heat transfer by pipes between components. The overall process of this system is similar to that of the reverse Carnot cycle, in which the fluid absorbs and releases heat while flowing through the heat exchanger components absorbing heat from surroundings through the evaporator, and releasing heat to surroundings through the condenser. The processes of an ideal vapor compression cycle are summarized below (Cengel, 2005):

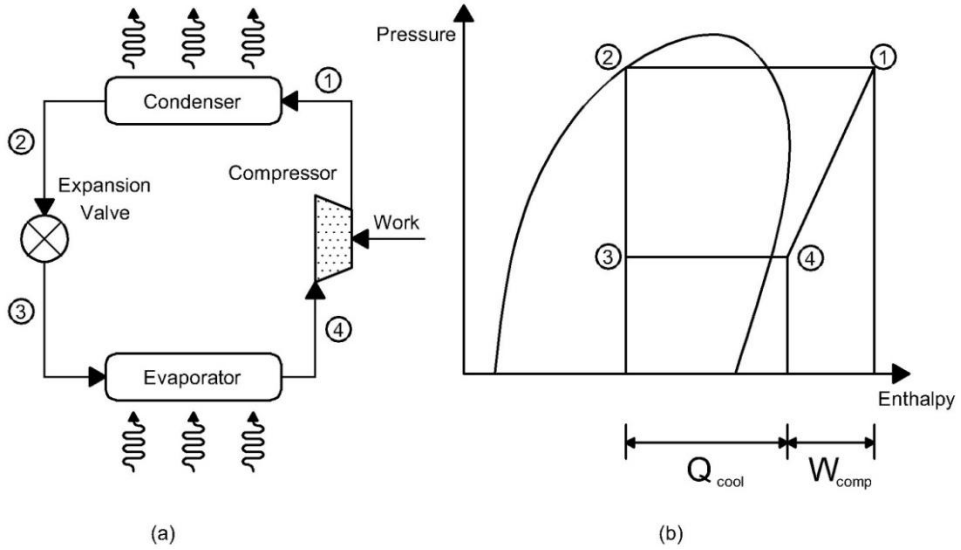

Figure 2-1: Typical vapor compression cycle (a) schematic and (b) P-h diagram (Energy Audit 2nd edition, Krarti)

- Compressor: Isentropic compression
- Condenser: constant pressure heat rejection
- Expansion device: throttling the saturated circular medium
- Evaporator: constant pressure heat absorption

According to basic principles of thermodynamics (Cengel, 2005), the refrigerant fluid at state 4 has low pressure and low temperature with a saturated vapor. This vapor enters the compressor and is compressed to a higher pressure during the compression process (i.e., the process from state 4 to state 1). The fluid becomes superheated vapor with the higher pressure and higher temperature. The temperature of the refrigerant at state 1 is typically higher than the surrounding temperature. The next stage at a condenser is the heat exchange. The superheated vapor of the circular medium rejects heat to the surrounding medium that is lower temperature than the refrigerant. During this stage (state 1 – state 2), the refrigerant becomes saturated liquid.

The saturated liquid (state 2) is still high pressure. However, in order for better phase change and heat transfer at evaporator, the high pressure of the saturated vapor needs to drop its pressure. This is based on the basic principle of phase changes: at lower pressure, liquid can be vaporized at lower temperature (Figure 2-1 (b)). Thus, in the ideal vapor-compression cycle, expansion device expands the refrigerant by throttling, so that the pressure of the circular medium is dropped as well as its temperature is decreased. During this stage (state 2 – state 3), the saturated liquid becomes low-quality saturated mixture. The final step of the cycle is the heat exchange at an evaporator. When the low-quality saturated mixture (state 3) passes through an evaporator, the low pressure, low temperature circular refrigerant absorbs heat from the surrounding medium, and is vaporized (state 3 – state 4). Thus, the circular refrigerant leaves the evaporator as saturated vapor state (state 4). And, then the cycle is repeated.

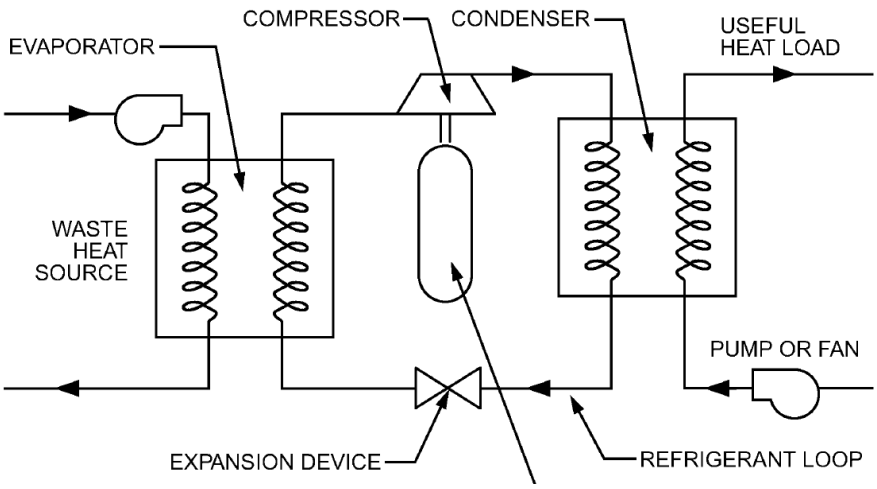

Figure 2-2: Closed Vapor Compression Cycle (ASHRAE Handbook HVAC Systems and Equipment 2008)

According to the ASHRAE Handbook (ASHRAE, 2008), heat pump systems are categorized by the type of heat sources/sinks: air, water, ground, solar energy, and industrial process. The

overall features of heat sources/sinks are summarized in Table 2-1. Air source is widely used for heat pumps, since air is readily available in the ambient environment. However, as the outside air temperature varies with time, the site outdoor air temperature must be considered when designing air-source heat pumps. When air temperature varies, it can result in a substantial decrease of the efficiency and capacity of a heat pump system. Specifically, the efficiency and the capacity of a heat pump decreases with a decreasing ambient air temperature during the heating mode. However, during the cooling mode, the efficiency and capacity of a heat pump can decrease as ambient air temperature increases. In addition, air source heat pump systems must consider the problems associated with frost formation, which affects the efficiency of a heat pump system because frost on an outdoor air coil causes a reduction in heat transfer.

Table 2-1: Common Heat Pump Sources and Sinks (ASHRAE Handbook – HVAC Systems and Equipment 2008)

Medium	Suitability	Availability	Cost		Temperature
			Installed	Operation and Maintenance	
Air	Good	Universal	Low	Moderate	Variable
Groundwater well	Excellent	Varies by depth and location	Varies by depth	Low, periodic maintenance	Generally excellent, varies by location
Surface water	Excellent for large water bodies or high flow rates	limited: depends on proximity	Depends on proximity and water quality	Depends on proximity and water quality	Usually satisfactory
Ground-coupled	Good if ground is moist; otherwise poor	Depends on soil suitability	High to moderate	Low	Usually good
Ground - Direct expansion	Varies with soil conditions	Varies with soil conditions	High	High	Varies by design
Solar Energy	Fair for heat source, poor for heat sink	Universal	Extremely high	Moderate to high	Varies by design

Meanwhile, compared to air source, water source provides an alternative to take advantage of an almost year-round constant temperature of groundwater (ASHRAE, 2007). However, when using water source, some additional considerations are required including testing of water quality and local soil and groundwater conditions. Indeed, groundwater and surface water temperature and depth depend on the site for each building. In order to use groundwater for GSHPs, accurate estimation of its depth is important not only for thermal performance, but also for determining the installation costs.

A ground source heat pump (GSHP) system uses ground as heat source or heat sink (Figure 2-3). Below a certain depth, the ground temperature is generally mild and remains constant throughout the year. However, in order to design ground-coupled heat pump system and analyze its performance, knowledge of soil composition and its thermal properties is critical (ASHRAE, 2007). Particularly, thermal conductivity is an important factor for estimating heat transfer rates. Moreover, moisture content affects thermal properties of soil (ASHRAE, 2008). In addition, the installation cost due to drilling work for boreholes depend on the soil type and is a significant factor to determine the cost-effectiveness of ground source heat pump systems, especially vertical loop systems.

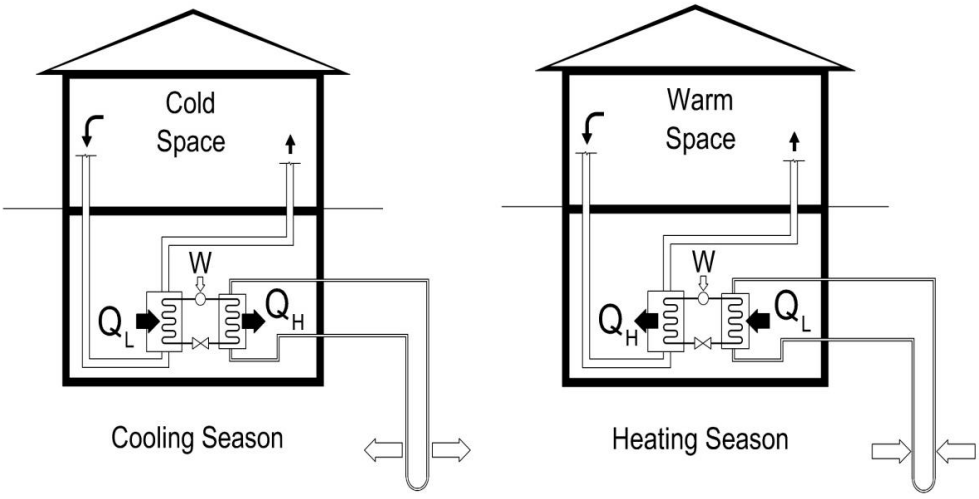

Figure 2-3: Ground-Coupled Heat Pump System for cooling season (left), and for heating season (right)

Thermal efficiency is an important factor to design and select heat pump systems. Indeed, heat pump systems need mechanical work to ensure their operation. The efficiency of heat pumps is expressed in terms of the Coefficient of Performance or COP defined as follows under ideal operation conditions:

$$\text{(Refrigerator)}\ \ \mathrm{COP_R} = \frac{\mathrm{Q_L}}{\mathrm{w_{net,in}}} = \frac{\mathrm{h_4 - h_3}}{\mathrm{h_1 - h_4}} \qquad \text{Equation 2-1}$$

$$\text{(Heat Pump)}\ \ \mathrm{COP_{HP}} = \frac{\mathrm{Q_H}}{\mathrm{w_{net,in}}} = \frac{\mathrm{h_1 - h_2}}{\mathrm{h_1 - h_4}} = \frac{\mathrm{Q_L}}{\mathrm{w_{net,in}}} + 1 = \mathrm{COP_R} + 1 \qquad \text{Equation 2-2}$$

where

Q_L = heat flow rate at an evaporator = $(h_4 - h_3) \cdot \dot{m}$

Q_H = heat flow rate at a condenser = $-(h_1 - h_2) \cdot \dot{m}$

h = enthalpy

w = the rate of energy input = $(h_1 - h_4) \cdot \dot{m}$

$\dot{m}$ = mass flow rate of circular medium (refrigerant)

As shown in the above equations, heat pumps' COP is always higher than 1 because of $COP_R > 0$. Thus, even in the worst cases, heat pumps provide heat into the space at least as the same amount of energy as they consume. It should be noted, however, that in reality the COP of heat pumps can be lower than the values provided by Equations 2-1 and 2-2 due various heat losses associated with both pipes and other devices. In particular, in the case of air-to-air heat pump systems, when outdoor temperature is too cold, it is possible for COP_{HP} to be less than 1 (Cengel, 2005). This possibility makes ground-coupled heat pumps attractive due to the rather constant ground temperatures. Indeed, while outdoor air temperatures can vary significantly with time and seasons, deep ground temperature is almost constant year-round. In addition, air-to-air heat pump systems can be subjected to frost conditions that inhibit heat transfer through evaporators, and thus additional systems and energy are required to defrost.

2.2. Existing Ground-Coupled Heat Exchanger Models

Since thermo-active foundations are essentially vertical ground coupled heat exchangers, the benefits associated with vertical ground source heat pumps are applicable to the thermo-active foundations. The performance of ground coupled heat exchanger systems is determined based on its ability of heat transfer over several time periods ranging from few minutes to 100 years between the heat exchanger pipes and the ground. So, in order to design thermo-active foundations, computationally efficient and accurate design models are required. Many researchers have been studied using empirical, analytical and numerical approaches to compute efficiently heat rejected to the ground from the heat exchanger pipes or extracted from the ground to the heat exchanger pipes.

2.2.1. Analytical Methods

Analytical solutions for ground coupled heat exchangers are based on several simplified assumptions. The primary assumptions include 'infinite line source' (Kelvin 1882; Ingersoll 1948, 1954; Mogensen 1983; Gehlin 1998; Witte et al. 2002) and 'cylindrical heat source' (Carslaw and Jaeger 1947; Ingersoll and Zobel 1954).

Line-source model

Kelvin (1861) developed the line source theory, and Ingersoll (1948, 1954) applied this theory to vertical ground coupled heat exchangers to calculate the temperature at any point in the infinite medium. Ingersoll's solution for ground temperature involves source heat transfer rate, distance from center line of pipe, and ground thermal properties. Specifically Ingersoll's solution assumes that heat flow is radial as depicted by Equations 2-3 and 2-4.

$$T - T_0 = \frac{Q'}{2\pi k}\int_x^\infty \frac{e^{-\beta^2}}{\beta} d\beta = \frac{Q'}{2\pi k} I(X) \qquad \text{Equation 2-3}$$

$$X = \frac{r}{2\sqrt{\alpha t}} \qquad \text{Equation 2-4}$$

where

T = Temperature of ground at any selected distance from the line source [℃]

T_0 = Initial temperature the ground [℃]

Q' = Heat transfer rate over the source [W/m]

r = Distance from center line of pipe [m]

k = Thermal conductivity of the ground [W/(m·℃)]

α = Thermal diffusivity of the ground =k/(ρ·c)

ρ = Density of the ground [kg/m^3]

β = Integration variable = $\frac{r}{2\sqrt{\alpha(t-t')}}$

t = Time

The Ingersoll solution is valid for a case of true line source. However, Ingersoll suggested that Equation 2-3 can be used for the case of small pipes of 2 inches or less in diameter without resulting in significant errors. Specifically, it is determined that the dimensionless term $\frac{\alpha t}{r^2}$ must be greater than 20 for practical applications to ensure small computational errors.

Hart and Couvillion (1986) developed another solution to estimate temperature distribution around a line source. They also used line source theory and considered an undisturbed far field temperature for better prediction of ground temperature distribution. In their solution, Hart and Couvillion assumed that the ground temperature is constant and undisturbed when the ground radius is greater than the far field radius. The proposed far field radius is defined as follows:

$$r_\infty = 4\sqrt{\alpha t} \qquad \text{Equation 2-5}$$

And, the temperature distribution around a line source is given by the following equation:

$$T - T_0 = \frac{Q'}{2\pi k}\left[\ln\frac{r_\infty}{r} - 0.9818 + \frac{4r^2}{2r_\infty^2} - \frac{1}{4x(2!)}\left(\frac{4r^2}{r_\infty^2}\right)^2 + \ldots\ldots + \frac{(-1)^{N+1}}{2Nx(N!)}\left(\frac{4r^2}{r_\infty^2}\right)^N\right] \qquad \text{Equation 2-6}$$

Where, r is the radial distance from the line source. Hart and Couvillion suggested that this equation applies for pipes when $\frac{r_\infty}{R}$ is greater than or equal to 15, where R is the pipe radius. The accuracy of Equation 2-6 depends on the ratio of $\frac{r_\infty}{R}$. When the value of this ratio is greater than or equal to 3, only 2 power series terms are needed, but for cases with a ratio of less than 3, the number of required power series terms is increased.

Cylindrical-source model

Kavanaugh (1985) used cylindrical source approximation to determine the temperature distribution and the heat transfer rate around a pipe embedded in the ground medium. The cylindrical source method was based on the Carslaw and Jaeger's solution (1947). Kavanaugh's cylindrical model used a finite cylinder in an infinite solid medium which has constant and uniform properties. The proposed solution is specific for a constant pipe surface temperature or for a constant heat transfer rate between the pipe and its surroundings. The thermal interference between boreholes is neglected in this solution.

The solution of Kavanaugh's cylindrical model is based on constant heat transfer rates and is given by the following equations:

$$T_{ff} - T_{ro} = \frac{Q'}{k} G(z, p) \qquad \text{Equation 2-7}$$

$$G(z, p) = \frac{1}{\pi^2} \int_0^\infty \frac{e^{-\beta^2 z} - 1}{J_1^2(\beta) + Y_1^2(\beta)} [J_0(p\beta) Y_1(\beta) - J_1(\beta) Y_0(p\beta)] \frac{1}{\beta^2} d\beta \qquad \text{Equation 2-8}$$

where

$$z = \frac{\alpha t}{r^2}, p = \frac{r}{r_0}, r_0 = \text{Outer pipe radius}$$

T_{ff} = Far-field temperature [^oC]

T_{ro} = temperature of outer pipe surface [^oC]

Meanwhile, in order to represent the number of legs of U-tube pipes in this solution, it is necessary to modify the diameter of the pipe. So, the equivalent pipe diameter is estimated as follows:

$$D_{eq} = \sqrt{n}\, D_0 \qquad \text{Equation 2-9}$$

where n is the number of U-tube legs in one borehole, D_0 is the original diameter of one U-tube leg , and D_{eq} is the equivalent diameter of a single pipe (Bose 1984).

Using this solution, using the energy balance, the outlet water temperature (T_{wo}) can be computed by the following equations:

$$T_{wo} = \frac{Q'L}{2 \cdot m_w c_{pw}} + T_{avgw} \qquad \text{Equation 2-10}$$

$$T_{wo} - T_{wi} = \frac{Q'L}{m_w c_{pw}} \qquad \text{Equation 2-11}$$

$$T_{avgw} = \frac{T_{wo} - T_{wi}}{2} \qquad \text{Equation 2-12}$$

$$T_{avgw} = T_{ff} + \left[\frac{Q'}{k} G(z, p)\right] + \Delta T_p \qquad \text{Equation 2-13}$$

$$\Delta T_p = \frac{Q'}{C \cdot N_i . 2\pi r_0 \cdot h_{eq}} \qquad \text{Equation 2-14}$$

where

T_{avgw}= average water temperature [^oC]

T_{wo} = outlet water temperature [^oC]

T_{wi} = inlet water temperature [^oC]

T_{ff} = far field ground temperature [^oC]

ΔT_p = temperature difference between outer pipe surface and fluid [^oC]

N_i = Number of U-tubes

C = Correction factor for non-uniform heat flow

(C = 0.85 when N_i = 2; C = 0.6-0.7 when N_i = 4)

2.2.2. Numerical Methods

As noted in the previous section, the analytical solutions described above are based on several simplifying assumptions to model ground coupled heat exchangers. In particular, these solutions ignore the effects of leg-to-leg thermal interferences as well as local geometries of the embedded heat exchangers. In order to consider these limitations of the analytical solutions, numerical methods have been utilized by several researchers to help estimate the performance of ground-coupled heat exchangers. Eskilson(1987) developed one of the first numerical solutions. This solution is the basis of several other numerical solutions reported for ground coupled heat exchangers. Eskilson's solution estimates the thermal performance of the ground loop heat exchangers using non-dimensional temperature response factors, called g-functions. In order to determine the response factors, both numerical and analytical models are employed.

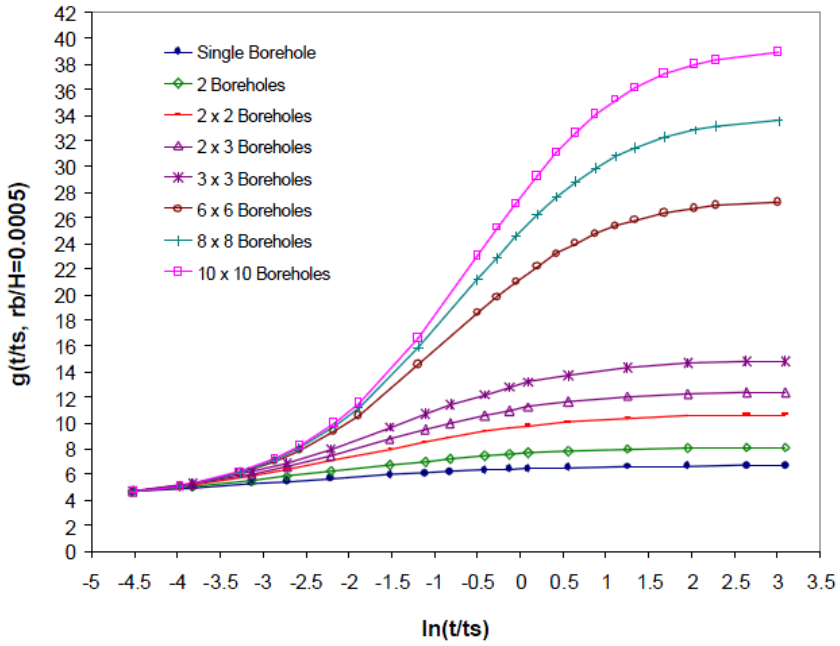

Figure 2-4: Temperature response factors (g-functions) for multiple borehole configurations (Spitler 2000)

Using a two-dimensional (radial-axial) explicit transient finite-difference method, the numerical solution for the Eskilson's determines the response to a unit step function heat pulse. In the Eskilson's method, the thermal capacitances of the individual borehole elements are neglected in the numerical analysis. By setting the temperature response of the borehole field to be dimensionless, the resulting non-dimensional ground temperatures and dimensionless times are g-functions (Figure 2-4).

However, even though the g-functions were developed for various borehole configurations, Eskilson's approach is only valid for long time steps. Thus, for short time steps, additional response function is required. Yavuzturk (1999) developed short time step response factors using two-dimensional implicit finite volume method applied to a cylindrical coordinate system. In this approach, the three-dimensional effects and the end of the U-tube are neglected. Compared to

Eskilson's approach, Yavuzturk's model accounted for individual borehole elements, and the effects of changing pipe temperature with depth are approximated.

Meanwhile, in cylindrical coordinates it is hard to model circular pipe. In order to represent the circular pipe of U-tube legs on polar grid, Yavuzturk employed a 'Pie-Sector' approximation (Figure 2-5). This discretization approach was also used by Rottmayer et al. (1997) for the quasi-three dimensional numerical U-tube heat exchanger model (Yavuzturk, 1999), (Rottmayer et al. 1997). In the method of pie-sector, a circular pipe is modeled as a pie-shaped pipe by defining the inside perimeter boundaries of the pie-sector as that estimated from the circular pipes with identical heat flux and resistance conditions used. In order to validate this approach, Yavuzturk used other cylindrical model which was an infinite cylinder model. It is concluded that the Pie-Sector approach was validated with an average relative error of less than 1%.

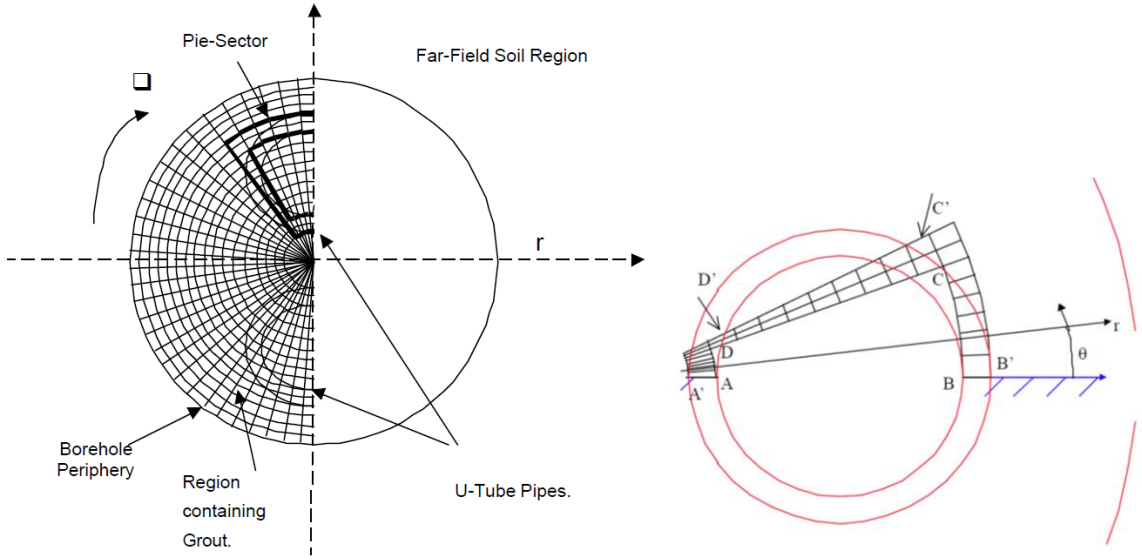

Figure 2-5: A schematic of Pie-Sector Approach: the borehole region on the numerical model domain is discretized using the pie-sector approximation for the U-tube pipes (left), the pie-sector representation of the U-tube pipes (right)

2.3. Thermo-active Foundation Systems

Thermo-active foundation (TAF) systems is the combination of ground loop heat exchanger pipes and building foundations used to heat and cool either partially or fully buildings. TAFs utilize building foundation elements (i.e., footings) in order to reduce the excavation costs associated with digging the boreholes for ground coupled heat exchange systems. TAF systems are also known as energy piles and foundation heat exchangers. Currently, there is a keen interest in installing TAF systems to meet heating and cooling requirements of a wide range of buildings especially in Europe and Japan (Brandl 2006, Laloui et al. 2006, Ooka et al. 2007). However, compared to vertical ground source heat pump systems, the performance of thermo-active foundation systems have not been widely studied and evaluated. Nevertheless, there have been some limited studies on the effectiveness of energy piles in extracting and rejecting heat in the ground medium using both numerical and empirical analyses (Adam et al. 2009). Some studies have analyzed both the thermal and mechanical performances of the thermo-active foundation systems (Brandl, 2006; McCartney et al.,2010).. Using a wide range of case studies, Brandl discusses the performance of thermo-active ground structures including energy foundations in terms of both thermal and mechanical responses. Brandl concluded that concrete has good thermal properties that enhance heat transfer between the ground and heat exchanger pipes, and that for general thermo-active ground structures, low-permeability soil and low hydraulic gradient of groundwater are favorable.

McCartney et al. (2010) performed a controlled laboratory experimental analysis using a centrifuge set-up to evaluate the soil-foundation interactions for geothermal foundations. The test was developed to evaluate the thermal and mechanical behavior of a small-scale thermo-active building foundation. From the testing results for the thermal response, it was observed that heat was

transferred effectively to the ground through the fluid circulating in the pipes embedded in the thermo-active foundation. Kaltreider (2011) used the test results of McCartney et al. (2010) to validate the predictions of a two-dimensional heat transfer mode for a thermo-active foundation.. Kaltreider found that several physical parameters can have a significant impact on the heat transfer rate between a thermo-active foundation and the ground including foundation depth, flow velocity, and shank space. In addition, Kaltreider found that there are potential thermal interactions between the building heating and cooling loads (through the foundation heat loss or gain) and the TAF system. .Specifically, when compared to the standard foundations (i.e., without embedded heat exchangers), TAF systems increase ground-coupled slab heat transfer. Kaltreider found that more heat losses occur during the heating season, and more heat gains are obtained during the cooling season.

In addition to laboratory testing, some researchers have focused on in-situ field experimental analysis using full-scale pile-foundation heat exchanger systems. In particular, Lyesse et al. (2006) performed the experiment for 97 piles of 25m length for a building in Switzerland to validate the predictions of their numerical model. Yasuhiro et al. (2007) monitored the performance of thermo-active foundation installed in a building located in Sapporo, Japan. It was found that the TAF system reduced the primary energy rate needed to heat and cool the building by 23.2%. Similar experimental analyses have been reported by Ryozo et al. in 2007 for a cast-in-place concrete pile foundation for a building in Japan, by Christopher et al. (2010) for a TAF system in UK, and by Jalaluddin et al. (2011) for 20m depth steel pile foundations with three types of ground heat exchangers (single U-tube type, double-tube type, and multi-tube type). Jalaluddin et al. found that the pile with double-tube exhibited the highest heat exchange rate, followed by the multi-tube, and U-tube type.

2.4. Summary

In this chapter, the reported thermal performance for both ground coupled heat exchangers and thermo-active foundation (TAF) systems are briefly summarized. For a conventional ground heat exchanger system, several analytical and numerical models have been developed to investigate heat exchanger rate and thermal performance associated to several TAF design and operating parameters. Based on the literature review for a conventional ground heat exchanger system, a detailed transient numerical model needs to be developed to evaluate the performance of thermo-active foundations. Analytical solutions while useful to provide some physical insights are not sufficient to develop design guidelines for TAF systems.

CHAPTER 3. TRANSIENT THREE-DIMENSIONAL NUMERICAL MODELING

3.1. Model Description

A three-dimensional numerical model for a thermal pile representing one thermo-active foundation is illustrated in Figure 3-1. The thermal pile includes two heat exchanger pipes embedded in the concrete foundation element surrounded by the ground medium. In this model, the heat exchanger U-tube pipes are simplified as two vertical pipes. The radius of the domain ground is chosen to be large enough to represent the undisturbed ground temperature boundary.

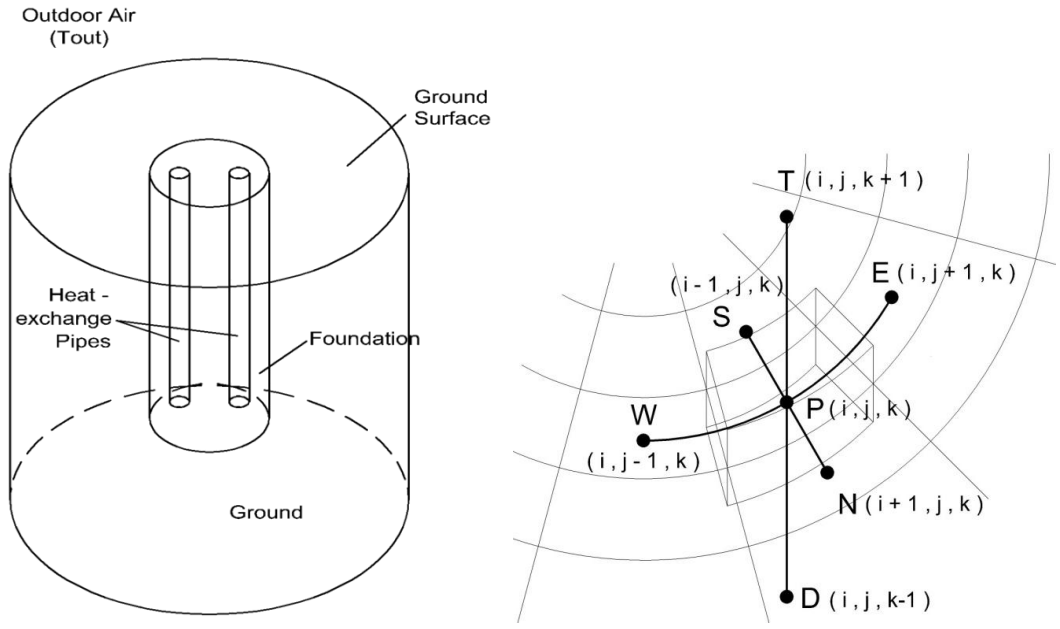

Figure 3-1: Simplified three-dimensional cylindrical thermal pile model (left), grid nodes (right)

The circular fluid flows into the inlet pipe of the U-tube at the ground surface level, and then flows out through the outlet pipe. According to Yavuzturk (1999), for the short time scale analysis pipe materials may have impact on short-term thermal performances of a vertical GCHP system, so that the thermal properties of a pipe are considered in this paper.

Building foundation is typically made up of concrete. Table 3-1 shows domain and foundation features as well as , its thermal properties considered in the analysis considered in this study. The common characteristics of the U-tube pipes are described in Table 3-2. The thermal properties of the circulating fluid are described in Table 3-3.

Table 3-1: Domain and foundation materials and properties

	Domain	**Foundation**
Material	Soil	Concrete
Diameter (m)	18.0	1.0
Depth (m)	20.00	10.00
Thermal Conductivity (W/m-K)	1.00	1.73
Density (kg/m^3)	2240	2600
Specific Heat (J/kg-K)	837	880

Table 3-2: Features of the U-Tube pipes

Radius (m)	0.025
Depth (m)	9.95
Shank Space (m)	0.100
Space between foundation to pipe	0.050
Thermal Conductivity (W/m-K)	0.36

Table 3-3: Thermal properties of the fluid circulating in the U-tube pipes

Thermal Conductivity (W/m-K)	0.58
Density (kg/m^3)	1000
Specific Heat (J/kg-K)	4181

3.2. Three-dimensional Finite Difference Method in Cylindrical Coordinates

The transient three-dimensional numerical model, developed as part of the study discussed in this thesis, uses an implicit finite difference discretization method associated with the cylindrical coordinates. Generally, heat transfer within the ground is complex and is affected by several mechanisms including conduction, radiation, convection, vaporization and condensation processes, ion exchange, and freezing-thawing processes (Brandl, 2006). However, conduction accounts for the most of heat transfer within the ground. So, in this study, the heat transfer within the ground is estimated assuming only conduction. The control volume of polar grid used to solve the transient heat conduction equation within and around the embedded TAF pipes is illustrated by Figure 3-2.

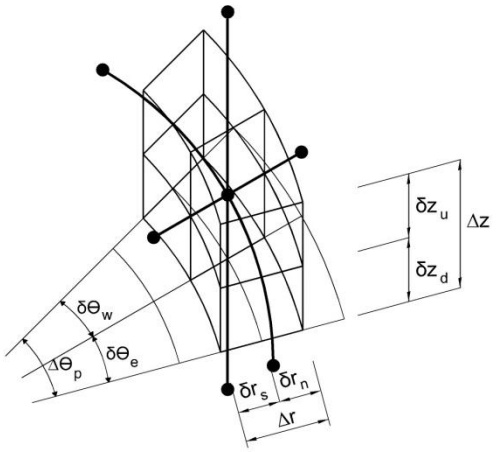

Figure 3-2: Control Volume for a regular node

The transient conduction equation in cylindrical coordinates can be expressed as follows:

$$\frac{1}{\alpha}\frac{\partial T}{\partial t} = \frac{\partial^2 T}{\partial r^2} + \frac{1}{r}\frac{\partial T}{\partial r} + \frac{1}{r^2}\frac{\partial^2 T}{\partial \theta^2} + \frac{\partial^2 T}{\partial z^2} \qquad \text{Equation 3-1}$$

The resulting implicit discretized equations for the heat conduction equation defined above are provided below. In the thermal pile model of Figure 3-1, it is assumed that there is no heat source in the ground. Thus, the conductive heat transfer equation is reduced to the following relationship between the temperatures of various nodes:

$$a_P T_P = a_E T_E + a_W T_W + a_N T_N + a_S T_S + a_U T_U + a_D T_D + b \quad \text{Equation 3-2}$$

where,

$$a_P = a_E + a_W + a_N + a_S + a_U + a_D + a_P^0 \quad \text{Equation 3-3}$$

$$a_E = \frac{k_e \Delta r_e \Delta z}{r_e (\delta\theta)_e} \quad \text{Equation 3-4}$$

$$a_W = \frac{k_w \Delta r_w \Delta z}{r_w (\delta\theta)_w} \quad \text{Equation 3-5}$$

$$a_N = \frac{k_n r_n \Delta\theta_n \Delta z}{(\delta\theta)_n} \quad \text{Equation 3-6}$$

$$a_S = \frac{k_s r_s \Delta\theta_s \Delta z}{(\delta\theta)_s} \quad \text{Equation 3-7}$$

$$a_U = \frac{k_u 0.5 * \Delta\theta * \left[\left(r + \frac{\Delta r_n}{2}\right)^2 - \left(r - \frac{\Delta r_s}{2}\right)^2\right]}{(\delta z)_u} \quad \text{Equation 3-8}$$

$$a_D = \frac{k_d 0.5 * \Delta\theta * \left[\left(r + \frac{\Delta r_n}{2}\right)^2 - \left(r - \frac{\Delta r_s}{2}\right)^2\right]}{(\delta z)_d} \quad \text{Equation 3-9}$$

$$a_P^0 = \frac{(\rho c)_P \Delta V}{\Delta t} \quad \text{Equation 3-10}$$

$$b = S_c \Delta V + a_P^0 T_P^0 \quad \text{Equation 3-11}$$

Since the vertical U-tube pipes have typically a narrow diameter and a long depth, some thermal properties are set as constant; such as thermal conductivity, density, specific heat, dynamic viscosity, and Prandtl Number of the circulating fluid within the pipes. The dominant heat transfer mechanisms within the fluid are convection and diffusion. Therefore, the advection heat transfer equations are employed.

$$a_P T_P = a_W T_W + a_E T_E + a_N T_N + a_S T_S + a_U T_U + a_D T_D + b \quad \text{Equation 3-12}$$

where,

$$a_W = D_W * (APe_W) + \max(F_W, 0) \quad \text{Equation 3-13}$$

$$a_E = D_E * (APe_E) + \max(-F_E, 0) \quad \text{Equation 3-14}$$

$$a_S = D_S * (APe_S) + \max(F_S, 0) \quad \text{Equation 3-15}$$

$$a_N = D_N * (APe_N) + \max(-F_N, 0) \quad \text{Equation 3-16}$$

$$a_U = D_U * (APe_U) + \max(F_U, 0) \quad \text{Equation 3-17}$$

$$a_D = D_D * (APe_D) + \max(-F_D, 0) \quad \text{Equation 3-18}$$

$$a_P^0 = \frac{\rho_{fluid} * Cp_{fluid} * \Delta V}{dy} \quad \text{Equation 3-19}$$

$$\Delta V = 0.5 * \Delta\theta * \left[\left(r + \frac{\Delta r_n}{2}\right)^2 - \left(r - \frac{\Delta r_s}{2}\right)^2\right] * \Delta z \quad \text{Equation 3-20}$$

$$b = a_P^0 * T_P^0 \quad \text{Equation 3-21}$$

The other terms are expressed in the following equations.

First, the conductance terms are defined as follows:

$$\text{(West)}\quad D_W = k_{fluid} * \frac{\Delta r * \Delta z}{r * \delta\theta_w} \qquad \text{Equation 3-22}$$

$$\text{(East)}\quad D_E = k_{fluid} * \frac{\Delta r * \Delta z}{r * \delta\theta_e} \qquad \text{Equation 3-23}$$

$$\text{(North)}\quad D_N = k_{fluid} * \frac{\left(r + \frac{\Delta r_n}{2}\right) * \Delta\theta * \Delta z}{\delta r_n} \qquad \text{Equation 3-24}$$

$$\text{(South)}\quad D_S = k_{fluid} * \frac{\left(r - \frac{\Delta r_s}{2}\right) * \Delta\theta * \Delta z}{\delta r_s} \qquad \text{Equation 3-25}$$

$$\text{(Up)}\quad D_U = k_{fluid} * \frac{0.5 * \Delta\theta * \left[\left(r + \frac{\Delta r_n}{2}\right)^2 - \left(r - \frac{\Delta r_s}{2}\right)^2\right]}{\delta z_u} \qquad \text{Equation 3-26}$$

$$\text{(Down)}\quad D_D = k_{fluid} * \frac{0.5 * \Delta\theta * \left[\left(r + \frac{\Delta r_n}{2}\right)^2 - \left(r - \frac{\Delta r_s}{2}\right)^2\right]}{\delta z_d} \qquad \text{Equation 3-27}$$

The flow rate terms are:

$$F_{W,E} = \rho_{fluid} * Cp_{fluid} * U_{W,E} * \Delta r * \Delta z \qquad \text{Equation 3-28}$$

$$F_N = \rho_{fluid} * Cp_{fluid} * U_N * \left(r + \frac{\Delta r_n}{2}\right) * \Delta\theta * \Delta z \qquad \text{Equation 3-29}$$

$$F_S = \rho_{fluid} * Cp_{fluid} * U_S * \left(r - \frac{\Delta r_s}{2}\right) * \Delta\theta * \Delta z \qquad \text{Equation 3-30}$$

$$F_{U,D} = \rho_{fluid} * Cp_{fluid} * U_{U,D} * 0.5 * \Delta\theta * \left[\left(r + \frac{\Delta r_n}{2}\right)^2 - \left(r - \frac{\Delta r_s}{2}\right)^2\right] \qquad \text{Equation 3-31}$$

The Peclet Number terms are defined:

$$Pe_{W,E} = F_{W,E}/D_{W,E}$$ Equation 3-32

$$Pe_{N,S} = F_{N,S}/D_{N,S}$$ Equation 3-33

$$Pe_{U,D} = F_{U,D}/D_{U,D}$$ Equation 3-34

The A(|Pe|) function is described using the Power Law Scheme:

$$APe_{W,E} = \max\left(0, \left(1 - 0.1 * \left|Pe_{W,E}\right|^5\right)\right)$$ Equation 3-35

$$APe_{N,S} = \max\left(0, \left(1 - 0.1 * \left|Pe_{N,S}\right|^5\right)\right)$$ Equation 3-36

$$APe_{U,D} = \max\left(0, \left(1 - 0.1 * \left|Pe_{U,D}\right|^5\right)\right)$$ Equation 3-37

While convective coefficients are employed to compute convection heat transfer as described in the above equations, it is difficult to determine adequate convective coefficients for the analysis since these coefficients depend on the flow rate, pipe size, and fluid temperature. As aforementioned, however, the effect of the fluid temperature on the convective coefficient is relatively small. In this analysis the impact of temperature is neglected, and the fluid is assumed to be at constant temperature, pipe size and flow rate. Thus, by using these values, Reynolds number and Nusselt number can be defined.

$$Re = \frac{(U * D_H)}{v}$$ Equation 3-38

$$D_H = \frac{(4 * A)}{P}$$ Equation 3-39

Where, D_H is hydraulic diameter, U is fluid velocity, v is kinematic viscosity, A is cross sectional area of pipe, and P is wetted perimeter of pipe. Since the pipe configuration in this analysis is modeled using the Pie-Sector approach, so that hydraulic diameter is used instead of actual pipe diameter for computing the convection coefficients. Based on the Reynolds number and the hydraulic diameter,, Nusselt number is calculated for both heating and cooling modes. For the case of turbulent flow $(\mathrm{Re} \geq 2300)$ in the pipes, Dittus-Boelter equation can be used.

$$\begin{cases} \mathrm{Nu} = 3.36 & (\text{if } \mathrm{Re} < 2300) \\ \mathrm{Nu} = 0.023 * \mathrm{Pr}^{n} * \mathrm{Re}^{0.8} & (\text{if } \mathrm{Re} \geq 2300) \end{cases} \qquad \text{Equation 3-40}$$

$$\begin{cases} n = 0.3 \text{ (for Cooling)} \\ n = 0.4 \text{ (for Heating)} \end{cases}$$

Where, Pr is Prandtl number. Thus, using Nusselt number, the convective coefficients of the fluid circulating within the pipes can be calculated:

$$\mathrm{h_{fluid}} = \frac{(\mathrm{Nu} * \mathrm{k_{fluid}})}{\mathrm{D_H}} \qquad \text{Equation 3-41}$$

However, in order to account for the pipe thickness and pipe thermal properties, an effective convective coefficient is employed:

$$\mathrm{h_{eff}} = (\mathrm{h_{fluid}} + \frac{\text{pipe thickness}}{\mathrm{k_{pipe}}}) \qquad \text{Equation 3-42}$$

Where, k_{pipe} is the thermal conductivity of the pipe material.

3.3. Boundary Conditions

Because of the cylindrical coordinates, boundary conditions of the Equation 3-1 are simplified. In particular, the top boundary is represented by a surface in contact with only the outside air temperature. Thus, the top surface is not in contact with inside air temperature within a building. Moreover, the outer edge of the ground medium is set as an adiabatic surface to model the far-field ground temperature.

In most US locations, ground temperature reaches steady and constant temperature after few feet of depth. In order to account for this effect, a constant ground temperature is used as the boundary condition at the bottom of the domain ground. Generally, boundary conditions are expressed by the following equation:

$$\alpha T + \beta \frac{\Delta T}{\Delta r} = C \qquad \text{Equation 3-43}$$

Type 1: $\alpha = 1$, $\beta = 0$, C = Constant Temperature

Type 2: $\alpha = 0$, $\beta = 1$, C = Constant Heat Flux

Type 3: $\alpha \neq 0$, $\beta \neq 0$

Based on the expression for boundary conditions, the top boundary and the bottom boundary conditions are of type 1 with prescribed temperature settings with outside air temperature and groundwater temperature, respectively. The outer edge boundary condition is of type 2 with an adiabatic surface (Table 3-4).

Table 3-4: Summary of boundary conditions for the cylindrical numerical model

Domain Boundary	Type	Settings
Top	Type 1	$\mathbf{T_{OA} = T_{OA,mean} - T_{OA,amp} \cdot \cos(w \cdot time)}$ [℃] Equation 3-44 $\mathbf{w = angular\ frequency = \frac{2\pi}{24}}$ $T_{OA,mean}$ = mean outside air temperature $T_{OA,amp}$ = amplitude of outside air temperature fluctuation
Bottom	Type 1	$\mathbf{T_{GW} = 10}$℃ (**50**℉) Equation 3-45
Outer edge	Type 2	**Adiabatic** $= \frac{\Delta T}{\Delta r} = 0$ Equation 3-46

The inlet fluid temperature is assumed to vary over time following a cosine function similar to the time variation of the outside air temperature. Its behavior follows the variation of the outside air temperature to account for the resulting variation of the building thermal loads. Specifically, the inlet fluid temperature is set to vary as 11℃ to 19℃ above the ground temperature (or groundwater temperature) during the cooling mode and 6 to 8℃ less than the ground temperature for during the heating mode (Kavanaugh, 2010).

$$T_{Inlet\ Fluid} = T_{Inlet\ Fluid,mean} - T_{Inlet\ Fluid,amp} \cdot \cos(w \cdot time)[℃] \quad \text{Equation 3-47}$$

where

$$w = \text{angular frequency} = \frac{2\pi}{(3600 \times 24 \times 365)}$$

$T_{Inlet\ Fluid,mean}$ = mean inflow fluid temperature (℃)

$T_{\text{Inlet Fluid,amp}}$ = amplitude of inflow fluid temperature fluctuation (°C)

3.4. Analysis of Impact of Grid Discretization

Generally, finite difference models based on finer grids generate more accurate solutions. However, because of limitations in computing capabilities, finer grids require more simulation time. Thus, a sensitivity analysis to determine the adequate grid scheme to be utilized is required.

For the sensitivity analysis on the grid dependence, a very fine grid scheme is used as a reference against which all the other discretization schemes are compared. For the comparative analysis, Root Mean Square Error (RMSE) method is used to measure of the magnitude of the differences between the predictions using the reference and any other schemes as illustrated in Equation 3-48:

$$\text{RMSE} = \sqrt{\frac{\sum_{i=1}^{n}(T_{1,i} - T_{2,i})^2}{n}} \qquad \text{Equation 3-48}$$

$$T_1 = [T_{1,1}, T_{1,2}, T_{1,3}, \dots, T_{1,n}] \quad \text{and} \quad T_2 = [T_{2,1}, T_{2,2}, T_{2,3}, \dots, T_{2,n}]$$

The RMSE values are shown in Figure 3-3 for several grid schemes. As shown in Figure 3-3, the finer is the grid, the more accurate is the numerical solution characterized by lower RMSE values. However, the computational efforts defined by the CPU time required for the numerical solution increases with the number of grid nodes. Based on the results of Figure 3-3, an adequate number for the grid nodes is 312,000. Indeed, after this threshold number, the required simulation time increases significantly as illustrated in Table 3-5 and Figure 3-3. In addition, the RMSE value for a grid made up of 312,000 nodes is relatively small attesting of the accuracy of the

numerical solution. Therefore, a grid with 312,000 nodes will be in most of the analysis of the TAF system performance discussed in the next chapters.

Table 3-5: The impact of grid node numbers of both CPU and RMSE values for the numerical solution

Case	NODE	CPU Time (seconds)	RMSE (℃)
case #1	288	0.10	2.83
case #2	1,680	0.87	0.49
case #3	15,120	9.16	0.24
case #4	23,520	14.26	0.16
case #5	33,600	36.74	0.19
case #6	47,040	65.62	0.12
case #7	54,720	90.49	0.17
case #8	63,840	109.65	0.12
case #9	77,280	158.54	0.12
case #10	86,400	183.75	0.12
case #11	97,920	224.73	0.12
case #12	112,320	272.19	0.12
case #13	144,000	489.13	0.07
case #14	160,800	576.53	0.05
case #15	198,000	663.90	0.07
case #16	221,760	839.18	0.06
case #17	312,000	1544.74	0.01
case #18	352,000	13149.30	0.06
case #19	416,000	14711.57	0.02
case #20	468,000	41971.27	0.00

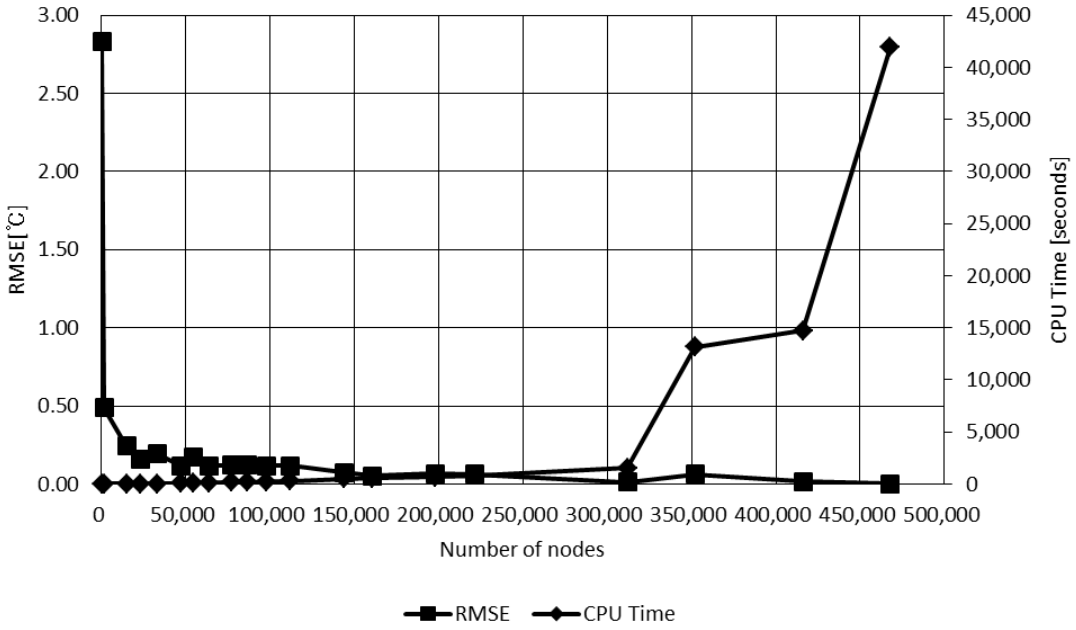

Figure 3-3: Variation of CPU time and RMSE value associated with the numerical solution as functions of the number of the grid nodes

3.5. Validation of the Three-Dimensional Numerical Model

3.5.1. Validation Method Description

In order to validate the predictions from the developed three-dimensional transient numerical model, experimental data from McCartney et al. (2010) are utilized. The experimental testing was performed at the Centrifuge Lab of the Geotechnical Engineering and Geo-mechanics, the University of Colorado at Boulder. Specifically, the experimental set-up consisted of a scale-model thermo-active foundation (Figure 3-4, Table 3-6), which had three independent U-tube loops. The scale-model was 24.6 times smaller than a typical real TAF foundation for a commercial building. The fluid used in the experiment is pure ethylene glycol heat transfer fluid. Table 3-6 shows the dimensions of the scaled experiment model.

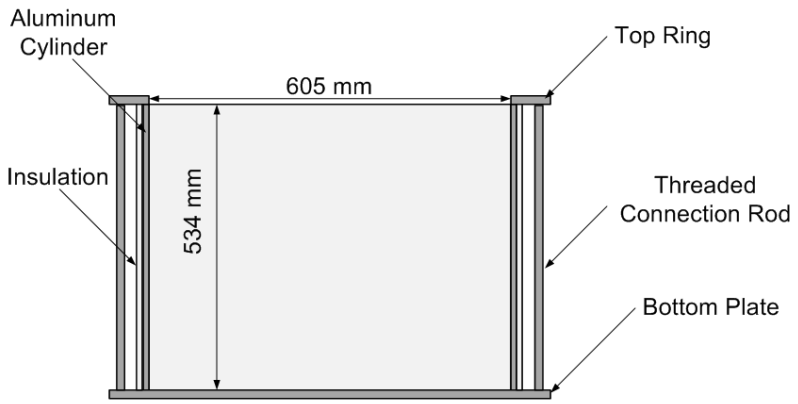

Figure 3-4: A scale-model for a thermo-active foundation set-up

Table 3-6: Basic dimensions of the small-scale thermo-active foundation model used in the experimental analysis

Domain Container	Diameter [mm]	605 mm
	Depth [mm)	534 mm
Foundation	Diameter [mm]	50 mm
	Depth [mm)	400 mm
U-Tube Pipe	Outer diameter [mm]	3.175 mm
	Inner diameter [mm]	1.588 mm

The measured parameters from the test set-up include ground temperatures, foundation temperatures, and inlet/outlet flow temperatures. To monitor the ground and foundation temperatures, 24 probes were used as illustrated in Figure 3-5. The specific locations of these temperatures probes are provided in Table 3-7.

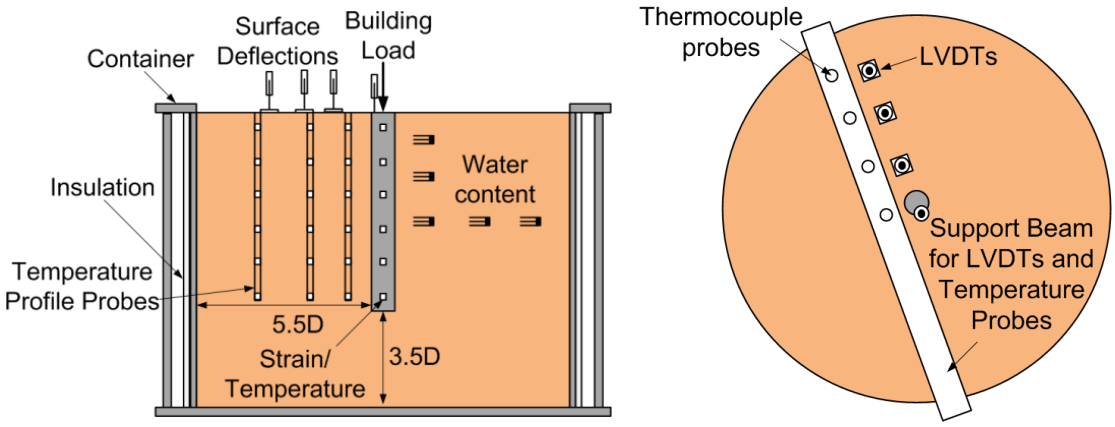

Figure 3-5: Locations of temperature probes within the tank

Table 3-7: Coordinates of the probe locations for the experiment test

r(cm) / Z(cm)	8.89	12.70	18.41	24.13
1.0	Probe 1-6	Probe 2-6	Probe 3-6	Probe 4-6
5.4	Probe 1-5	Probe 2-5	Probe 3-5	Probe 4-5
9.8	Probe 1-4	Probe 2-4	Probe 3-4	Probe 4-4
14.2	Probe 1-3	Probe 2-3	Probe 3-3	Probe 4-3
18.6	Probe 1-2	Probe 2-2	Probe 3-2	Probe 4-2
23.0	Probe 1-1	Probe 2-1	Probe 3-1	Probe 4-1

As part of the experimental set-up, four operation modes were considered to mimic operation of TAF system under various building thermal load conditions including: heating start-up, steady state heating, cooling start-up, and steady state cooling as shown in Figure 3-7 showing the heat exchanger fluid outlet temperature variation with time. Hot fluid was pumped up at the beginning of the experiment to increase the temperature of a heat exchanger pipes in the foundation, and then maintained at a fairly constant temperature (ranging from 30°C to 35°C). After one hour from the beginning of the experiment, the fluid flow was stopped to cool down the foundation and soil medium. Then, the fluid temperature is kept at a constant temperature (about 20°C).

Since the heat pump in the experimental set-up was not capable to pump cool fluid, a simple flow control method was used. This method resulted in the oscillations in the temperature variation during the heating mode as shown in Figure 3-7. In an attempt to maintain fairly constant outlet temperature around at 30℃, the pump is set frequently on and off until the temperature reached 30℃.

Since the specific thermal properties of various materials (such as soil and concrete) used in the experimental set-up were not given or tested, a sensitivity analysis was carried for the calibration process. In addition, the bottom of the domain cylinder was not adiabatic surface since it is exposed to the ambient air. The lower boundary condition in the numerical model had to be adjusted based on the ground temperature profiles measured during the experimental analysis.

Table 3-8: Thermal properties of the materials used in the experimental set-up

	Pipe	**Foundation**	**Soil**
Thermal Conductivity (W/m K)	0.42	1.76	1.43
Density (kg/m3)	-	2240	2400

Specific Heat (J/kg K)	-	874	852

3.5.2. Results

To validate the numerical model predictions, the calculated ground and outlet temperatures from the numerical solution are compared with measurements. Table 3-9 summarizes the comparative analysis results for the ground temperatures using the root mean square error (RMSE) values for 5 hours. Generally, it is observed that the simulation results match well the experimental measurements.

Table 3-9: RMSE values between mode predictions and measurements for the ground temperatures during five hours

	1 hour	**2 hour**	**3 hour**	**4 hour**	**5 hour**
RMSE [°C]	0.30	0.34	0.28	0.26	0.24

Figure 3-6 shows the far-field temperature variation with time as measured from the experimental set-up and as used in the numerical model. The three-dimensional numerical model successfully made the similar pattern of temperature rise of the far-field ground temperature.

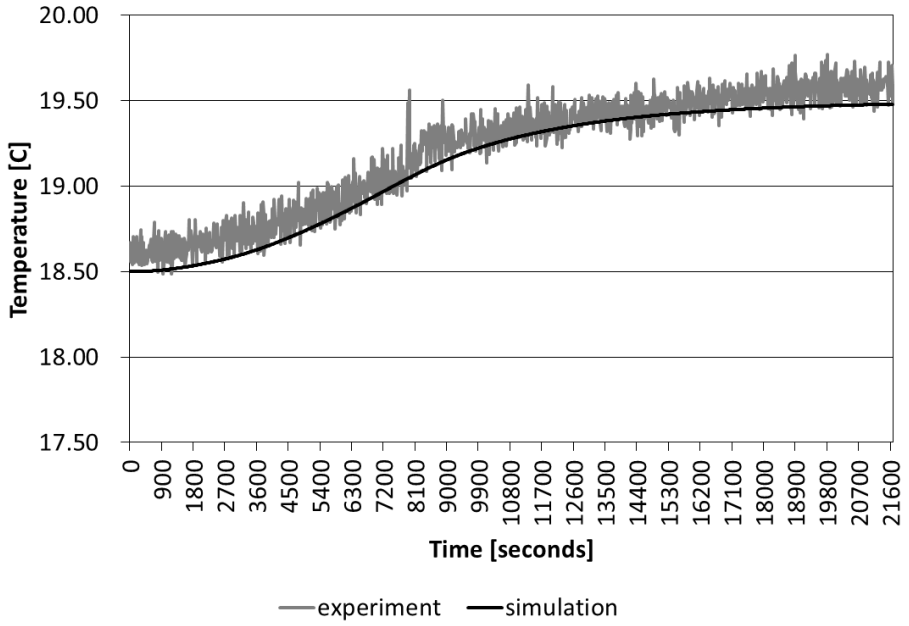

Figure 3-6: Far field ground temperature variation with time

Table 3-10 and Figure 3-7 compare the outlet temperatures obtained from the model predictions and measurements for various time intervals. Similar to the results found for the ground temperatures, the numerical solution predictions agree well with the experimental data. More detailed validation results are described in Appendix-A.

Table 3-10: Difference between model predictions and measurements for the outlet fluid temperatures

Time [t, sec]	t=3600	t=7200	t=10800	t=14400	t=18000	t=21600
Experiment [℃]	30.32	20.39	20.05	19.63	19.37	19.27
Simulation [℃]	29.95	20.61	20.11	19.78	19.64	19.57
Error [℃]	0.37	-0.22	-0.06	-0.16	-0.27	-0.30

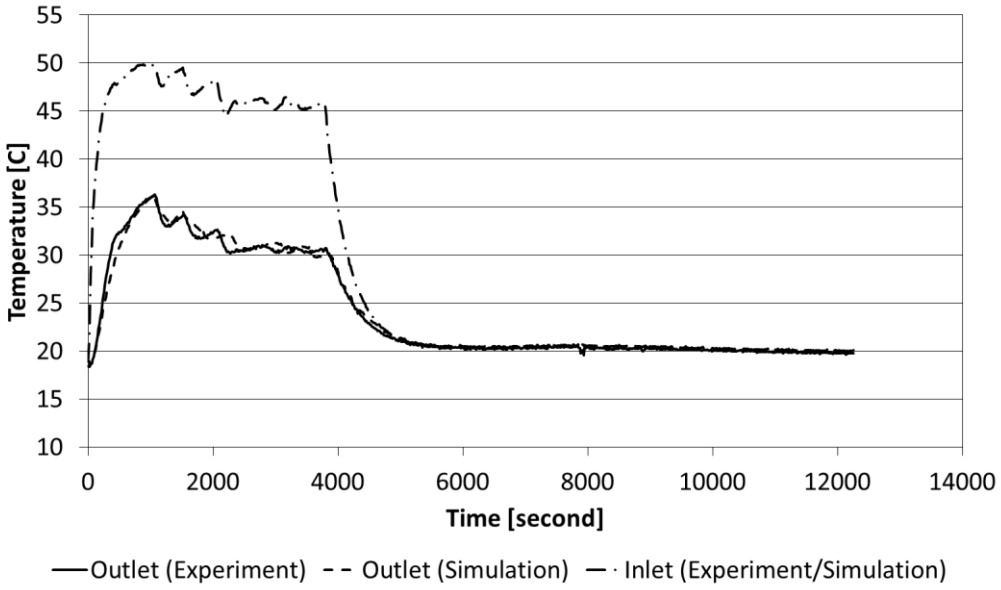

Figure 3-7: Variation of fluid outlet temperature with time based on model predictions and testing measurements

3.6. Sensitivity Analysis

In order to evaluate the thermal performance of a thermo-active foundation, the impact of several parameters is investigated using the validated numerical model. Generally, the ground is a large medium and has high thermal capacitance. However, the specific properties of the ground depend on a wide range of factors including type of soil, moisture content, soil layers, and groundwater level. In reality, it is very difficult to determine ground characteristics and properties with expensive testing set-up. Therefore, in this study, the ground is assumed to have uniform thermal properties and with no groundwater flow.

The parameters that are investigated in this study consist of foundation depth, fluid velocity in the heat exchanger loops, radial distance between U-tube pipes (also called shank space), and the number of U-tube loops in one pile. The main factor to evaluate the impact of each parameter is the

heat flux transferred between circulating fluid and the ground medium. This heat flux is estimated using both inlet and outlet temperatures as indicated by Equations 3-49 and 3-50.

$$Q = \rho_{fluid} * cp_{fluid} * V * (T_{outlet} - T_{inlet}) \quad \text{Equation 3-49}$$

$$\text{Percent increase in heat transfer} = \frac{(Q - Q_{base})}{Q_{base}} \times 100\% \quad \text{Equation 3-50}$$

where

Q = heat flux [w]

ρ_{fluid} = density of fluid [kg/m^3]

cp_{fluid} = specific heat of fluid [J/kg]

V = volumetric flow rate [m^3/sec]

T_{outlet} = outlet temperature of fluid [℃]

T_{inlet} = inlet temperature of fluid [℃]

Q_{base} = heat transfer of the base case

3.6.1. Impact of foundation depth

Similar to the vertical GSHPs, thermo-active foundation systems utilize deep constant ground to extract or reject heat. Therefore, the foundation depth can significantly affect the thermal performance of TAF systems. Figure 3-8 illustrates the variation of the heat exchange rate (expressed in percent as defined by Equation 3-50) as a function of normalized foundation depths for various fluid velocities. As shown in Figure 3-8, as the foundation pile is deeper, more heat can be exchanged to or from the ground especially for higher fluid velocities Therefore, when

selecting a depth for a thermo-active foundation, it important to also consider the fluid velocity within the geothermal exchanger loops.

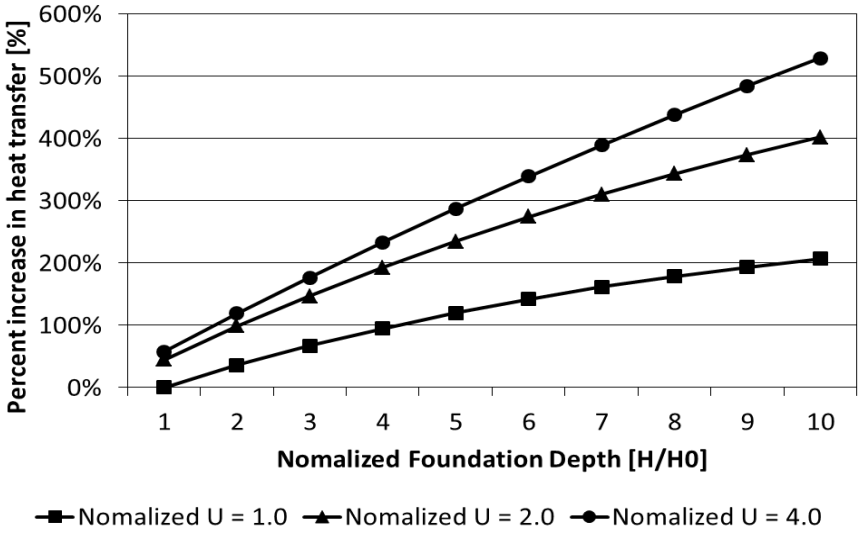

Figure 3-8: Impact of foundation depth for various normalized fluid velocities

3.6.2. Impact of fluid velocity

The effect of fluid velocity in the U-tube loops on the performance of thermo-active foundation is shown in Figure 3-9. As expected, the exchanged heat transfer increases as the fluid velocity increases. In addition, at the point that a shift from a laminar flow to a turbulent flow (i.e., when Re ≥ 2300) occurs, there is a sudden increase of the heat transfer rate. This change is due to the fact that turbulent flow increases the convective coefficient along the pipe walls, and therefore increases heat transfer through the pipe walls.

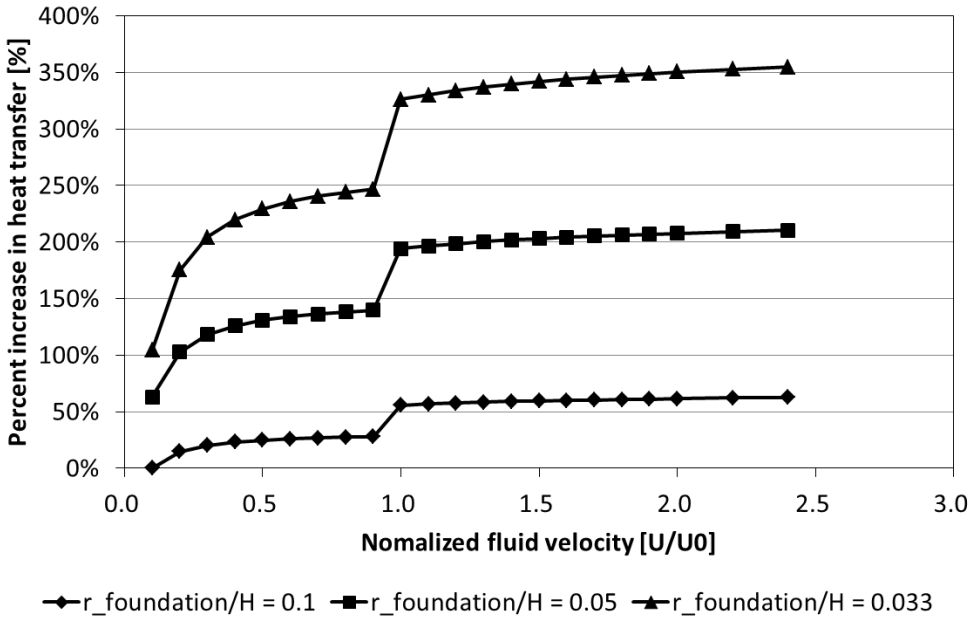

Figure 3-9: Impact of fluid velocity for various ratios of borehole radius to foundation depth

However and as shown in Figure 3-9, the increasing rate of heat transfer is rather slow after the shift from laminar flow to turbulent flow. Indeed, due to the higher fluid velocity there is not enough time for heat exchanges between the fluid and the ground. Thus, the temperature differences between the inlet and outlet becomes rather small.

3.6.3. Impact of the shank space

Within a thermo-active foundation, there is thermal interference between U-tube pipes. The impact of the distance between two loops, typically referred as the shank space, is evaluated. Figure 3-10 illustrates the percent increase in heat transfer between the thermo-active foundation and ground as a function of the ratio of shank space to foundation radius for various foundation radii.

Figure 3-10 indicates that the heat transfer through the pipes increases as the shank space

increases. A higher shank space implies that there is less thermal interactions between the U-tube pipes. In addition, larger foundation radius results in higher heat transfer by the thermo-active foundation due to larger surface area

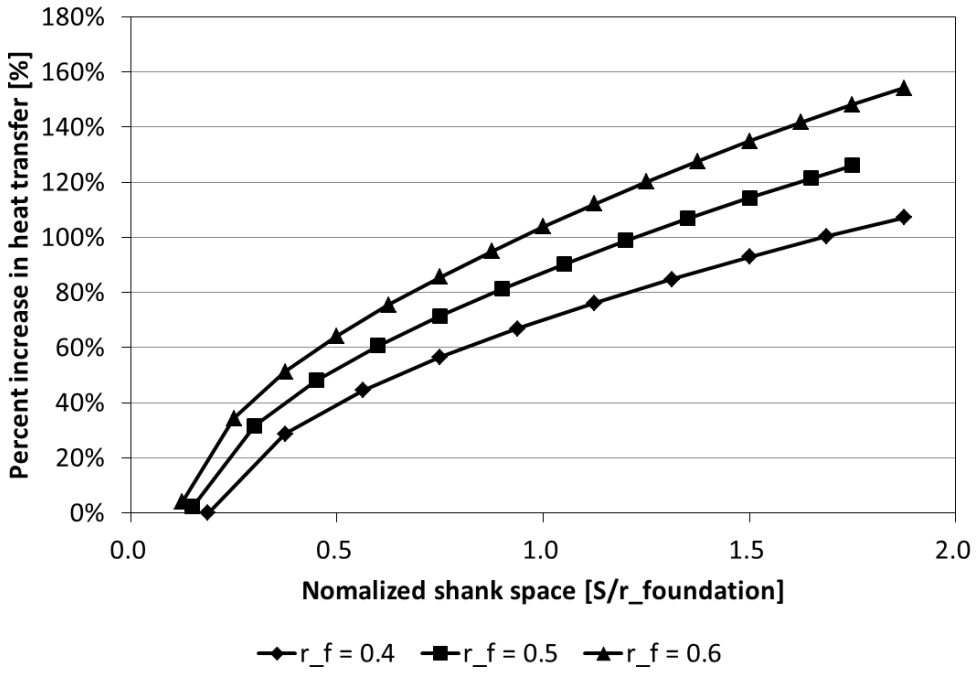

Figure 3-10: Impact of shank space ratio for various foundation radii

3.6.4. Impact of the number of U-tube loops

To evaluate the effect of the number of U-tube loops on thermal foundation of a thermo-active foundation, a sensitivity analysis was performed as shown in Figure 3-11. As expected, increasing the number of U-tube loops in a foundation increases the heat transfer between the fluid and the ground, improving the thermal performance of a thermo-active foundation.

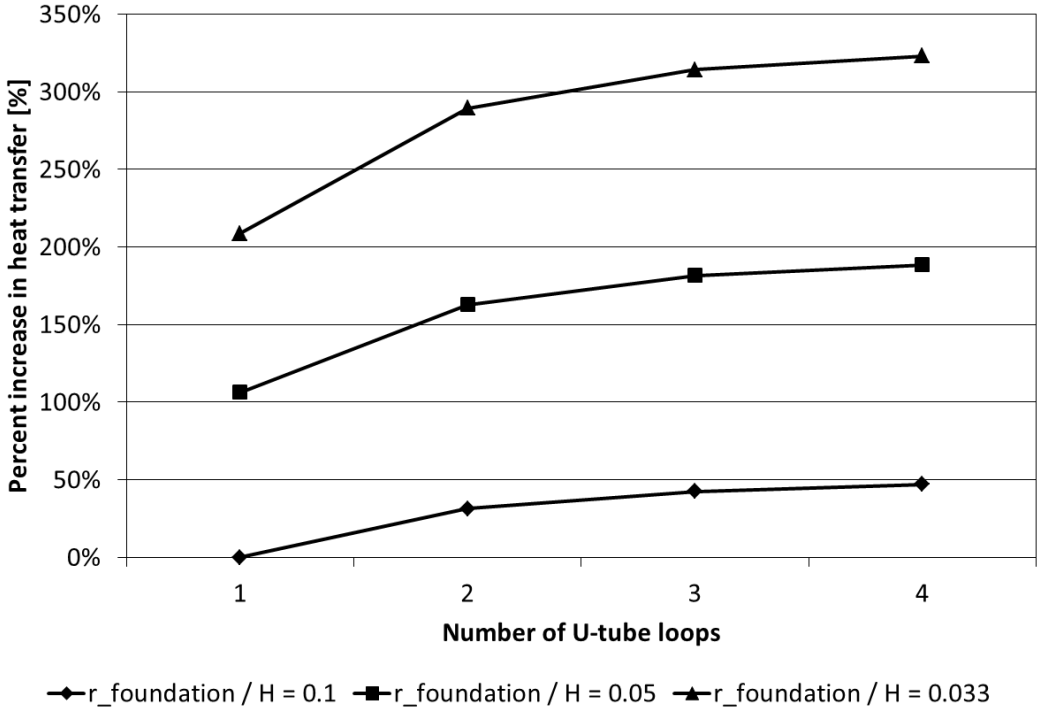

Figure 3-11: Impact of the number of U-tube loops on heat exchange rate for various ratios of borehole radius to foundation depth

3.7. Summary

In this chapter, a three-dimensional transient numerical model for a thermo-active foundation has been developed using cylindrical coordinate system. The numerical model is based on the implicit finite difference method. The numerical model considered in this study is representative of a concrete pile foundation and can be used estimate the heat transfer exchanged between the thermal pile and the ground medium under various design and operating conditions.

Using a proper discretization scheme to optimize the accuracy and the computational efforts, , the transient three-dimensional numerical has been validated with the experimental data obtained from a laboratory set-up in the Centrifuge Lab of the Geotechnical Engineering and

Geomechanics, the University of Colorado at Boulder. The experimental set-up was specific for a small scale model thermo-active foundation with a pile diameter of 605 mm and a depth of 534 mm. The scale-model set-up is 24.6 times smaller than an actual prototype foundation for a commercial building. Based on the results of the validation analysis, the numerical solution predictions agree well with the measured data with RMSE values of less than 0.5℃ for all temperature measurements.

Utilizing the 3D numerical model developed in this chapter, a series of sensitivity analyses has been carried out to determine the impact of selected design and operating parameters on the performance of thermo-active foundations. It is found that higher heat transfer exchanged between the thermo-active foundation and ground can be achieved by increasing either the foundation depth, the fluid velocity, or shank space of the U-tube loops within the same pile.

CHAPTER 4. THERMAL RESPONSE FACTOR MODEL

4.1. Introduction

The fluid temperature outlet from the U-tube loops is needed to estimate the energy efficiency of thermo-active foundation systems. . The thermal response factor method (also called g-function) has been used to integrate GSHP model within detailed building energy simulation tools. Both short-time and long-time step g-functions have to generated to model properly the thermal performance of GSHPs. Eskilson's g-approach is utilized to calculate long-time step g-function (Eskilson, 1987) while Yavuzurk method is used to estimate short-time step g-function (Yavuzturk, 1999). It should be noted that for the short-time step analysis, the time step is from 2.5 min to 200 hours. For long-time step analysis, the time step is over 200 hours. To determine the response of boreholes to a step function heat pulse, Eskilson utilized a superposition approach as illustrated in Figure 4-1.

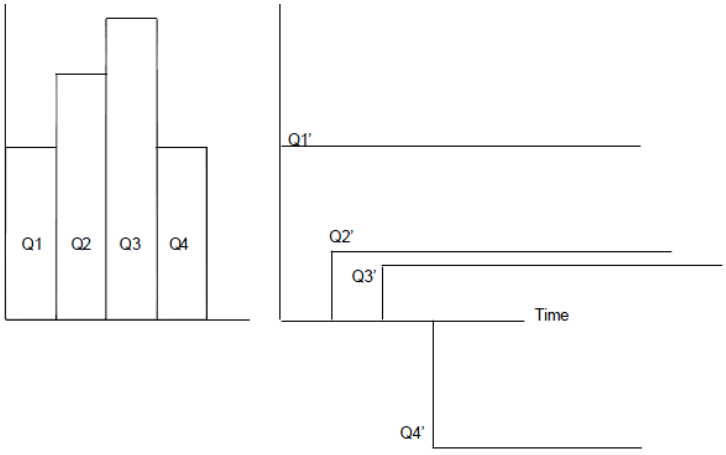

Figure 4-1: Superposition of piece-wise linear step heat inputs (Spitler 2000)

Temperature change at the borehole wall is calculated using g-functions in response to a unit time step heat input pulse. Once the temperature response of the borehole field to a single unit step heat pulse is determined, the response to ground coupled heat exchangers to any heat (rejection/extraction) rate can be determined by decomposing the heat rejection/extraction rate into a series of unit step pulses. Then, to obtain the overall response, the response to each unit step pulse is superimposed. Using the superposition principle, the borehole wall temperature at the end of the n^{th} time period is described in the following equation (Spitler 2000):

$$T_{borehole} = T_{ground} + \sum_{i=1}^{n} \frac{(Q_i - Q_{i-1})}{2pk} g\left(\frac{t_n - t_{i-1}}{t_s}, \frac{r_b}{H}\right) \quad \text{Equation 4-1}$$

where

t = Time

t_s = Time scale = $H^2/9\alpha$

H = Borehole depth

k = Ground thermal conductivity

$T_{borehole}$ = Average borehole temperature

T_{ground} = Undisturbed ground temperature

Q = Step heat rejection/extraction pulse

r_b = Borehole radius

i = Index to denote the end of a time step

4.2. Description of Three-dimensional Numerical Model

The three dimensional numerical model developed and validated in Chapter 3 is used to calculate the average foundation wall temperature. In particular and in order to generate g-

functions, the boundary conditions of the numerical model are modified. For long-time steps, the three-dimensional numerical model and associated boundary conditioned are illustrated in Figure 4-2.

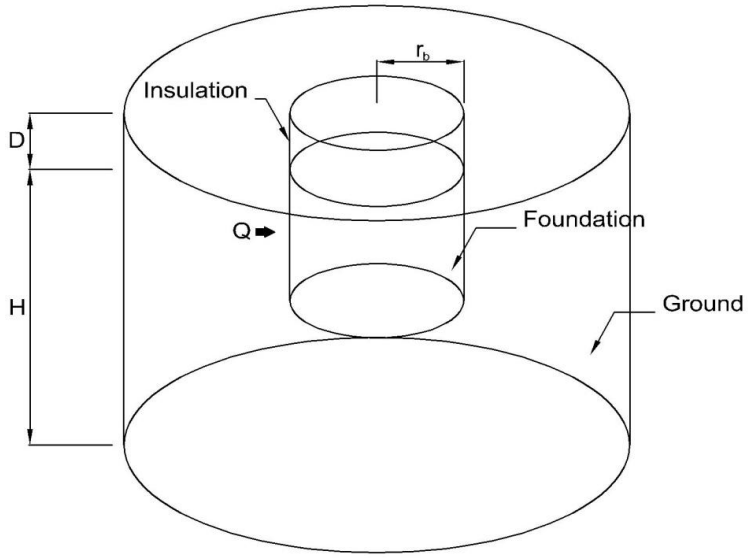

Figure 4-2: Numerical model for long-time step g-function estimation

For short-time step g-function calculation, an overall thermal resistance of the thermo-active foundation should be defined. This resistance should include convective resistance for the circulating fluid, the conductive thermal resistance of the U-tube pipes, and the conductive thermal resistance of the foundation material.

$$R_{total} = R_{fluid} + R_{pipe} + R_{foundation} \qquad \text{Equation 4-2}$$

where

R_{total} = total thermal resistance of a thermo-active foundation [℃-m/W]

R_{fluid} = convective thermal resistance of a circular fluid [℃-m/W]

R_{pipe} = conductive thermal resistance of a pipe [℃-m/W]

$R_{foundation}$ = conductive thermal resistance of foundation material [℃-m/W]

Figure 4-3 illustrates the model to estimate the short-time step g-function.

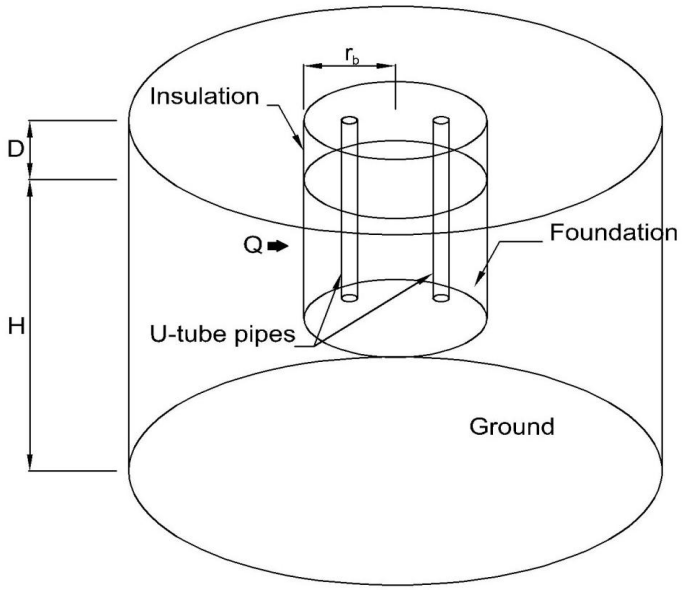

Figure 4-3: Numerical model for the short-term g-function

Table 4-1 and Table 4-2 describe the geometric and material properties used in the analysis as well as the boundary and initial conditions considered for the numerical model. These features including the boundary and initial conditions are based on analyses carried out by Eskilson's and Yavuzturk's studies.

Table 4-1: Properties of thermo-active foundation model

Depth of insulation (D)	5 m
Depth of foundation (H)	110 m
Radius of foundation (r_b)	0.055 m
Thermal conductivity of soil (k_{soil})	3.5 W/m-K

Thermal diffusivity of soil	1.62 X 10^{-6} m^2/s
Thermal conductivity of foundation (k_{conc})	1.73 W/m-K (for Long-time step model only)
Thermal diffusivity of foundation	1.44 X 10^{-6} m^2/s (for Long-time step model only)
Heat extraction rate (Q)	22 W/m
Far field temperature (T_{om})	8 ℃

Table 4-2: Boundary and Initial conditions of thermo-active foundation model

Boundaries	Conditions
Top of domain	Constant temperature $T(r, \theta, z=1, t) = T_{om}$
Outer edge of domain	Constant temperature $T(r, \theta, z=1, t) = T_{om}$
Bottom of domain	Adiabatic
Foundation wall	Constant heat flux
Bottom of foundation	Adiabatic (for Long-time step model only)
Insulation layer	Adiabatic
Initial condition	$T(r, \theta, z, t=0) = T_{om}$

4.3. Thermal response factors

From the numerical solution, the average temperature of the foundation wall is calculated. To compute g-functions, Eskilson's and Yavuzturk's g-function equations are employed. The Eskilson's equation was modified by Yavuzturk to consider the temperature changes due to the thermal effects of borehole materials (i.e., Equation 5-3 and Equation 5-4). Utilizing the g-function equations, the thermal response factors of a thermo-active foundation are then calculated for both short-time step and long-time step:

[Long-time step g-function] $$\mathbf{g}\left(\frac{t_n - t_{i-1}}{t_s}, \frac{r_b}{H}\right) = \frac{2 \times \pi \times k_{ground}(T_{borehole} - T_{ground})}{Q}$$ Equation 4-3

[Short-time step g-function] $$\mathbf{g}\left(\frac{t_n - t_{i-1}}{t_s}, \frac{r_b}{H}\right) = \frac{2 \times \pi \times k_{ground}(T_{borehole} - R_{total} \cdot Q - T_{ground})}{Q}$$ Equation 4-4

To verify the calculation procedure for the thermal response factors of thermo-active foundations developed in this chapter, the thermal response factors of TAF systems is compared with those obtained by Eskilson's and Yavuzturk's vertical GSHP model for long-time steps and short-time steps, respectively.

4.3.1. Long Time-Step Thermal response Factors

The three-dimensional numerical model is adjusted to model vertical GSHP and is then used to generate the Eskilson's long-time step g-function by setting thermal conductivity of the concrete to be the same as that of the soil. Figure 4-4 and Figure 4-5 illustrates the comparative results of the 3-D numerical model predictions to those obtained by the Eskilson's borehole model.

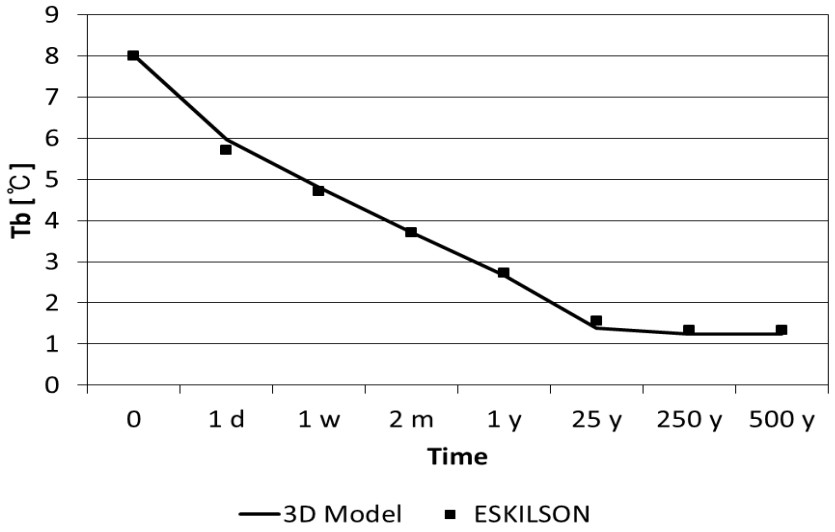

Figure 4-4: Time variation of the average borehole wall temperature (T_b)

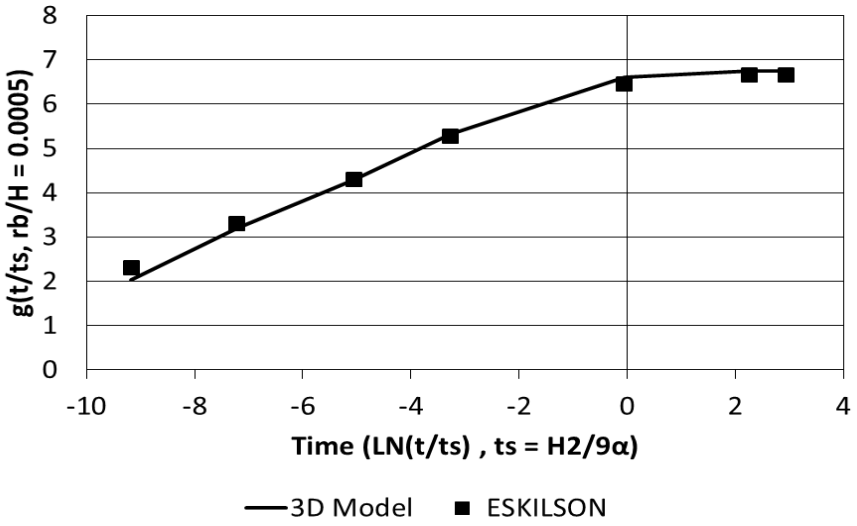

Figure 4-5: Long-time step g-function variation (with $t_s = H^2/9\alpha$)

As an application of the long-time step model, the average fluid temperature can be calculated:

$$T_{fluid} = T_{foundation} + R_{total} \times Q \qquad \text{Equation 4-5}$$

Where,

T_{fluid} = average fluid temperature (℃)

$T_{foundation}$ = average foundation wall temperature (℃)

Q = unit heat extraction/rejection rate (W/m)

R_{total} = total thermal resistance of foundation (m/W)

4.3.2. Short Time-Step Thermal response Factors

For short-time step, the thermal performance within the thermo-active foundation is determined. In order to validate the calculation approach, g-function obtained by Yavuzturk's short-time step model for a borehole with a ratio of radius to depth, r_b/H, of 0.0005. Figure 4-6 illustrates the resulting g-function from Yavuzturk's model and from the three-dimensional numerical model. The g-function obtained from the three-dimensional model developed in this paper matches well with that by the Yavuzturk's model.

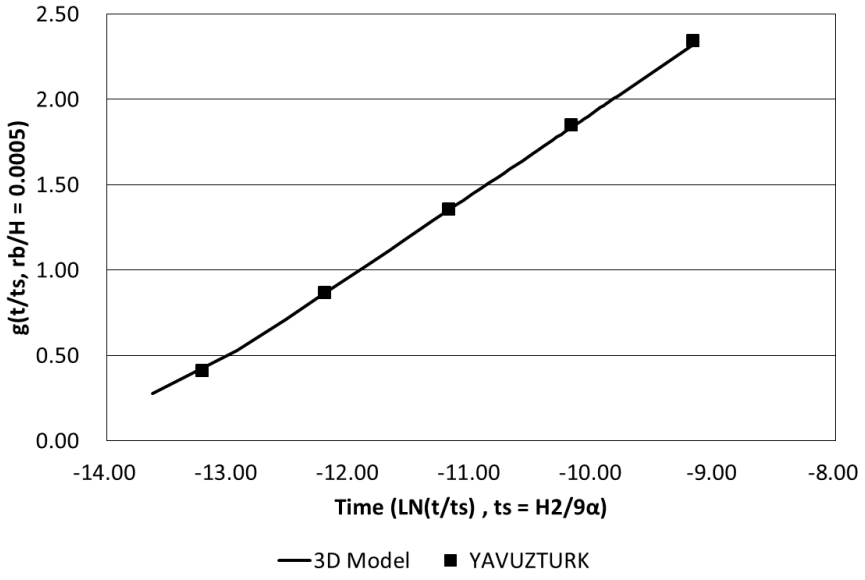

Figure 4-6: Short-time step g-function variation

In Figure 4-7, the short-time step g-function developed using the numerical model is well lined up with the long-time step g-function. Thus, to model the thermal performance of any thermo-active foundation system, the three-dimensional numerical model can be utilized to generate g-function.

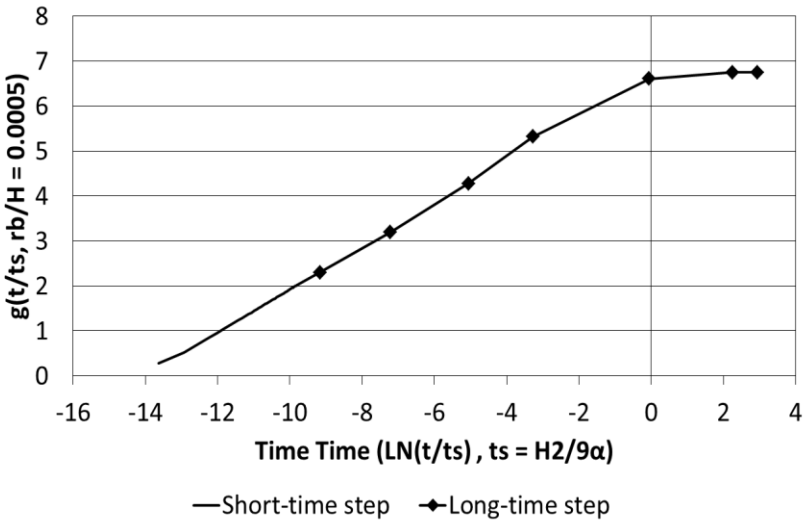

Figure 4-7: Long-time step and short-time step g-function obtained from the 3-D numerical model

4.4. Sensitivity Analysis of the Thermal response factor

Based on the sensitivity analysis discussed in Chapter 3, it is found that several design and operating parameters can affect the thermal performance of thermo-active foundation systems. In this section, a similar sensitivity analysis is carried out but specific to the impact of the design and operating parameters on the variations of the thermal response factors.. These parameters include foundation depth, foundation radius, shank space, and thermal conductivities of both soil and foundation material (i.e., concrete).

4.4.1. Foundation Depth

In Figure 4-8, thermo-active foundation g-function variation with the time expressed with the term $Ln(t/t_s)$ is illustrated for various foundation depths. It should be noted that based on the

equation to calculate t_s (i.e., $t_s = H^2/9\alpha$), foundation depth affects the time scale expressed in natural logarithm.

Based on the g-function curves, it is clear that foundation depth is a significant parameter to estimate the thermal performance of TAF systems. Indeed, different foundation depths have distinct g-function curves. As shown in Figure 4-8, TAFs with deeper foundation has higher g-function values, and thus would be able to transfer more heat.

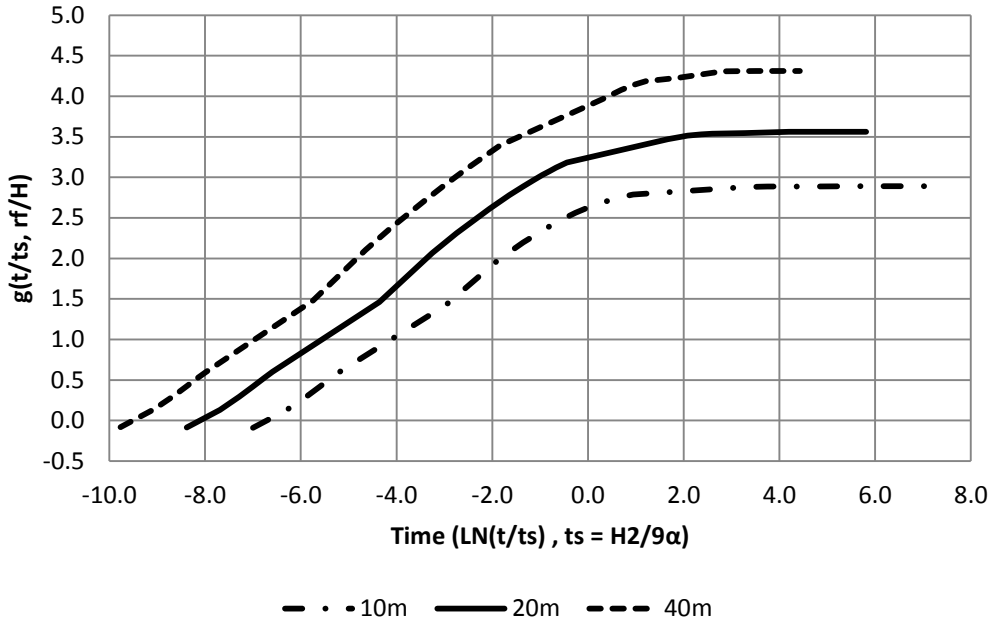

Figure 4-8: G-function of a thermo-active foundation for various foundation depths (with foundation radius = 0.055m, H =foundation depth, and α = ground thermal diffusivity)

4.4.2. Shank Space

Figure 4-9 and Figure 4-10 show the g-functions for various shank space values. The shank space is defined as the distance between U-tube legs. It is normalized by the diameter of the foundation. Since the long-time step thermal performance of a thermo-active foundation occurs

from the foundation wall, the g-function for long-time step is independent of the shank space. However, for short-time step performance, the g-function is affected by the shank space, even though the difference between g-function curves is rather small.

Figure 4-10 indicates that higher g-function is obtained for larger distance between the U-tube legs. The larger shank space reduces the thermal interactions between the U-tube pipes.

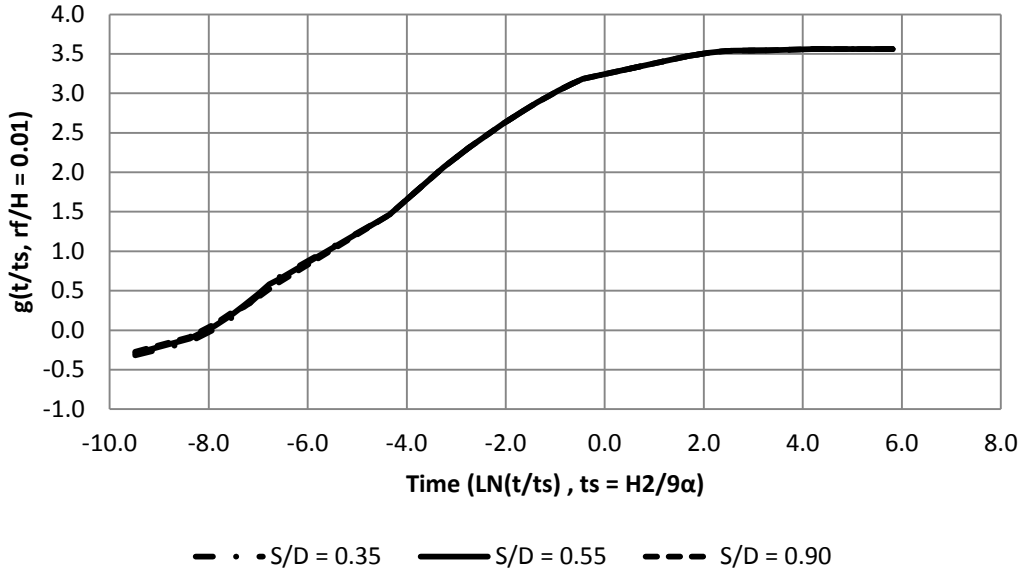

Figure 4-9: Variation of g-function for various shank space values (with foundation radius = 0.055m, D = foundation diameter of 0.11m, H =foundation depth of 13m, and α = ground thermal diffusivity)

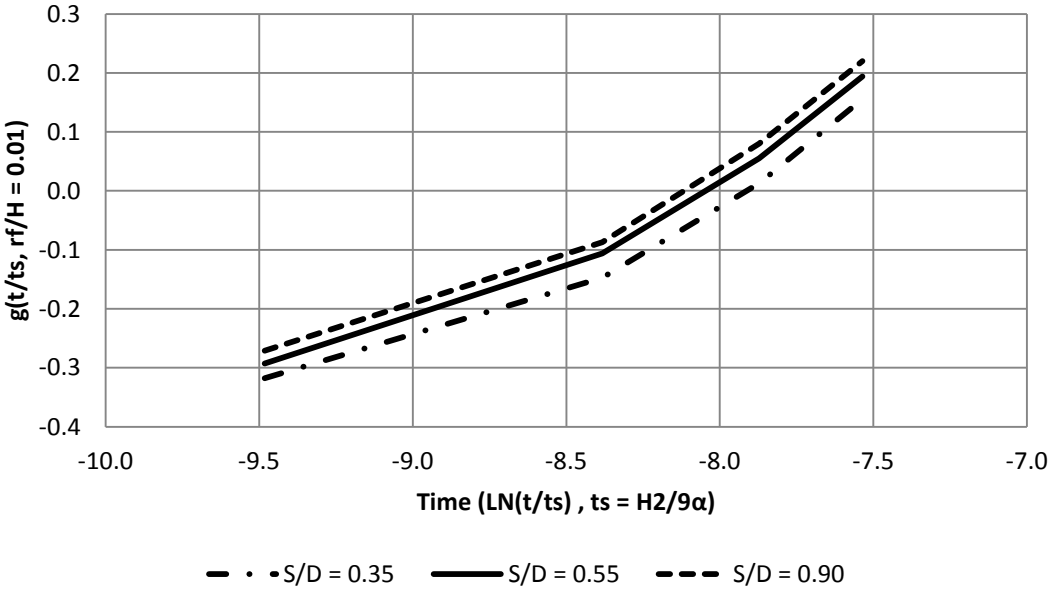

Figure 4-10: Variation of short-time g-functions for various shank space values (with foundation radius = 0.055m, D = foundation diameter of 0.11m, H = foundation depth of 13m, and α = ground thermal diffusivity)

4.4.3. Thermal Conductivity of Foundation Material

For short-time steps, the elements within the thermal piles affect the performance of thermo-active foundations. Figure 4-11 and Figure 4-12 illustrate the impact of the concrete thermal conductivity on short-time and log-time steps on g-function of a thermo-active foundation. Higher concrete thermal conductivity results in higher values for the g-function are obtained. By reviewing the equation to compute g-functions (Equation 5-4), it can be seem that the thermal conductivity of foundation is needed to estimate thermal resistance and therefore the foundation wall temperature. Thus, higher foundation thermal conductivity values increase the temperature differences between the ground and the foundation wall..

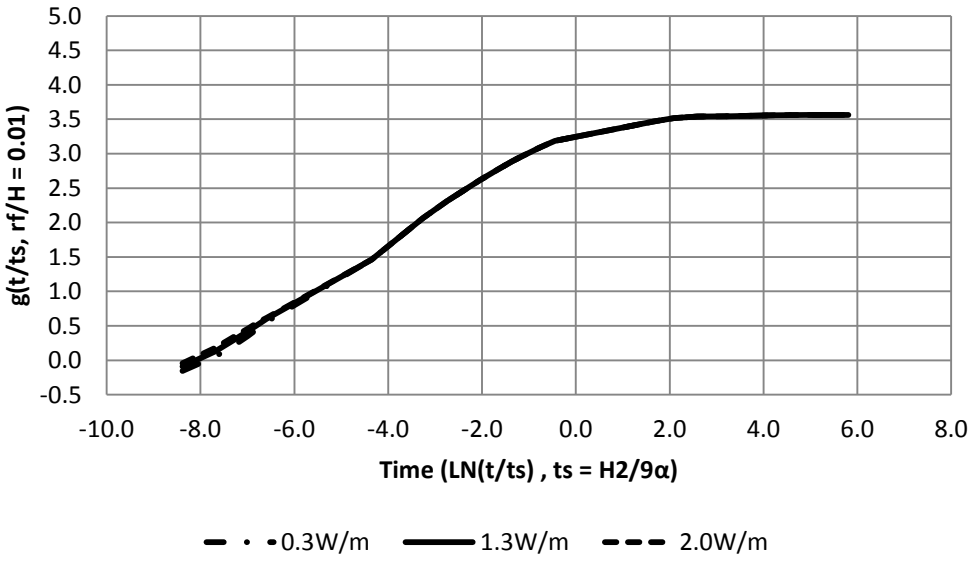

Figure 4-11: Variation of g-function for the various concrete thermal conductivity values (with foundation radius = 0.055m, H =foundation depth of 13m, S = shank space of 0.03124m, and α = ground thermal diffusivity)

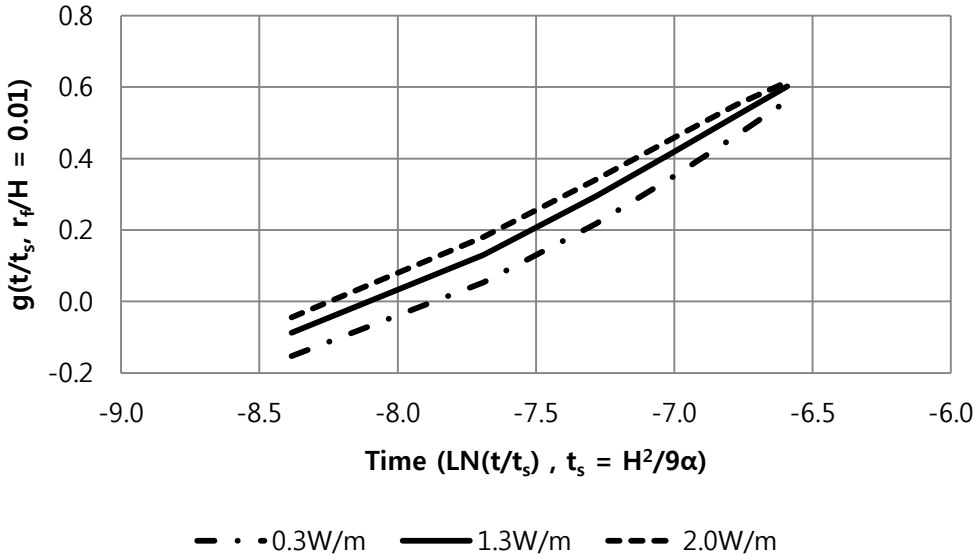

Figure 4-12: Variation of short-time step g-function for various concrete thermal conductivity values (with foundation radius = 0.055m, H =foundation depth of 13m, S = shank space of 0.03124m, and α = ground thermal diffusivity)

4.4.4. Soil Thermal Conductivity

Soil thermal conductivity is an important parameter that affects the capability of the ground-coupled heat exchangers to reject or extract heat to/from the ground. Several factors can affect soil thermal conductivity including but not limited to moisture content, soil decomposition, soil surface condition, and depth. To account for these factors, effective or apparent soil thermal conductivity is typically used in ground-couple heat transfer analysis (ASHRAE Fundamentals, 2009). Soil thermal conductivity is required for the calculation of g-function (refer to Equation 5-4)as illustrated in Figure 4-13.. Soils with lower soil thermal conductivity have higher values of short-term thermal response factors.

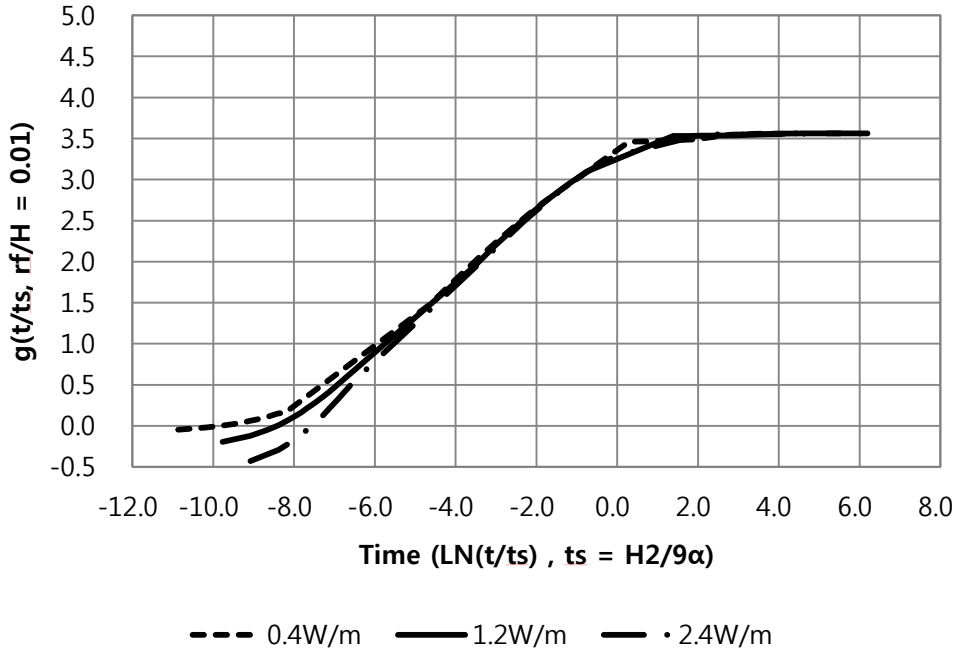

Figure 4-13: Variation of g-function for the various soil thermal conductivity values (with foundation radius = 0.055m, H =foundation depth of 13m, S = shank space of 0.03124m and α = ground thermal diffusivity)

4.4.5. Fluid Flow Rate

The heat transfer rate exchanged by a thermo-active foundation is directly affected by the fluid mass flow rate. In addition, flow rate and fluid velocity affects the convective coefficients along the tubes.

Figure 4-14 illustrates the variation of g-function as a function of the normalized time for various volumetric fluid flow rates. The first fluid flow rate (V = 1.765E-5 m3/s) results in a laminar flow, and the other rates result in turbulent flow within the heat exchanger loops. As shown in Figure 4-14, the g-function does not change with the flow rate. So, it can be concluded that while flow rate affects heat transfer rate, it does not impact the g-function.

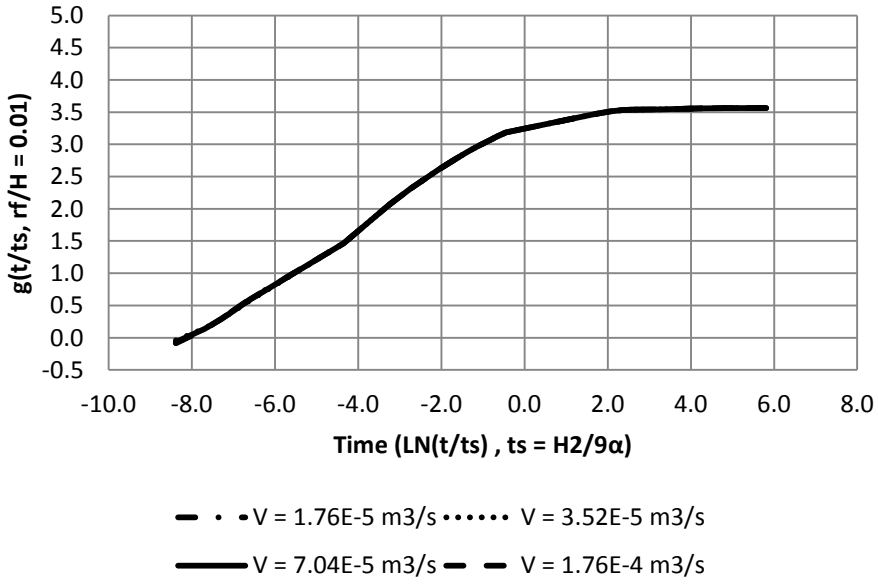

Figure 4-14: Variation of g-function for various fluid flow rates (with foundation radius = 0.055m, H =foundation depth of 13m, S = shank space of 0.03124m and α = ground thermal diffusivity)

4.5. Comparison Analysis of Thermal response factors

In order to evaluate the differences in thermal response factors of a thermo-active foundation (TAF) and a vertical ground source heat pump (GSHP), a comparative analysis is

performed. In this analysis, the basic features for both TAF and GSHP models are the same including the borehole characteristics, ground thermal properties, and temperature settings. The only difference between the two models is the medium surrounding the boreholes. For GSHP model, soil is typically used around a borehole, while for TAF, it is concrete. The values of soil thermal conductivity used in this analysis are described in Table 4-3, while the concrete thermal conductivity is assumed to be 1.8 W/m. Since medium material around heat exchanger pipes affect only the short-term performance of TAF and GSHP systems this analysis is performed for short-term thermal response factors.

Table 4-3: Soil thermal conductivity values used in the comparative analysis of thermal response factors

	Thermal Conductivity
Soil 1	0.6 [W/m]
Soil 2	0.8 [W/m]
Soil 3	1.0 [W/m]
Soil 4	1.2 [W/m]
Soil 5	1.4 [W/m]
Soil 6	1.6 [W/m]
Soil 7	1.8 [W/m]
Soil 8	2.0 [W/m]
Soil 9	2.2 [W/m]
Soil 10	2.4 [W/m]
Soil 11	2.6 [W/m]
Soil 12	2.8 [W/m]
Soil 13	3.0 [W/m]

Figure 4-15 illustrates the results of the comparative analysis of the g-function (i.e., thermal response factor) evaluated at 15 hour between GSHP and TAF systems. It is clear from the

results outlined in Figure 4-15 that GSHP is influenced by soil thermal conductivity more than TAF. This result is expected since GSHP boreholes are directed in contacted with soil while TAF heat exchangers are embedded in the concrete foundation. As shown in Figure 4.15, when soil thermal conductivity increases, the difference in thermal response factors between GCHP and TAF increases. The two systems have the same response factors when the soil thermal conductivity is equal to 1.8 W/^{o}C-m which is the concrete thermal conductivity.

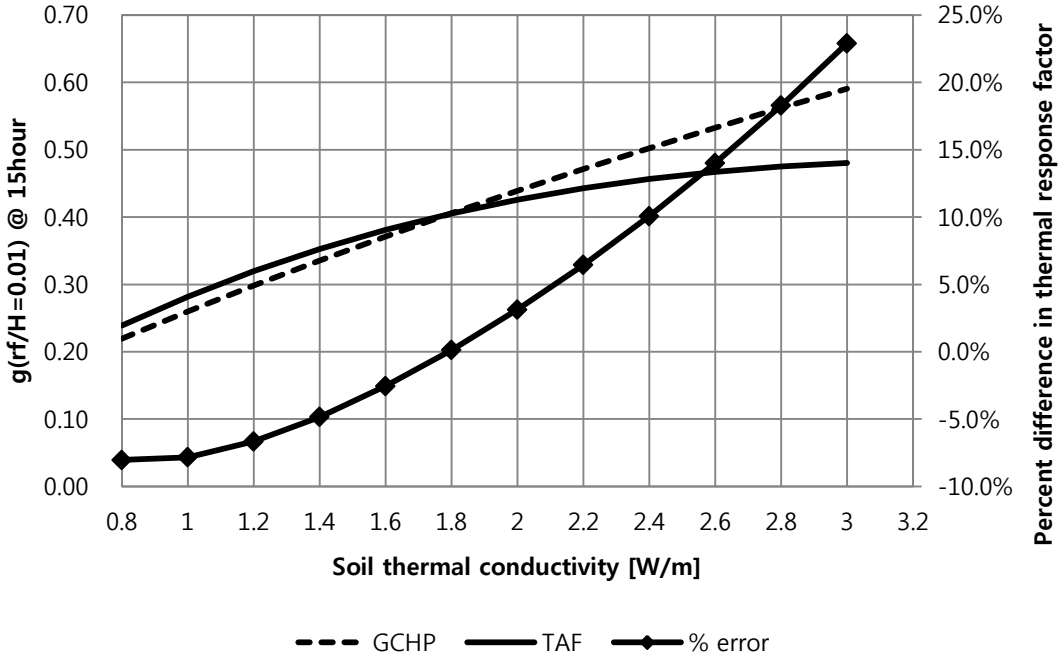

Figure 4-15: Thermal response factor at 15 hour for various soil thermal conductivity values associated with GCHP and TAF systems, and percent difference of between TAF and GCHP thermal response factors, (Percent difference in thermal response factor = (GCHP – TAF) / TAF * 100%)

Figure 4-16 and Figure 4-17 provide the variations of respectively, the cooling and heating energy end-uses associated to of GSHP and TAF systems when the soil thermal conductivity changes from the reference value of 1.8 W/^{o}C-m. As expected, the GSHP is more affected by the variation of soil thermal conductivity than TAF.

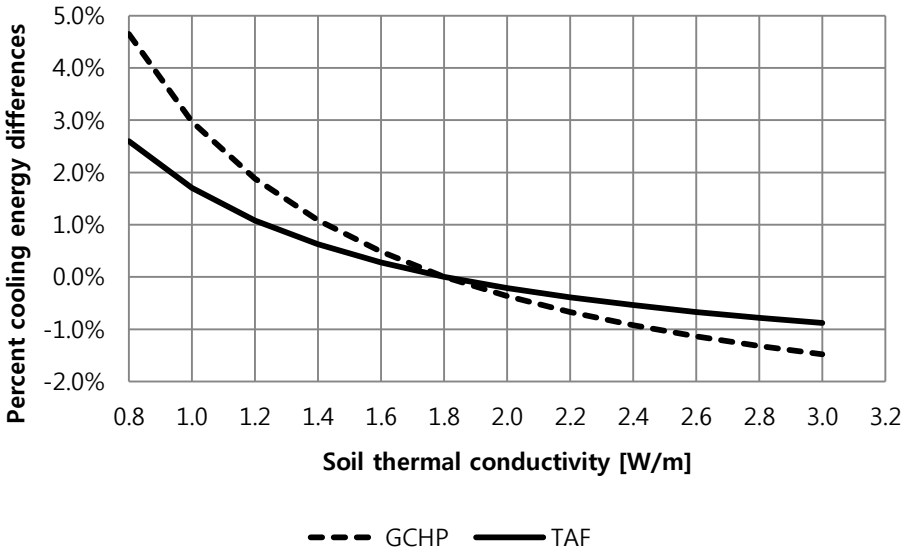

Figure 4-16: GSHP and TAF cooling energy consumption variations with soil thermal conductivity

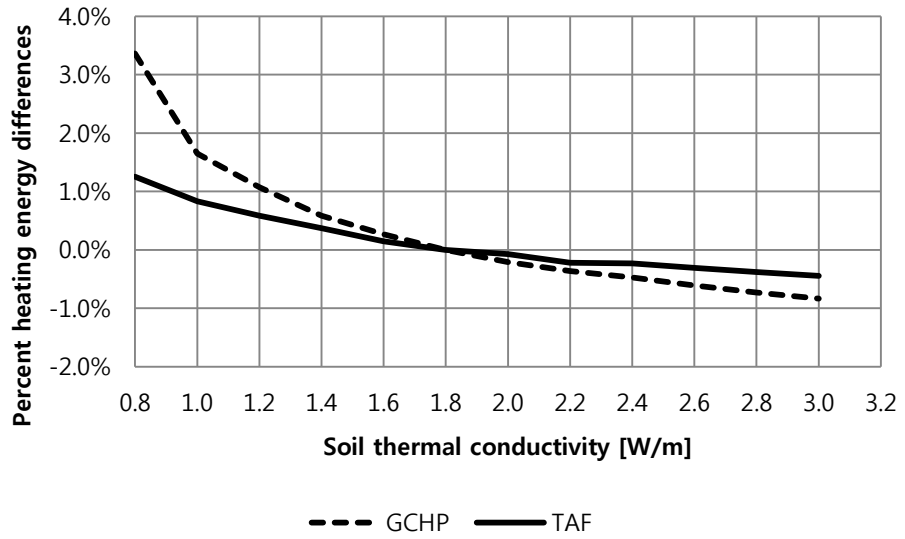

Figure 4-17: GSHP and TAF heating energy consumption variations with soil thermal conductivity

In the comparative analysis, the concrete (i.e., foundation) thermal conductivity is set to 1.8 W/m for all TAF cases. For soils with thermal conductivity lower than 1.8 W/^{o}C-m, the energy used by GSHP system are higher than that consumed by TAF due to lower thermal performance. For soils

with higher soil thermal conductivity, TAF consumes more energy than GSHP. Figure 4-18 shows the percent difference in both cooling and heating energy end-uses between the two systems.

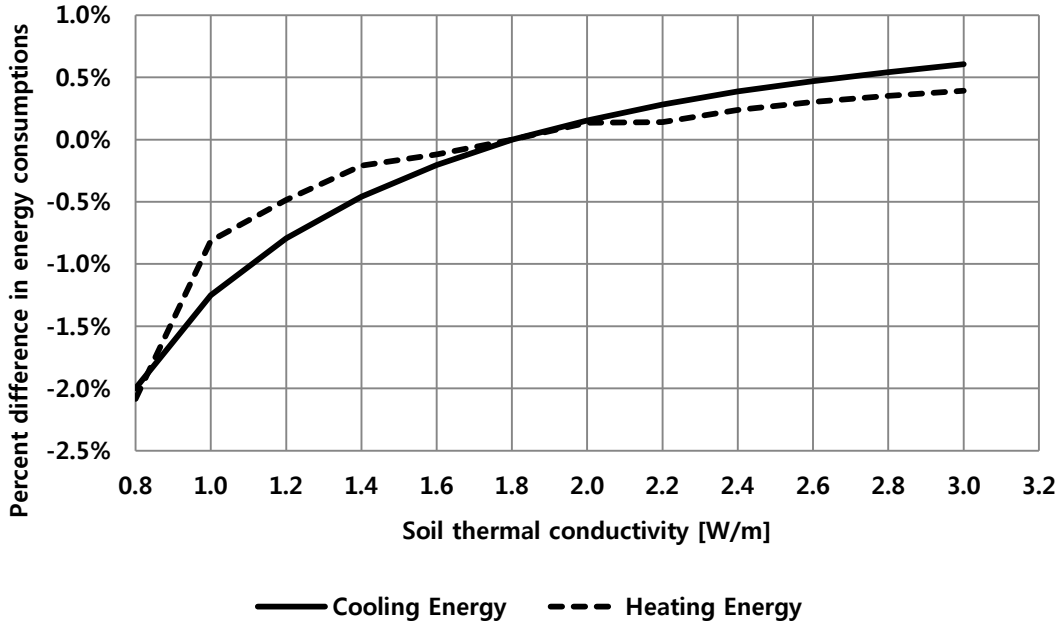

Figure 4-18: Comparison of cooling/heating energy use between GSHP and TAF systems

4.6. Summary

In this chapter, the thermal response factor for a thermo-active foundation model was developed using the g-function approach. In particular, a three-dimensional numerical model was defined with a constant heat flux to develop short-time step g-function. To validate the thermal response factor developed in this chapter, the new g-function for a thermo-active foundation model was compared with the existing g-function models established for GSHP systems. In the validation analysis, it is found that the new thermal response factor for a thermo-active foundation provide good match to the existing g-function values when the same input data are used.

Using the validated three-dimensional thermal response factor model for a thermo-active foundation, a series of sensitivity analyses is performed to investigate the impact of design and operating parameters on the g-function variation associated with thermo-active foundations. The parameters studied in this chapter include the foundation depth, the shank space, the thermal conductivities of both soil and foundation elements, and the working fluid flow rate within the heat exchanger loops. It is found that foundation depth affects most the g-function calculation. The shank space and the foundation thermal conductivity influenced the TAF g-functions associated with short-time steps. Lastly, the volumetric fluid flow rate is found to have no significant impact on TAF g-function variations..

CHAPTER 5. INTEGRATION OF THERMO-ACTIVE FOUNDATION MODELING IN ENERGYPLUS

5.1. Introduction

The thermal response factor (g-function) of a thermo-active foundation (TAF) is useful to model the thermal performance of TAF systems in detailed building energy simulation tools, such as EnergyPlus and DOE-2. As a first step, the average foundation wall temperature is estimated using Equation 5-1. Then, the average circulating fluid temperature is calculated from Equation 5-2. Finally, the average circulating fluid temperature is used to compute the outlet TAF fluid temperature. This outlet TAF temperature is the entering fluid temperature into a heat pump. Based on the efficiency of a heat pump system, climate conditions, and building thermal loads, the energy consumption of a building is computed using hourly or sub-hourly building energy simulation tools.

$$T_{foundation} = T_{ground} + \sum_{i=1}^{n} \frac{(Q_i - Q_{i-1})}{2pk} g\left(\frac{t_n - t_{i-1}}{t_s}, \frac{r_b}{H}\right) \quad \text{Equation 5-1}$$

$$T_{fluid} = T_{foundation} + R_{total} \times Q \quad \text{Equation 5-2}$$

where

t = Time

t_s = Time scale = $H^2/9\alpha$

H = Foundation depth

k = Ground thermal conductivity

$T_{foundation}$ = Average foundation wall temperature

T_{ground} = Undisturbed ground temperature

T_{fluid} = Average fluid temperature

Q = Step heat rejection/extraction pulse

r_b = Borehole radius

i = Index to denote the end of a time step

R_{total} = Total thermal resistance of a foundation

In this chapter, thermal response factor calculation approach for TAF systems are integrated into EnergyPlus to estimate the effectiveness of TAF systems in meeting heating and cooling loads for a typical office building in selected US locations. Furthermore, to evaluate the effect of design and operating parameters of TAF system performance, a series sensitivity analyses is carried out. The parameters considered include foundation pile depth, foundation pile radius, shank space, and concrete thermal conductivity. The analysis is performed using EnergyPlus tool to estimate the energy use for a prototypical office building located in selected US climates.

5.2. Building Model

A small office building is used for the simulation analysis carried out using EnergyPlus tool to assess the effectiveness of TAF systems. Most of the sensitivity analysis is performed using weather data for Chicago, IL using Typical Meteorological Years (TMY). Chicago climate is characterized by hot and humid during the summer season extending from July through September, and cold, snowy, and windy during the winter season. Figure 5-1 illustrates the monthly dry-bulb temperature for Chicago. In Figure 5-2, the floor plan of the office building is provided. The building has five zones, and the floor area is 463.6m^2 (4990ft^2).

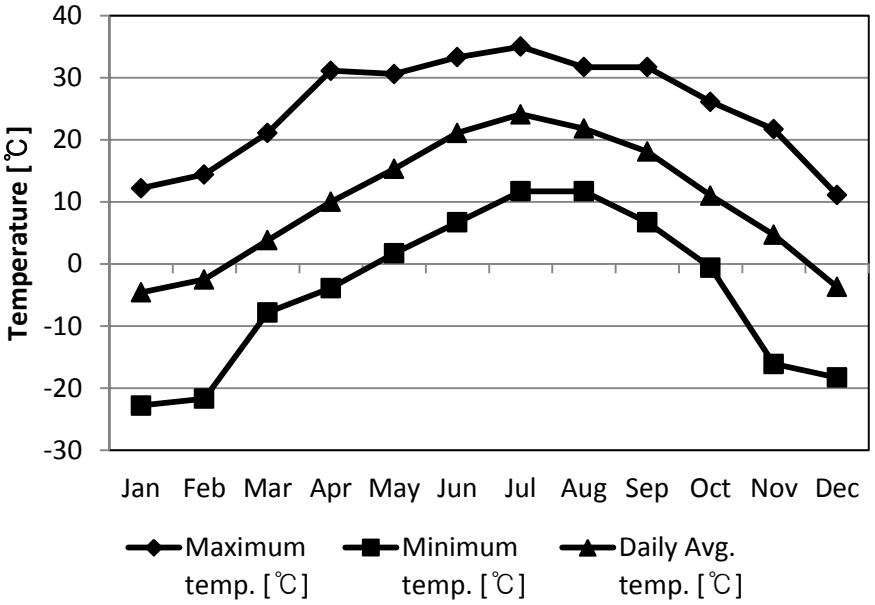

Figure 5-1: Monthly dry-bulb temperature for Chicago, IL (data from TMY3: Chicago, IL)

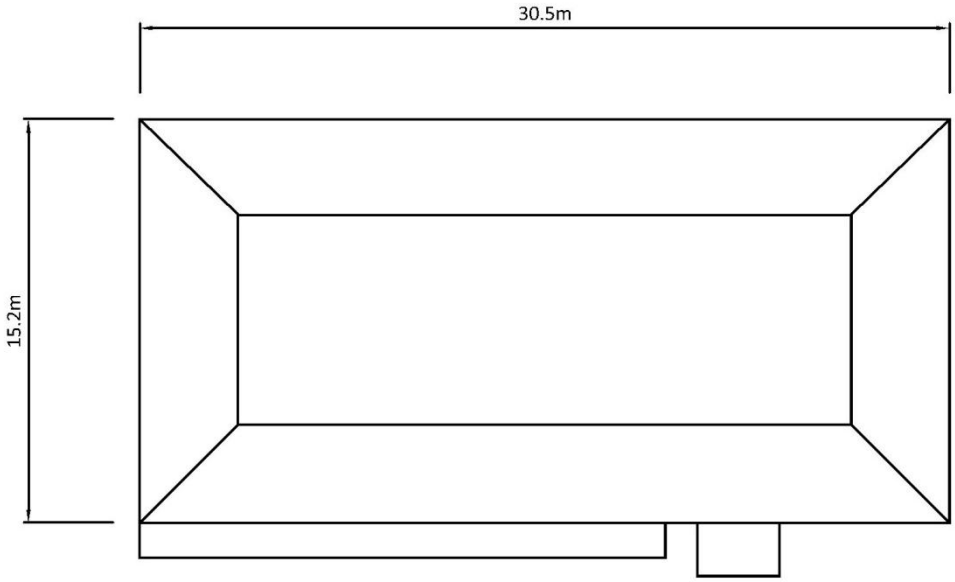

Figure 5-2: Floor plan of the office building modeled in EnergyPlus

The prototypical office building with its baseline system uses a standard VAV system, temperature based outside air economizer, hot water reheat coils served by a hot water boiler, and chilled water cooling coil served by an electric compression chiller with air cooled condenser.

Figure 5-3 and Figure 5-4 provide the monthly electricity and gas consumptions of the baseline building model (i.e., using the central chiller and boiler without geothermal heat pump system).

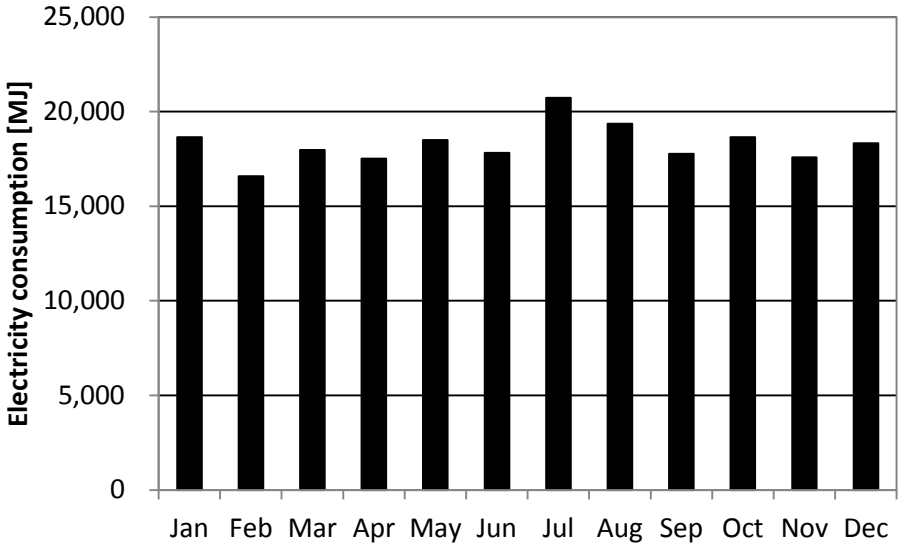

Figure 5-3: Monthly electricity consumption for the baseline building model [MJ]

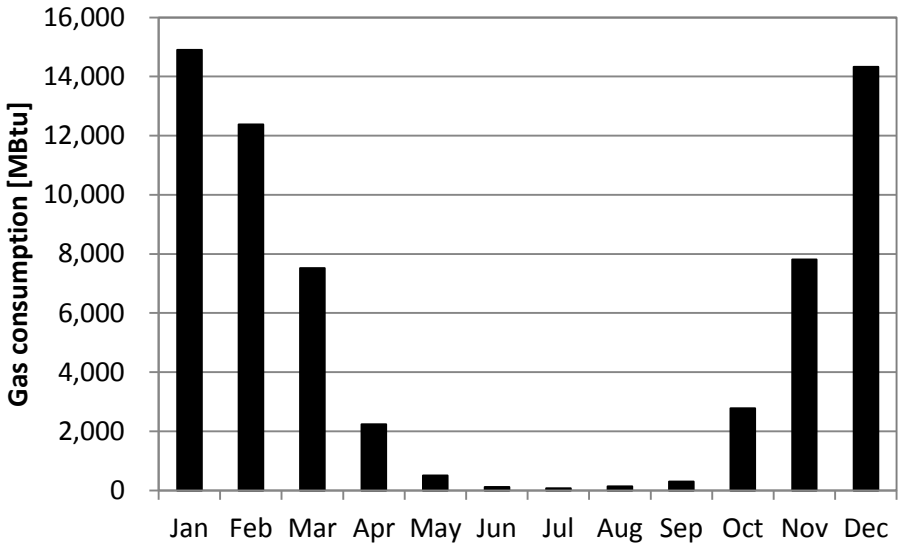

Figure 5-4: Monthly gas consumption for the baseline building model in [MBtu]

The assumptions for the sensitivity analyses using EnergyPlus simulation tool include:

- Each foundation has one U-tube heat exchanger loop

- There are no thermal interactions between TAF piles

- There are no thermal interactions between ground floor and TAF piles

- The total number of foundations for the prototypical office building is 12.

- The distances between foundation piles are 10.2m and 7.6m in x-axis and y-axis, respectively.

The input data for the thermo-active foundation are summarized in Table 5-1. Figure 5-5 illustrates the location of the 12 foundation piles along the building slab surface. Table 5-2 describes the specifications of the geothermal heat pump used in the simulation energy model.

Table 5-1: Model input data for the thermo-active foundation system used in EnergyPlus

Ground thermal diffusivity [m2/sec]	$9.41 * 10^{-7}$
Ground thermal conductivity [W/m·K]	1.60
Concrete thermal conductivity [W/m·K]	1.30
Pipe thermal conductivity [W/m·K]	0.36
Foundation depth [m]	20.0
Foundation radius [m]	0.20
Number of thermo-active foundation	12.0

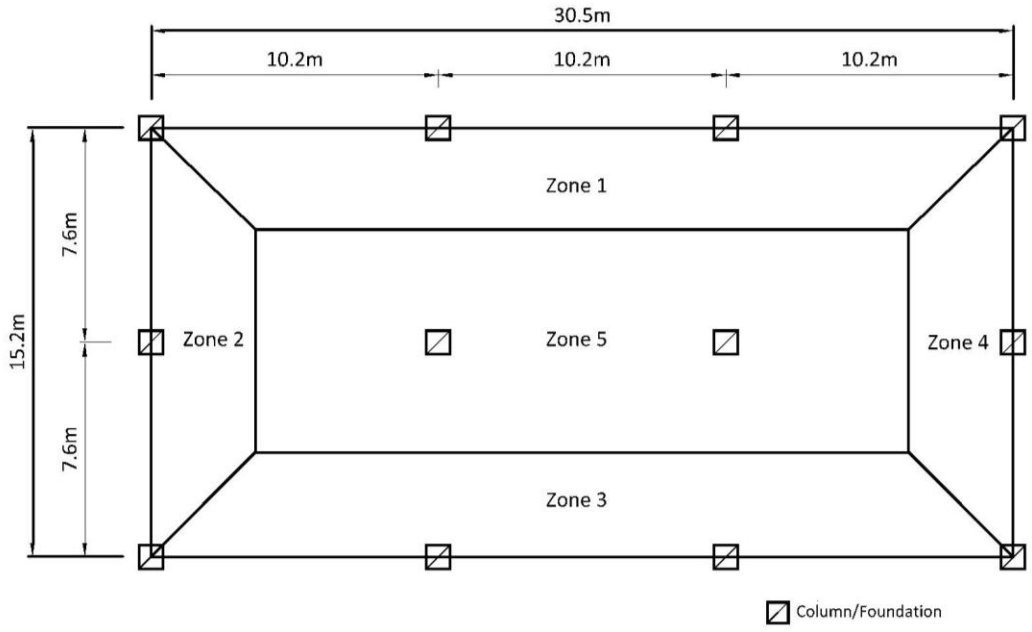

Figure 5-5: Location of foundation piles along the slab floor

Table 5-2: Geothermal heat pump specifications

Company	Model	Type	Cooling 77°F(25℃) Source 53.6°F(12℃) Load		Heating 32°F(0℃) Source 104°F(40℃) Load	
			Capacity Btu/h	EER Btu/h·W	Capacity Btu/h	COP
WaterFurnace. Inc.	ENVISION NSW 018	Water to Water	17,300	16.6	14,700	3.0

5.3. Impact of Foundation Depth and Shank Space

As found in Chapter 3, foundation depth and shank space are the most influential factors affecting the thermal performance of thermo-active foundations. Generally, deeper foundation piles provide more surface area to transfer heat between the ground and the heat exchanger pipes, and

thus are able to reject or extract more heat to or from the ground. In addition, when the distance between U-tube pipes are small, the inlet fluid temperature influences the outlet fluid temperature through the grout material as a heat transfer medium. Thus, it is preferable to have sufficient a distance between U-tube pipes to prevent or minimize the thermal interaction between the U-tube legs.

Table 5-3 lists the various combinations of foundation depths and shank spaces used in the simulation analysis to evaluate the effectiveness of TAF systems to meet the heating and cooling load of the prototypical office building located in Chicago, IL. The percent energy reduction is based on the configuration correspondent to 5m foundation depth and 0.14m shank space..

Table 5-3: Configurations of foundation depth and shank space used in the simulation analysis

Shank space (S)	0.14m	0.22m	0.3m	0.36m	**-**	**-**
Nomalized by diameter (D)	0.35	0.55	0.75	0.90	-	-
Depth (H)	5m	10m	20m	30m	40m	45m
Nomalized by 5m (H_0)	1	2	4	6	8	9

Figure 5-6 and Figure 5-7 present the results of the EnergyPlus simulation analysis in terms of percent energy use reduction associated with cooling and heating, respectively. The deeper the foundation pile, the more energy use reduction is achieved. In addition, as the distance between U-tube pipes becomes wider, the more energy used for heating and cooling is reduced. However, for deep foundations, the impact of shank space is not significant.

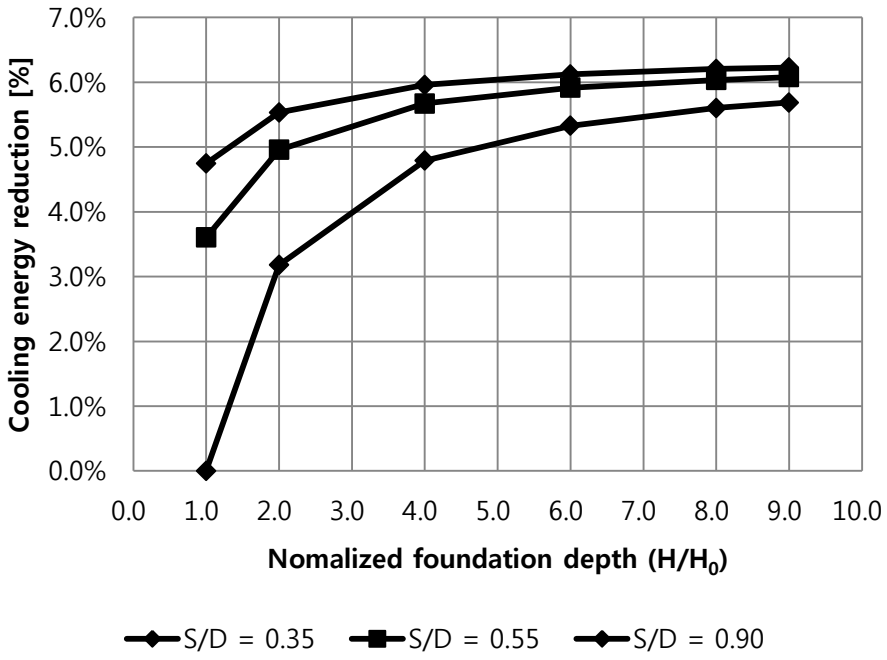

Figure 5-6: Percent cooling energy reduction for various combinations of shank spaces and foundation depths (reference values: Diameter, D = 0.4m, H_0 = 5m)

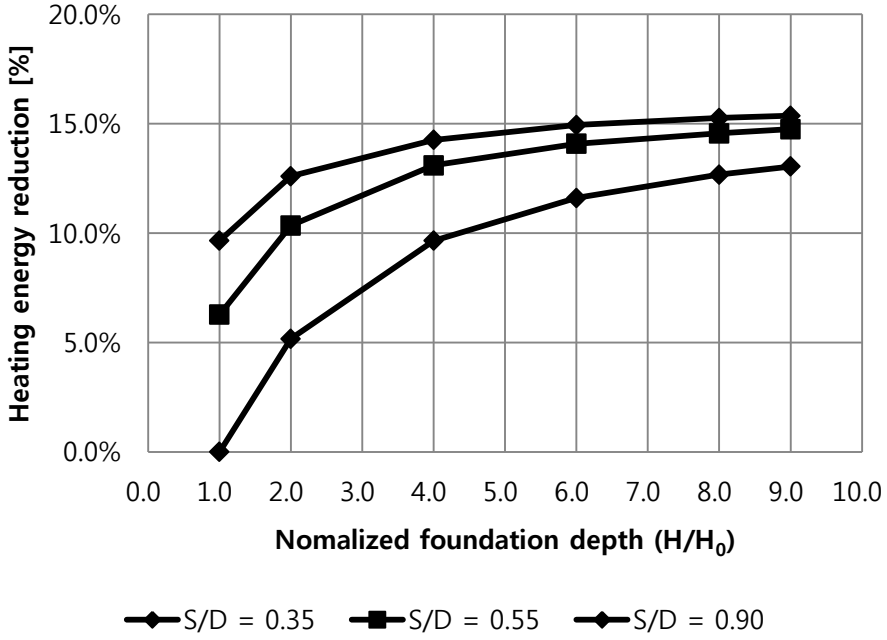

Figure 5-7: Percent heating energy reduction for various combinations of shank spaces and foundation depths (reference values: Diameter, D = 0.4m, H_0 = 5m)

5.4. Impact of Foundation Depth and Soil Thermal Conductivity

Soil thermal properties are important factors to be considered for accurate estimation of thermal performance of TAF systems. However, it is difficult to determine specific soil thermal properties due to several influential mechanisms such decomposition of soil materials, migration of moisture, phase change due to freezing and thawing cycles as illustrated in Figure 5-8 and Table 5-4 (ASHRAE Fundamental, 2009). As shown in Figure 5-8, the impact of moisture content can be accounted for using the concept of apparent soil thermal conductivity. Typically, soil thermal conductivity increases with moisture content.

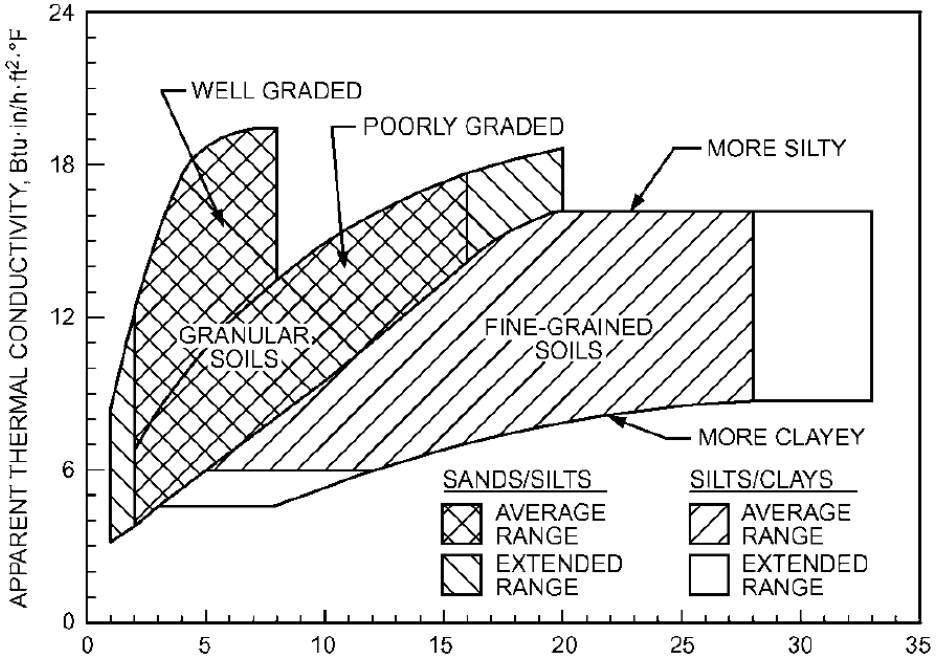

Figure 5-8: Apparent thermal conductivity for moist soils (Source: ASHRAE Fundamental, 2009)

Table 5-4: Typical soil thermal conductivity values (ASHRAE Fundamental, SI & IP, 2009)

Soil types	Normal range [W/(m·K)]	Recommended values	Normal range [Btu·in/h·ft²·F]	Recommended values

		[W/(m·K)]			[Btu·in/h·ft²·F]	
		Low	**High**		**Low**	**High**
Sands	0.6 to 2.5	0.78	2.25	4.2 to 17.4	5.4	15.6
Silts	0.9 to 2.5	1.64	2.25	6 to 17.4	11.4	15.6
Clays	0.9 to 1.6	1.12	1.56	6 to 11.4	7.8	10.8
Loams	0.9 to 2.5	0.95	2.25	6 to 17.4	6.6	15.6

Table 5-5 summarizes the specifications of various combinations of soil thermal conductivities and foundation depths used in the simulation energy analysis. The simulation results are expressed in terms of percent energy use reduction based on the case of 10m depth and 0.4W/m soil thermal conductivity.

Table 5-5: Combinations of soil thermal conductivities and foundation depths

Soil conductivity	0.4W/m	0.8W/m	1.2W/m	1.6W/m	2.0W/m	2.4W/m
Nomalized by 0.4W/m	1	2	3	4	5	6
Depth (H)	10m	20m	40m	-	-	-
Nomalized by 10m (H_0)	1	2	4	-	-	-

Figure 5-9 and Figure 5-10 provides the results of the EnergyPlus simulation analysis. Compared to the impact of foundation depths, soil thermal conductivity has less effect on energy use reduction for both heating and cooling of the prototypical office building. This impact decreases as the foundation depth increases. As illustrated in Figure 5-9 and Figure 5-10, high soil thermal conductivity result in more significant energy use reductions for both cooling and heating end-uses.

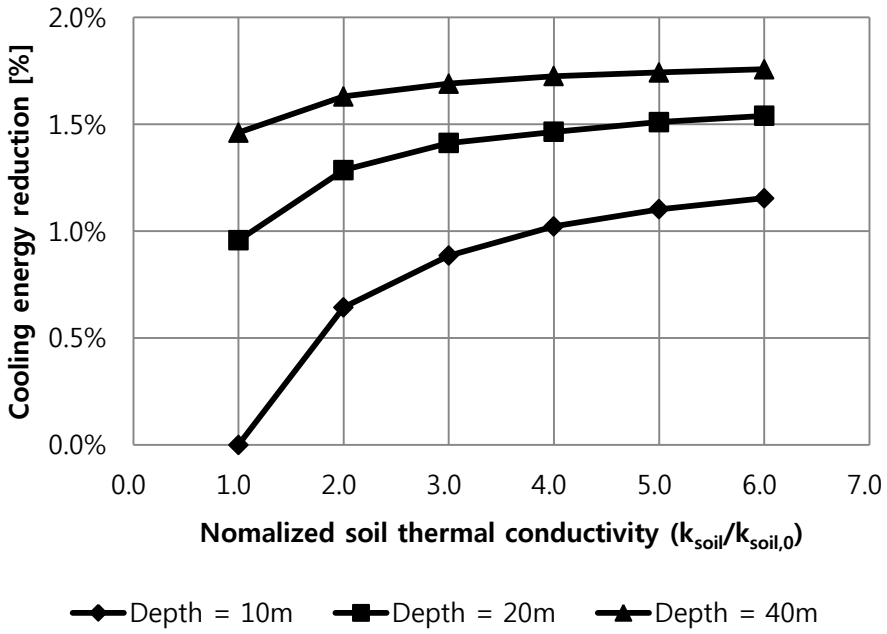

Figure 5-9: Percent cooling energy use reduction for various combinations of soil thermal conductivity and foundation depths (reference values: Ho= 10 m and $k_{soil,0}$ = 0.4W/m·K)

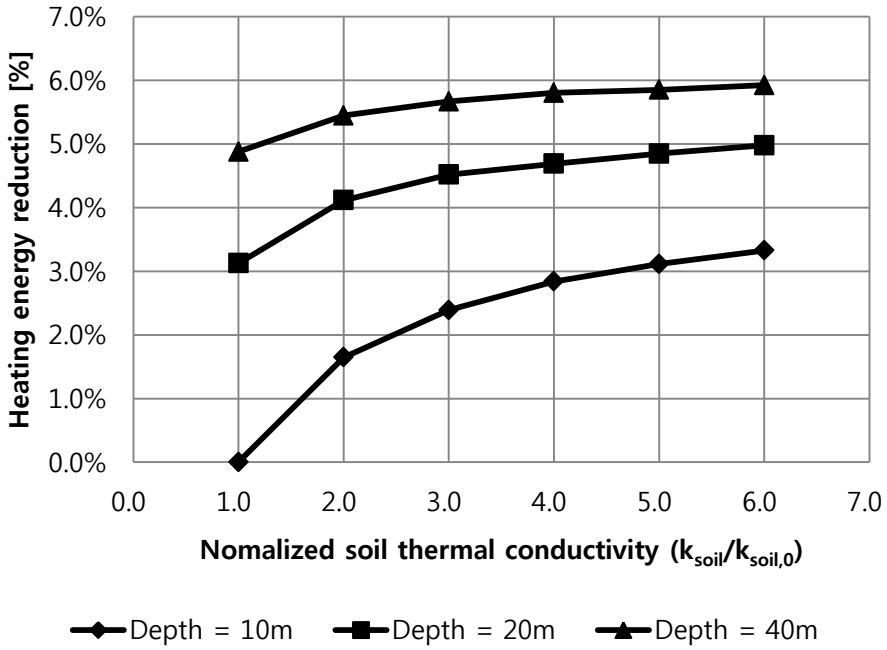

Figure 5-10: Percent heating energy use reduction for various combinations of soil thermal conductivity and foundation depths (reference values: Ho= 10 m and $k_{soil,0}$ = 0.4W/m·K)

5.5. Foundation Depth and Concrete Thermal Conductivity

Table 5-6 summarizes the combinations of values for both concrete thermal conductivity and different foundation depth considered in the sensitivity analysis to assess their impact on heating and cooling energy end-uses.

Table 5-6: Combinations of concrete thermal conductivities and foundation depths

Concrete conductivity (k_{conc})	**0.3W/^{o}C-m**	**0.8W/^{o}C-m**	**1.3W/^{o}C-m**	**1.65W/^{o}C-m**	**2.0W/^{o}C-m**
Nomalized by 0.3W/m ($k_{conc,0}$)	1	2.7	4.3	5.5	6.7
Depth (H)	10 m	20 m	40 m	-	-
Nomalized by 10m (H_0)	1	2	4	-	-

Figure 5-11 and Figure 5-12 illustrate the results of the EnergyPlus simulation analysis for concrete thermal conductivity and foundation depths. The results indicate that higher concrete thermal conductivity leads to reduced energy use. In addition, the deeper foundation results in higher energy reductions for all concrete thermal conductivity values. Moreover, the impact of concrete thermal conductivity decreases as the foundation depth increases.

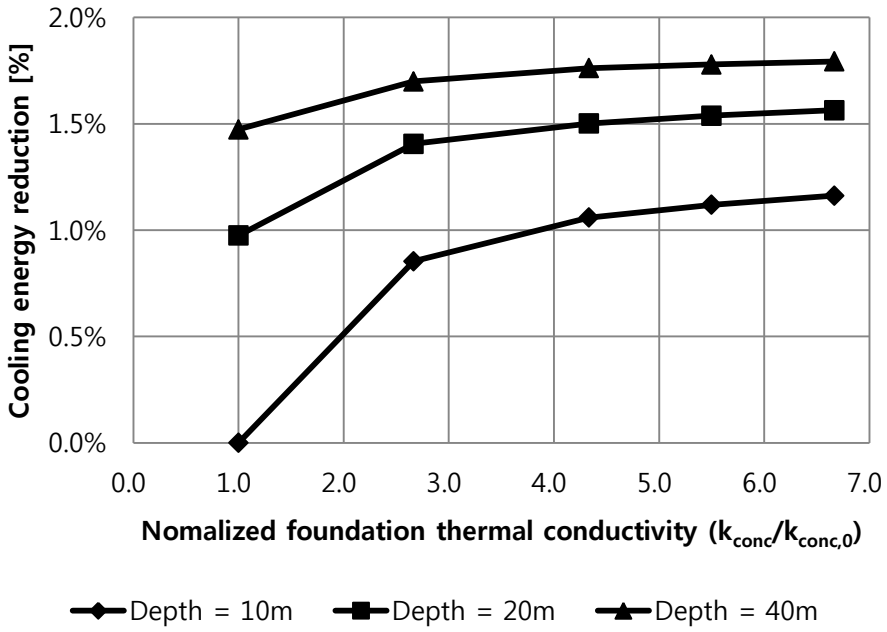

Figure 5-11: Percent cooling energy use reduction for various combinations of foundation thermal conductivity and foundation depth (reference values: Ho= 10 m and $k_{conc,0}$ = 0.3W/m·K)

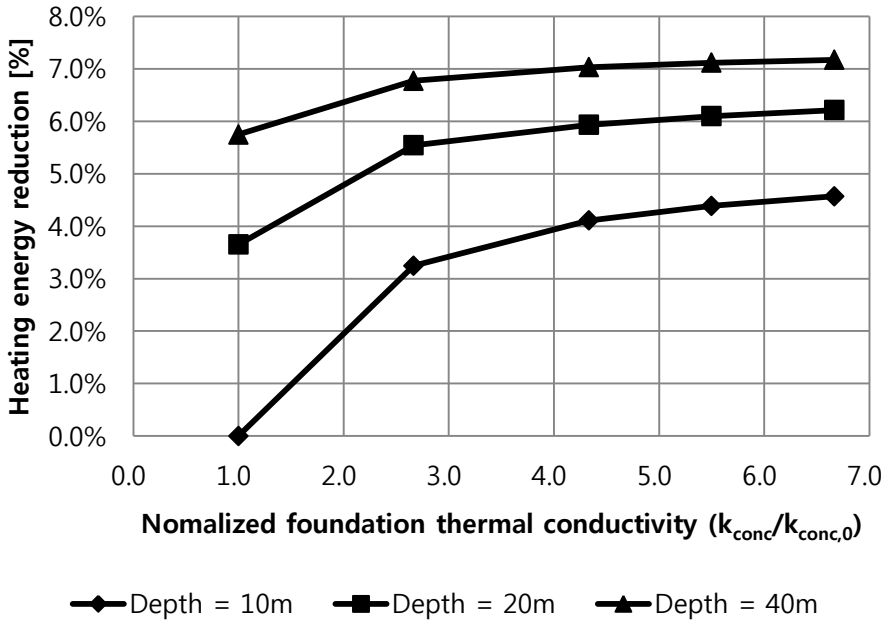

Figure 5-12: Percent heating energy use reduction for various combinations of foundation thermal conductivity and foundation depth (reference values: Ho= 10 m and kconc,0 = 0.3W/m·K)

5.6. Fluid Flow Rate

As discussed in Chapter 3, fluid flow rate affects convective coefficients, and thus the performance of thermo-active foundation systems. Table 5-7 provides the fluid rates as well as foundation depths considered in the simulation analysis. The results are expressed in percent energy use reduction for both heating and cooling using the case with a foundation depth of 10 m and a volume flow rate of 1.75E-5 m3/s.

Table 5-7: Combinations of fluid flow rates and foundation depths

Volume flow rate [m3/s] (V)	1.75E-5	3.50E-5	7.00E-5	1.05E-4	1.75E-4
Nomalized by 1.75E-5 m3/s (V_0)	1	2	4	6	10
Flow type	Laminar	Turbulent	Turbulent	Turbulent	Turbulent
Depth (H)	10m	20m	40m	-	-
Nomalized by 10m (H_0)	1	2	4	-	-

Figure 5-13 and Figure 5-14 illustrates the results of the EnergyPlus simulation analysis for various combinations of fluid flow rates and foundation depths. The simulation results clearly show that higher volumetric flow rate reduces energy end-uses for both cooling and heating regardless of the foundation depth. However, as the flow rate increases, the rate of energy use reduction decreases. This result is due to the fact that heat transferred between the fluid and the foundation/ground medium decreases as the flow rate increases, even though the convective coefficient is higher. Thus, it can be concluded that a proper flow rate should be selected to optimize the energy performance of the thermo-active foundation while minimizing pump energy use.

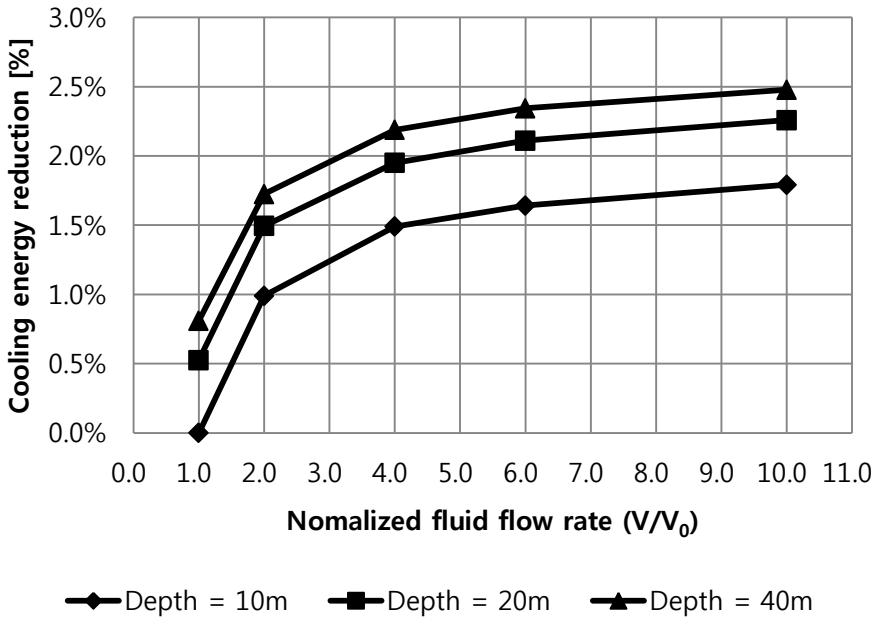

Figure 5-13: Percent cooling energy use reduction for various combinations of volumetric flow rate and foundation depths (reference values: Ho = 10 m and V_0 = 1.75E-5 m^3/sec)

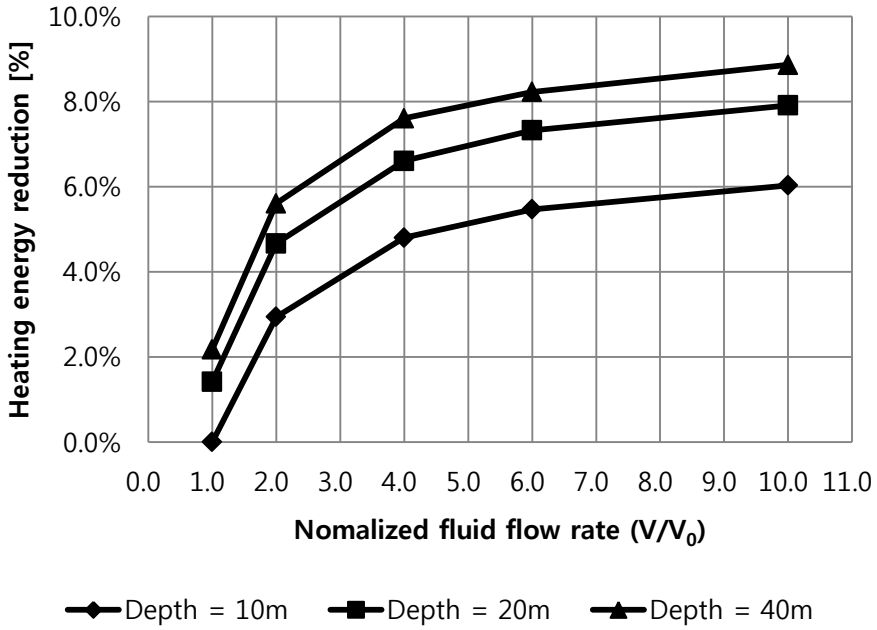

Figure 5-14: Percent heating energy use reduction for various combinations of volumetric flow rate and foundation depths (reference values: Ho = 10 m and V_0 = 1.75E-5 m^3/sec)

5.7. Summary

In this chapter, the thermal response factors developed in Chapter 4 are integrated within EnergyPlus to perform a series of sensitivity analyses to assess the energy use impact of a thermo-active foundation system to heat and cool a prototypical office building located in Chicago, IL. Specifically, the impact of design and operating parameters is evaluated including foundation depth, shank space, soil thermal conductivity, concrete thermal conductivity, and volumetric flow rate of the fluid circulating in the heat exchanger loops.

The results from the energy simulation analyses indicate that: Deeper foundation depth increases heat transfer surfaces, and lead to reduced energy end-uses for both cooling and heating.

- Increasing the distance between U-tube legs reduces thermal interactions between pipes and improves the efficiency of TAF systems.

- Soils with high thermal conductivity enhances heat transfer rate which results in higher energy use reduction for heating and cooling. Concrete with higher thermal conductivity increases exchanged heat transfer and reduce heating and cooling energy end-uses.
- Higher volumetric fluid flow rate can increase ground-coupled heat transfer. However, the effectiveness of high fluid flow rates is reduced after a threshold value. An optimal value for fluid flow rate needs to be considered to minimize pumping energy use while optimizing TAF system performance.

In summary, the thermal response factors of a thermo-active foundation developed in this thesis can be integrated seamlessly in any detailed building energy simulation program. The

simulation analysis can then be used to optimize the design and operation of TAF systems. Some design guidelines for TAF systems are presented in the following chapters.

CHAPTER 6. DESIGN GUIDELINES FOR THERMO-ACTIVE FOUNDATIONS

6.1. Background

Geothermal energy is considered as an attractive renewable energy source especially for cooling and heating buildings. Indeed, earth is typically cooler than ambient air during cooling season, and is warmer than ambient air during heating season in most US climates. There have been several studies to assess the thermal performance of ground-source heat pump systems (GSHP), and to develop design strategies for these systems to meet building thermal loads. One of the common problems with GSHP systems is under-sized ground heat exchanger loop. Indeed, Shonder et al. (1998, 2002) reported that the ground loop capacity is the most important factor that determines the outlet loop fluid temperature which is the entering temperature to the heat pump. In their study, they found that the recommended maximum outlet fluid temperature for cooling-dominated climates was 95°F(35℃). When the outlet temperature is above this recommended threshold, the efficiency of the heat pump began to decrease substantially. For heating dominated climates or seasons, it was also observed that the efficiency of the heat pump decreases when the outlet fluid temperature is below 30°F (-1.0℃). Chiasson and Yavuzturk (2009) discussed the possible problems related to improper sizing of heat exchanger loops for GSHP systems. In particular, they indicated that when ground-coupled heat exchanger loop size is undersized, the fluid outlet temperatures are affected by the imbalances in the thermal load. For heating-dominated regions the fluid outlet temperature progressively drops to the freezing point. For cooling-dominated regions, the fluid outlet temperatures can increase significantly. Moreover, Kavanaugh (2010) noted that short ground loops can cause lower efficiencies of the heat pump systems.

Under-sizing of ground-coupled heat exchanger loops can lead to more severe problems for a thermo-active foundation system that those for GSHPs. Indeed, thermo-active foundation systems have additional design constraints due to the structural considerations associated to the building foundations. These constraints include foundation pile depth, foundation radius, and total number of foundation piles. In this chapter, the thermal response factors integrated within detailed building energy simulation tool are used to develop design guidelines for thermo-active foundation systems. In particular, the proper number of foundation piles suitable for a specific heat pump type and capacity is determined for select US climate zones. Furthermore, the impact of building foundation design on selecting the heat pump capacity is also investigated in the analysis carried out in this chapter.

6.2. Description of the Case Model Simulated in EnergyPlus

A prototypical office building is considered to perform the required analysis to develop design guidelines for TAF systems. The building has one-story with five thermal zones as shown in 1. The building floor area is 463.6m^2 (4990ft^2). The number of foundation piles is assumed to be 12 based on structural analysis as illustrated in Figure 6-2.

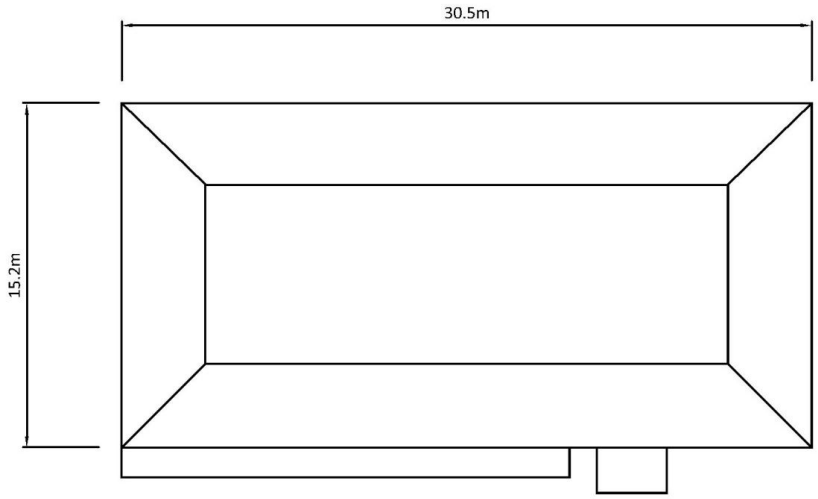

Figure 6-1: Floor plan of the five-zone office building

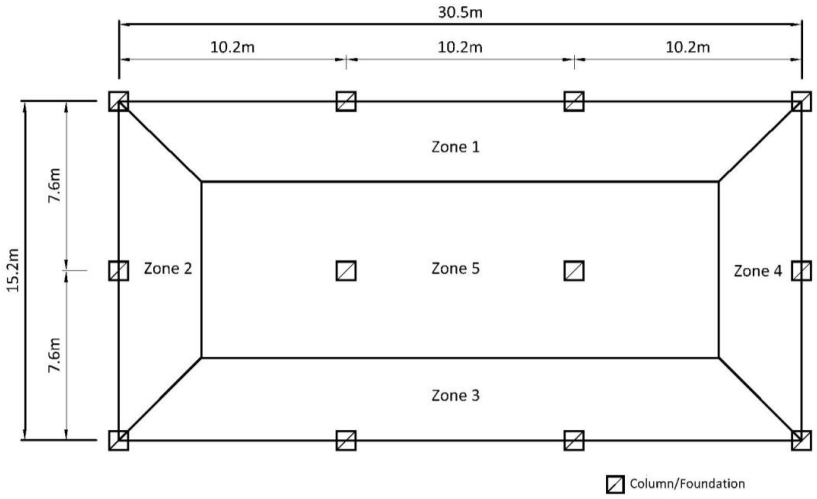

Figure 6-2: Floor plan and location of foundation piles

In EnergyPlus, a thermo-active foundation system is modeled with an auxiliary heating/cooling system. A schematic HVAC system as modeled in EnergyPlus is illustrated in Figure 6-3. The overall system information for the prototypical office building is described as:

- Standard VAV system
- Temperature based outside air economizer

- Hot water reheat coils with a hot water boiler
- Chilled water cooling coil with an electric compression chiller and an air cooled condenser
- Water-to-water geothermal heat pump system

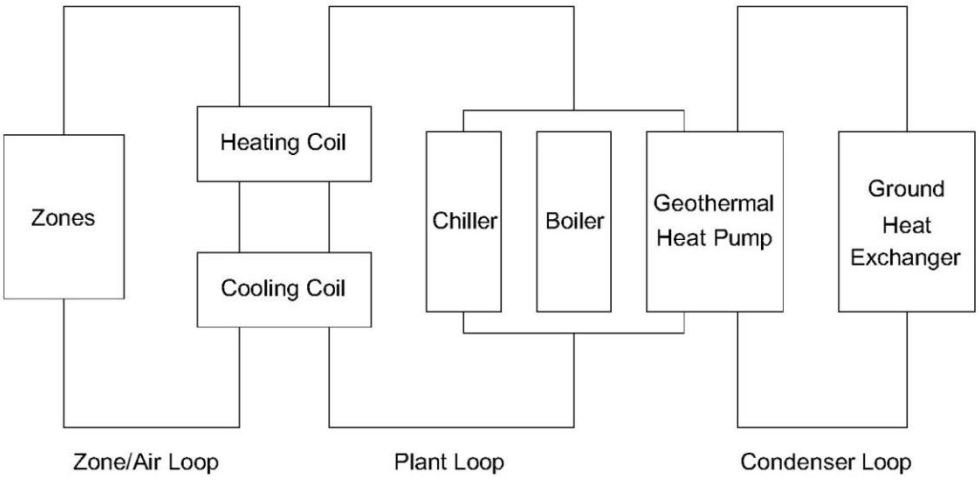

Figure 6-3: Schematic HVAC system with ground heat exchangers and a geothermal heat pump as modeled in EnergyPlus

In this chapter, several parametric analyses are performed to investigate the impact of climate conditions and building foundation features on the proper design of TAF systems. For this analysis, some assumptions are employed including:

- In one foundation pile, only one U-tube heat exchanger is installed,

- There are no thermal interactions between adjacent foundation piles.

- The total number of foundation piles for the building is set to be 12 based on structural loading

- The distances between two foundation piles are 10.2m and 7.6m in x-axis and y-axis, respectively as shown in Figure 6.2.

The input data used to model TAF systems in EnergyPlus are provided in Table 6-1. Table 6-2 lists the specifications of the geothermal heat pump used in the building energy simulation analysis.

Table 6-1: The input data used for modeling TAF system in EnergyPlus

Ground thermal diffusivity [m²/sec]	9.41 X 10^{-7}
Ground thermal conductivity [W/m·K]	1.60
Concrete thermal conductivity [W/m·K]	1.30
Pipe thermal conductivity [W/m·K]	0.36
Foundation depth [m]	20.0
Foundation radius [m]	0.20
Number of thermo-active foundation	12.0

Table 6-2: Specifications of geothermal heat pump system

Company	**Model**	**Type**	**Cooling 77˚F(25˚C) Source 53.6˚F(12˚C) Load**		**Heating 32˚F(0˚C) Source 104˚F(40˚C) Load**	
			Capacity Btu/h	EER Btu/h·W	Capacity Btu/h	COP
WaterFurnace. Inc.	ENVISION NSW 018	Water to Water	17,300	16.6	14,700	3.0

6.3. Description of the Climate Conditions

In this chapter, six sites are considered in the simulation analysis to cover six different US climate zones. The sites and associated ASHRAE climate zones are described in Table 6-3 and

Figure 6-4. In the simulation analysis performed with EnergyPlus, the same soil thermal properties are assumed for all sites. However, the site-specific variations of the ground temperatures are considered for both developing the thermal response factors and performing the energy simulation using EnergyPlus for each climate zone.

For all climate zones, weather data in the form of Typical Meteorological Years (TMY) format is utilized. For each site, specific heating and cooling schedules specific to each site are developed based outdoor air temperature variations.

Table 6-3: Summary of US sites and associated ASHRAE climate zones used in the energy analysis (ASHRAE Standard 90.1-2004)

Region	ASHRAE Climate zone	Outdoor air temperature		Climate conditions	Annual average ground temperature (T_{ground})*
		Summer	Winter		
Cheyenne, WY	Zone 6B	19.0℃	-0.8℃	Cold / Dry	7℃ (44.6°F)
Chicago, IL	Zone 5A	22.0℃	-0.4℃	Cool / Humid	10℃ (50.0°F)
Denver, CO	Zone 5B	22.3℃	2.5℃	Cool / Dry	10℃ (50.0°F)
New York, NY	Zone 4A	22.5℃	3.2℃	Mixed / Humid	12℃ (53.6°F)
Phoenix, AZ	Zone 3B	29.4℃	14.3℃	Warm / Dry	23℃ (73.4°F)
Tampa, FL	Zone 2A	24.8℃	15.3℃	Hot / Humid	22℃ (71.6°F)

*The reference of the annual average ground temperature is TMY3 data.

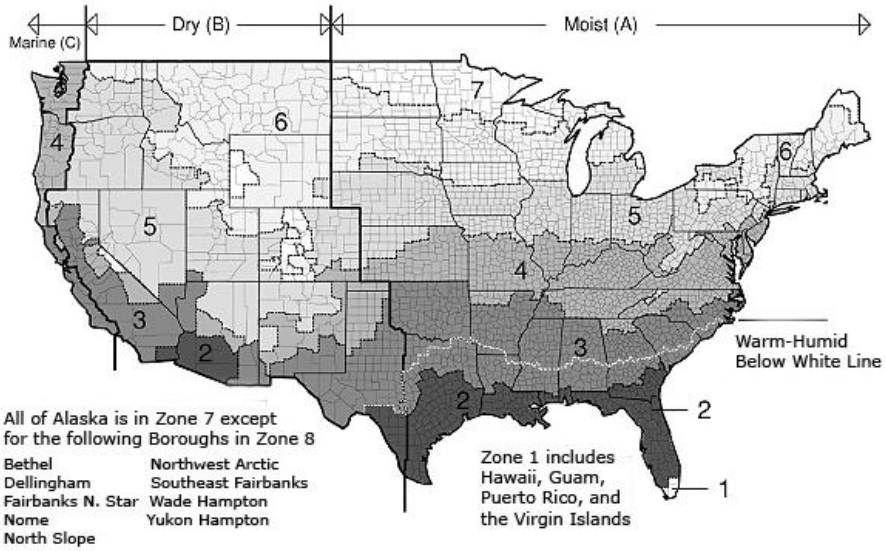

Figure 6-4: US ASHRAE Climate zones (ASHRAE Standard 90-1-2004)

6.4. Design Criteria of Number of Thermo-Active Foundations

In order to determine the proper design specifications for TAF systems, consistent design criteria are established for all the climate zones. For TAF systems, the design criteria are based on fluid outlet temperatures (which are also the entering fluid temperatures to the heat pump systems). After reviewing several references and manufacturers' product information for heat pumps used in this chapter, it is found that the maximum recommended exiting water temperature (EWT) range is 25℃ to 35℃, and the minimum EWT is around 0℃ (Shonder et al. 1998, 2002, WaterFurnace, 2012).

It should be noted that the working fluid circulating in the ground loops is assumed to be water, which is freezes at 0℃. Thus, the acceptable minimum EWT should be above the freezing point. In summary, the main design criteria include a maximum acceptable EWT is 30℃, and the minimum recommended value for EWT is 2℃.

6.5. Number of Thermo-active Foundation Piles

6.5.1. Models of TAF systems for Different Climate Zones

Utilizing the three-dimensional numerical model developed in Chapter 4, the thermal response factors were created for the different climate conditions. And the interesting results were observed that the thermal response factors were the same for all cases (Figure 6-5). This result might be caused by that soil thermal properties were the same for all cases, and only undisturbed ground temperatures were different for different climate conditions. And it resulted in that the foundation wall temperature and the fluid temperature were changed proportionally to the undisturbed ground temperature changes when the other boundary conditions were not changed.

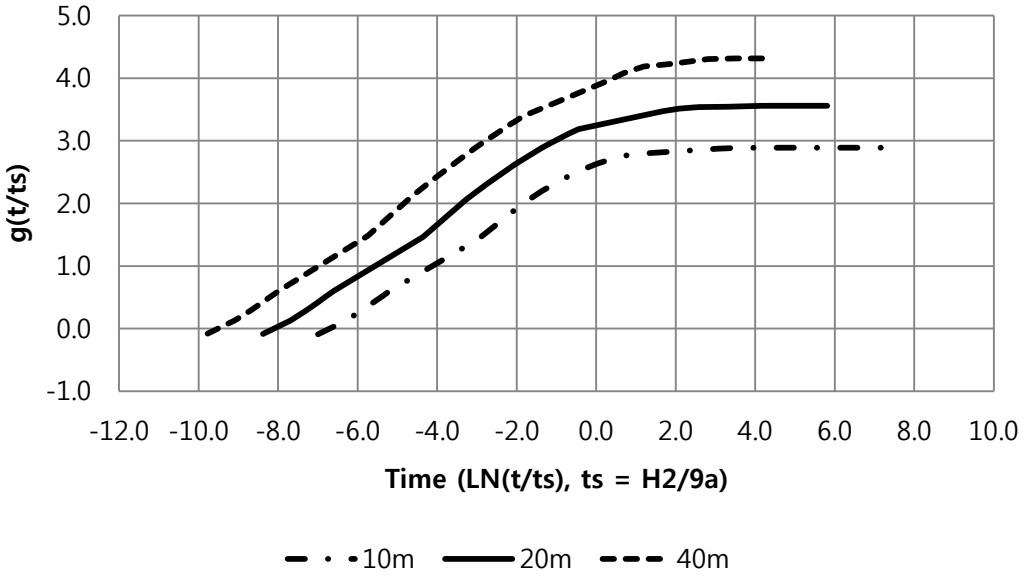

Figure 6-5: Thermal response factor (g-function) variations for various foundation depths

6.5.2. Number of Thermo-Active Foundations for Cheyenne, Wyoming

Cheyenne, WY is characterized by cold and dry climate with an average summer temperature of 20℃.Figure 6-6, Figure 6-7 and Table 6-4 illustrate the results of the simulation

analysis to estimate the number of foundation piles and the exiting water temperatures for various foundation depths for both heating and cooling modes. The results shown in Figure 6-6 and Figure 6-7, shorter foundations need longer ground heat exchangers to achieve the desired exiting water temperature (EWT) to be below or equal to the design temperature (30℃)during the cooling mode, and to remain above the design temperature (2℃) during the heating mode.

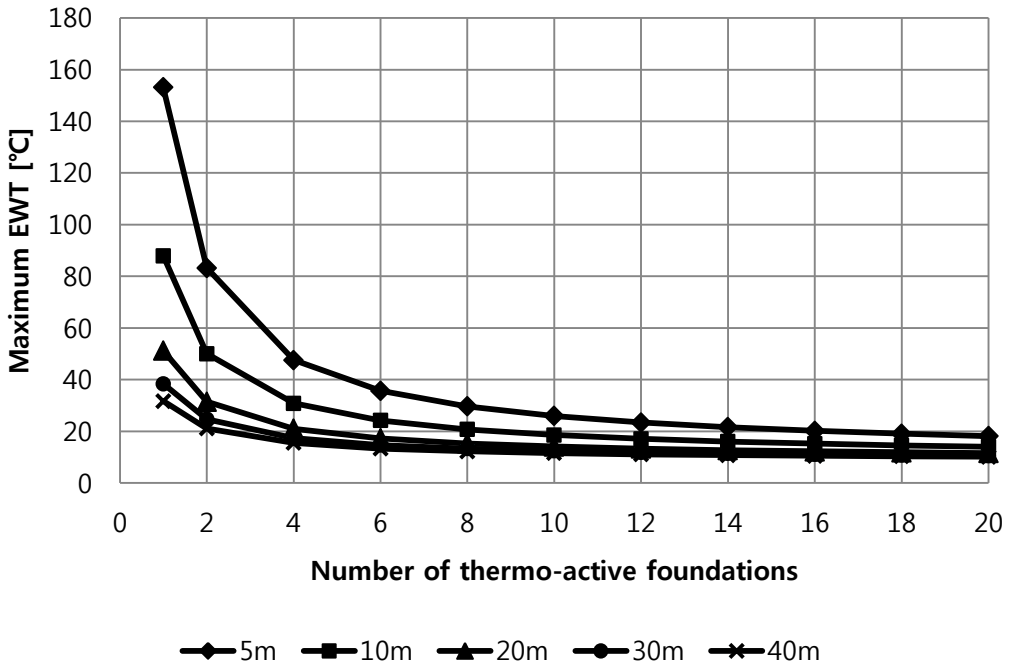

Figure 6-6: Maximum exiting water temperature variation for select foundation depths during cooling mode, Cheyenne, WY.

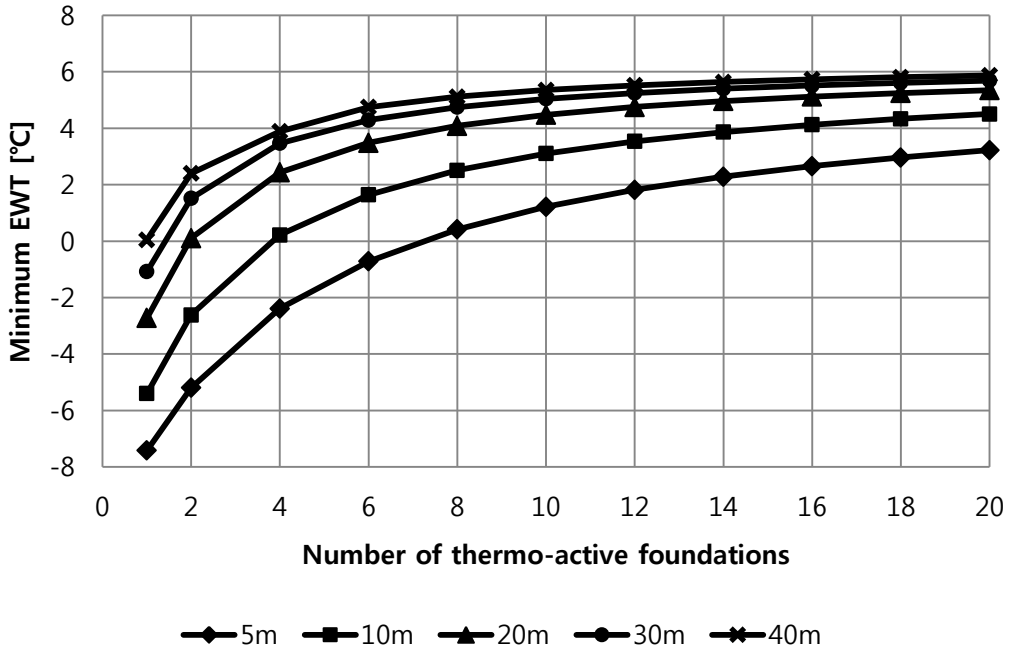

Figure 6-7: Minimum exiting water temperature variation for select foundation depths during heating mode, Cheyenne, WY.

Table 6-4 compares the minimum number of thermo-active foundation piles provided in order to achieve reasonable efficiency of heat pump during both cooling mode and heating mode. As shown in Table 6-4 and since Cheyenne has a heating-dominated climate, the minimum number of thermo-active foundation piles is found to be selected based on the heating mode in which the minimum EWT is considered.

Table 6-4: The minimum number, N, of thermo-active foundation piles for Cheyenne, WY (T_{ground} = 7℃)

	Foundation Depths				
	5m	**10m**	**20m**	**30m**	**40m**
Cooling mode EWT ≤ 30℃	N ≥ 8	N ≥ 5	N ≥ 3	N ≥ 2	N ≥ 2
Heating mode EWT ≥ 2℃	N ≥ 13	N ≥ 7	N ≥ 4	N ≥ 3	N ≥ 2

6.5.3. Number of Thermo-Active Foundations for Chicago, Illinois

Chicago, the largest city in Illinois, is located near Lake Michigan and has a humid continental climate. Typically, Chicago is hot and humid during the summer, and cold, snowy, and windy during the winter. During the winter season, outdoor air temperature is often below freezing level. Spring and fall seasons are generally moderate with low humidity.

Figure 6-8 and Figure 6-9 show the required number of thermo-active foundation piles for various foundation depths. Similar to the results found for Cheyenne, WY., short foundation depths require higher number of piles to obtain reasonable exiting fluid temperature for Chicago, IL.

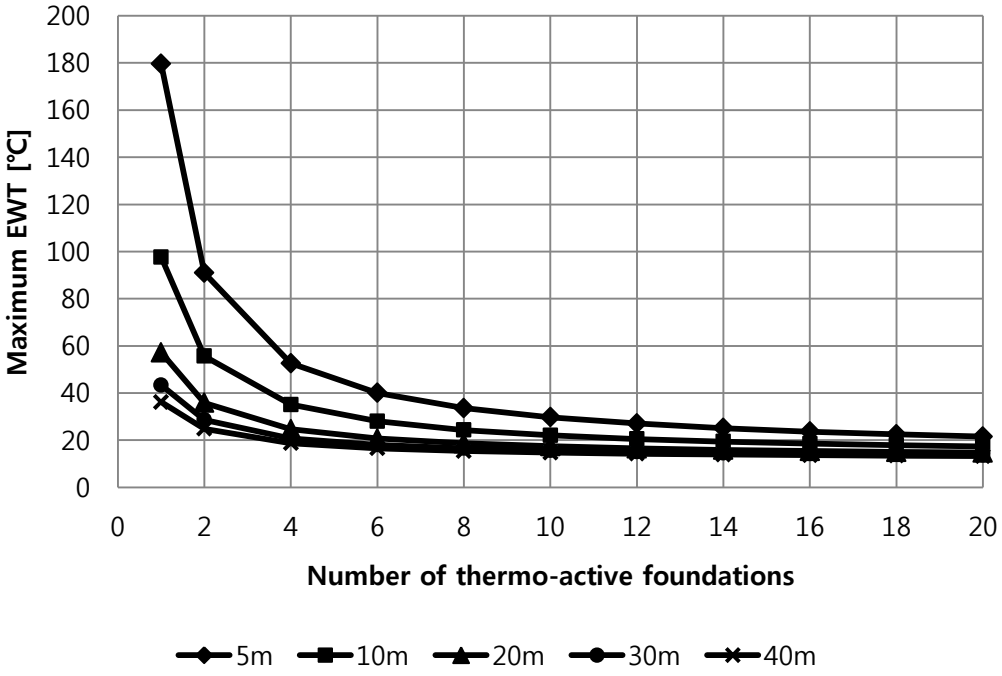

Figure 6-8: Maximum exiting water temperature variation for select foundation depths during cooling mode, Chicago, IL.

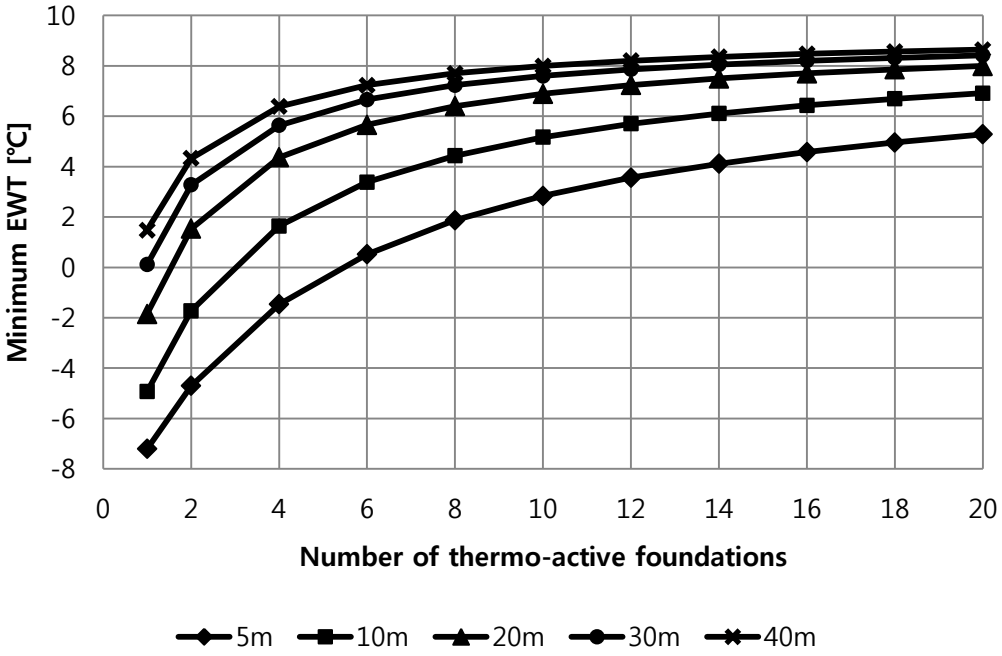

Figure 6-9: Minimum exiting water temperature variation for select foundation depths during heating mode, Chicago, IL.

In Table 6-5, the minimum number of thermo-active foundation piles is provided to achieve reasonable efficiency of heat pump for both cooling mode and heating mode. As shown in Table 6-5, the number of foundation piles required for cooling mode is higher than that needed for heating mode.

Table 6-5: Minimum number, N, of thermo-active foundation piles for Chicago, IL(T_{ground} = 10℃)

	Foundation Depths				
	5m	**10m**	**20m**	**30m**	**40m**
Cooling mode EWT ≤ 30℃	N ≥ 10	N ≥ 6	N ≥ 3	N ≥ 2	N ≥ 2
Heating mode EWT ≥ 2℃	N ≥ 8	N ≥ 5	N ≥ 3	N ≥ 2	N ≥ 2

6.5.4. Number of Thermo-Active Foundations for Denver, Colorado

Denver has a continental climate with cool and snowy winters, and mild to hot and dry summers. The average summer temperature is 22℃, and the average winter temperature is 2.5℃. The annual average ground temperature is 10℃ (i.e., same as Chicago, IL). Figure 6-10 and Figure 6-11 outline the variations of both maximum and minimum EWTs as functions of the number of thermo-active foundation piles and foundation depths. The results obtained for Denver are similar to those found for Chicago in terms of the required number of thermo-active foundation piles.

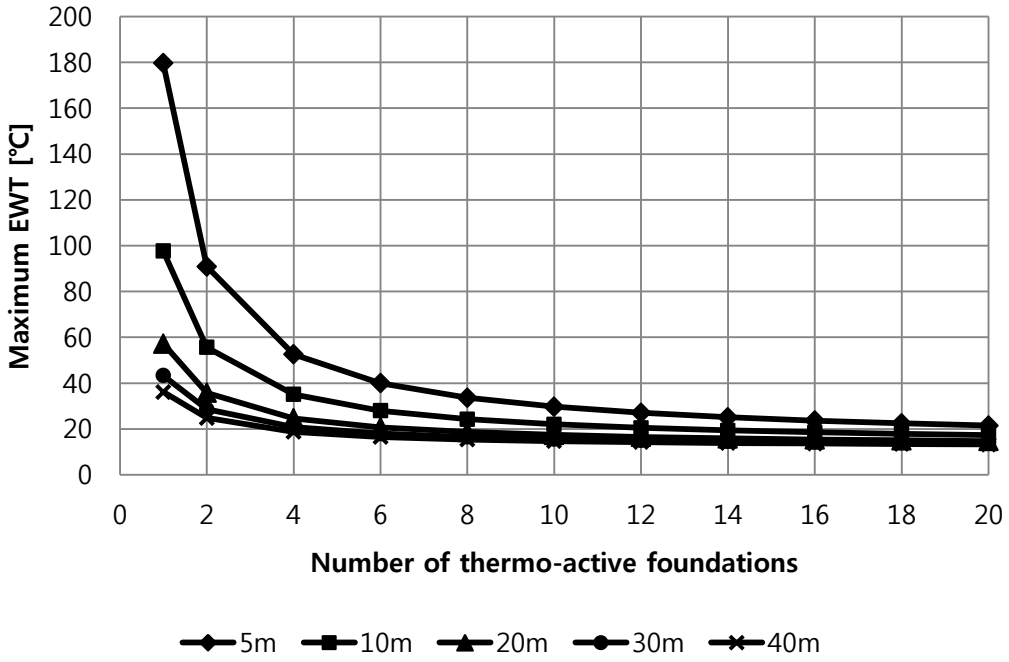

Figure 6-10: Maximum exiting water temperature variation for select foundation depths during cooling mode, Denver, CO.

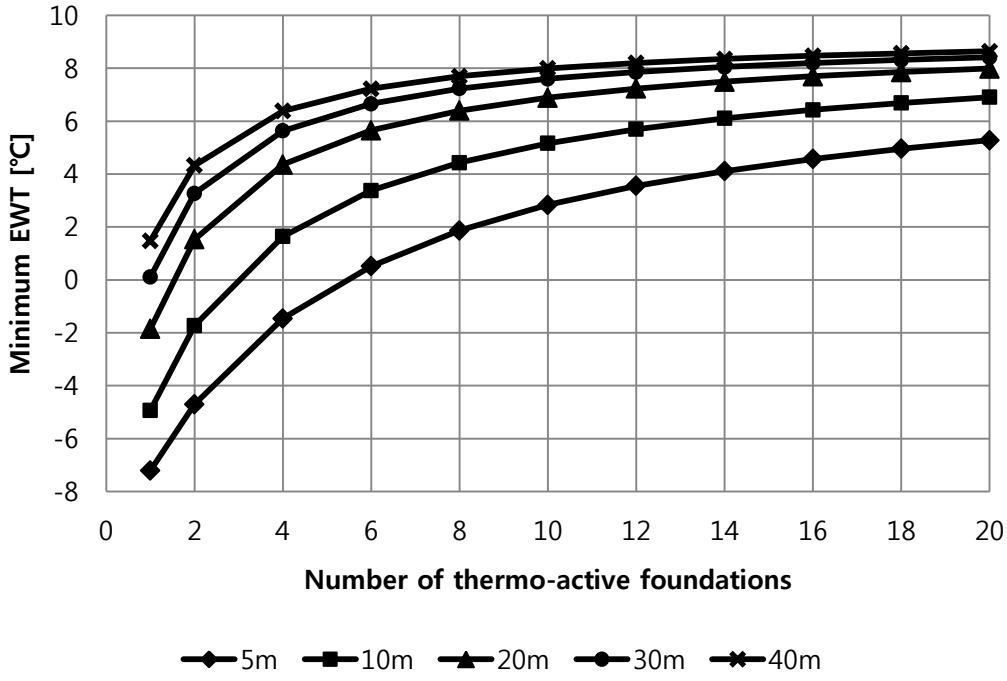

Figure 6-11: Minimum exiting water temperature variation profile for select foundation depths during heating mode, Denver, CO.

The required number of thermo-active foundation piles is listed in Table 6-6 for both cooling and heating modes. As indicated for Chicago, the design of TAF systems, including the heat exchanger loop length and the number of thermo-active foundation piles, is determined by the cooling mode when the building is located in Denver.

Table 6-6: Minimum number, N, of thermo-active foundation piles for Denver, CO. (T_{ground} = 10℃)

	Foundation Depths				
	5m	**10m**	**20m**	**30m**	**40m**
Cooling mode EWT ≤ 30℃	N ≥ 10	N ≥ 6	N ≥ 3	N ≥ 2	N ≥ 2
Heating mode EWT ≥ 2℃	N ≥ 8	N ≥ 5	N ≥ 3	N ≥ 2	N ≥ 2

6.5.5. Number of Thermo-Active Foundations for New York, New York

Because of Atlantic and the Appalachians, New York is kept warmer during the winter season with an average temperature of 3.2℃. During the summer, the climate is hot and humid with an average temperature is 22.5℃. The annual average ground temperature is 12℃ as estimated from TMY3 weather data.

Figure 6-12 and Figure 6-13 represent the variations of maximum and minimum EWT as functions of the number of thermo-active foundation piles and foundation depths.

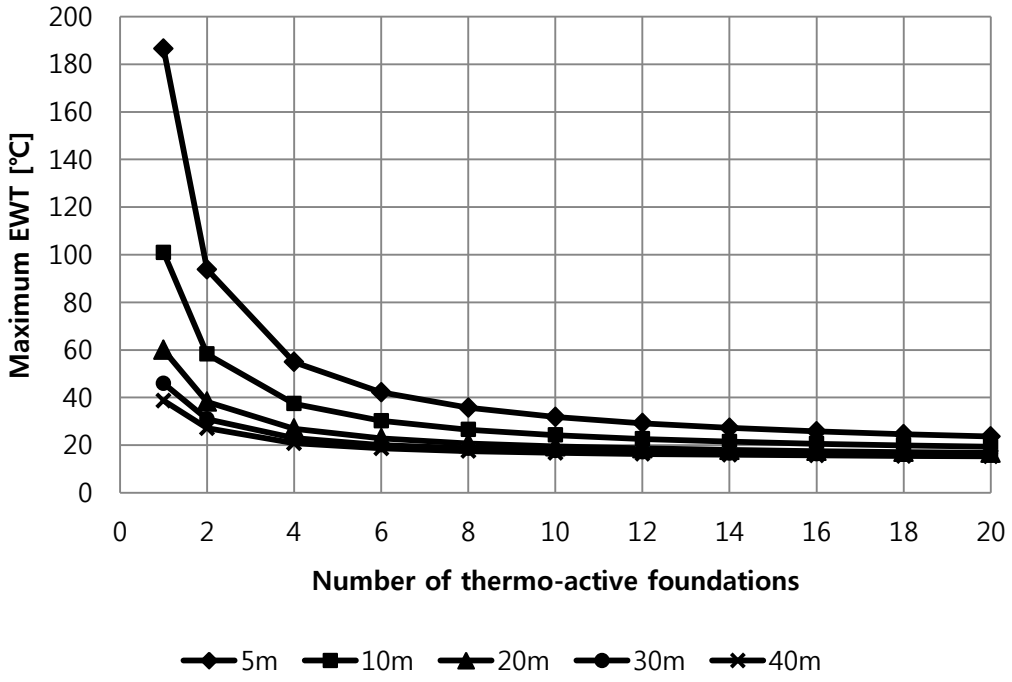

Figure 6-12: Maximum exiting water temperature variation for select foundation depths during cooling mode, New York, NY.

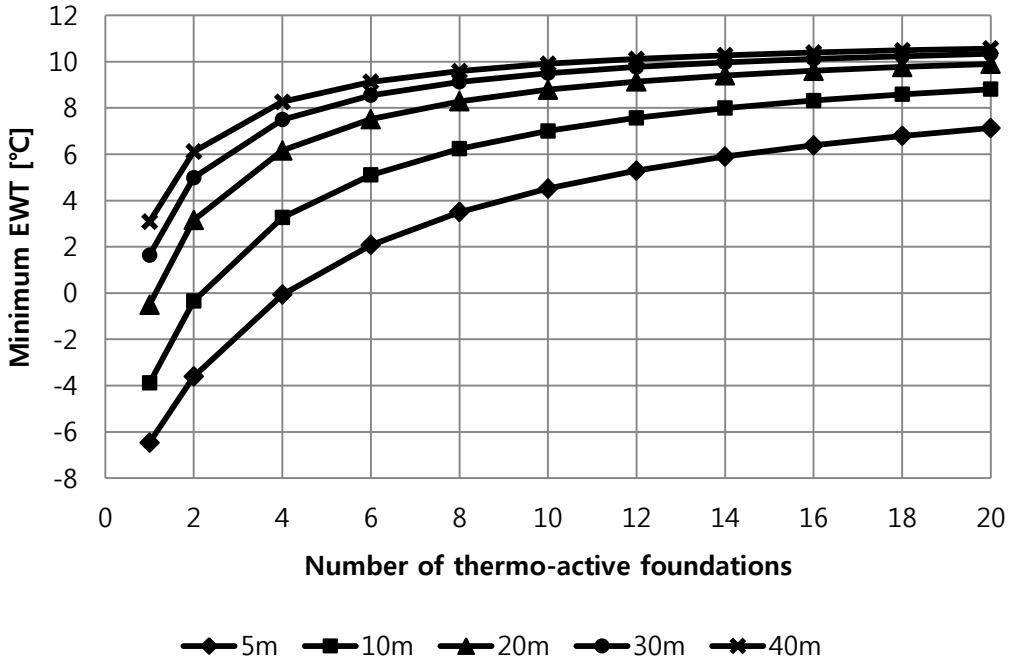

Figure 6-13: Minimum exiting water temperature variation for foundation depths during heating mode, New York, NY.

Table 6-7: Minimum number, N, of thermo-active foundation piles for New York, NY (T_{ground} = 12℃)

	Foundation Depths				
	5m	**10m**	**20m**	**30m**	**40m**
Cooling mode EWT ≤ 30℃	N ≥ 12	N ≥ 7	N ≥ 3	N ≥ 3	N ≥ 2
Heating mode EWT ≥ 2℃	N ≥ 6	N ≥ 4	N ≥ 2	N ≥ 2	N ≥ 1

Table 6-7 shows the minimum number of thermo-active foundation piles needed to meet the operation requirements of the heat pump system. Since the winter in New York is warmer than that in Cheyenne and Chicago, the minimum number of piles is less than that needed in Cheyenne and Chicago. However, building cooling loads in New York are than those found in

Cheyenne and Chicago, more thermo-active foundation piles are needed than Cheyenne and Chicago during cooling mode.

6.5.6. Number of Thermo-Active Foundations for Phoenix, Arizona

Phoenix has a subtropical desert climate with is hot and dry conditions especially during the summer period. The average outdoor air temperature is 29.4℃ during summer and 14.3℃ during winter. Figure 6-14 and Figure 6-15 illustrate the results obtained for maximum and minimum EWT as functions of the number of foundation piles, respectively. In particular, it is found that short foundation depth needs more thermo-active foundation piles in order to ensure acceptable exiting water temperature.

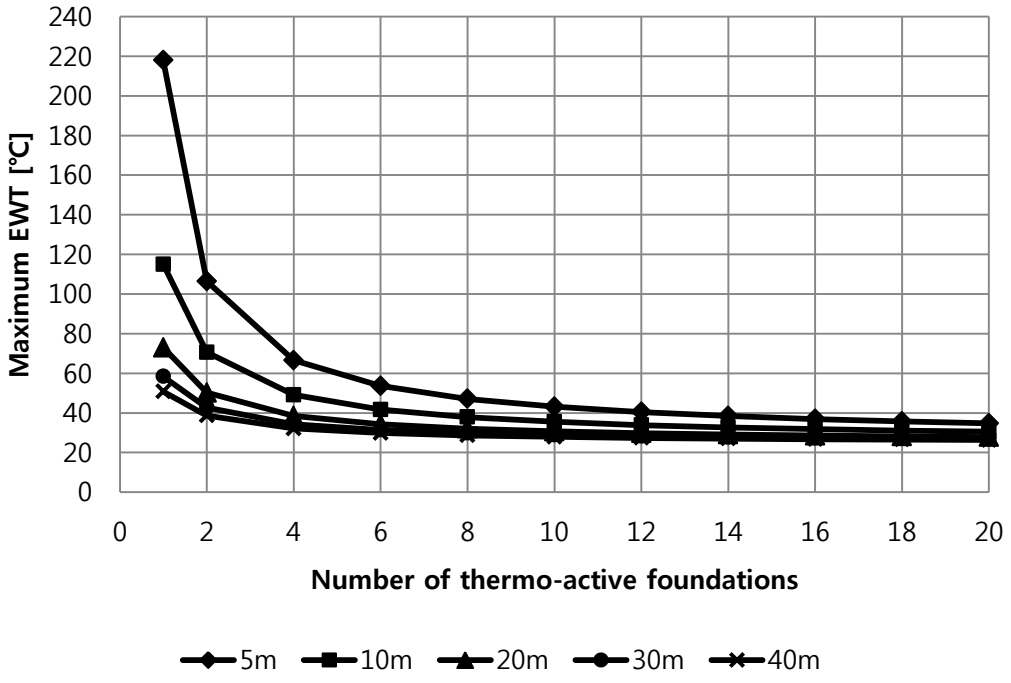

Figure 6-14: Maximum exiting water temperature variation for select foundation depths during cooling mode, Phoenix, AZ.

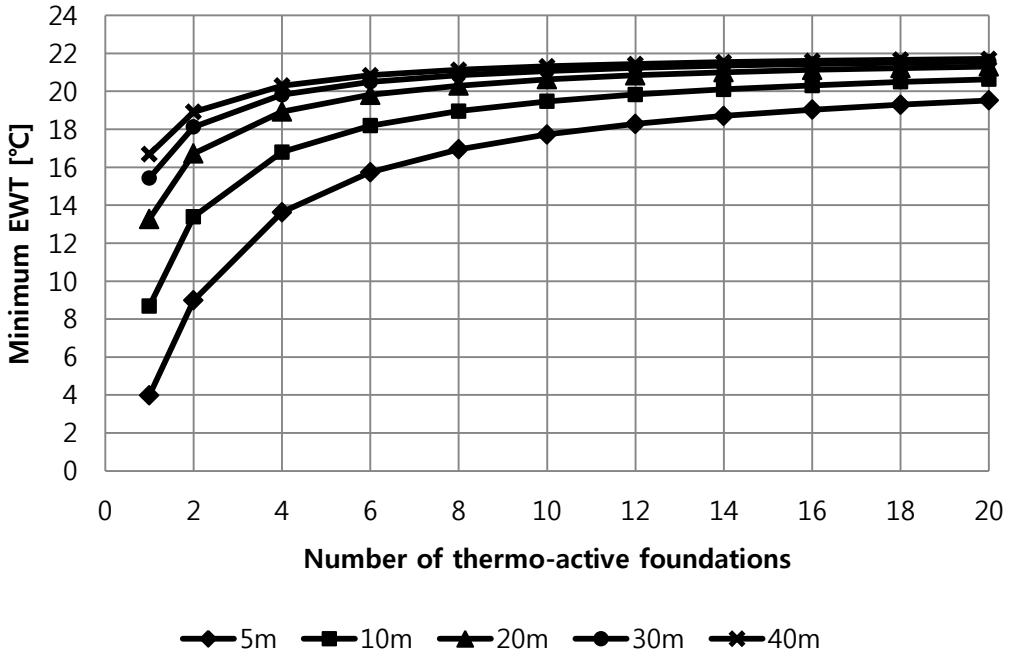

Figure 6-15: Minimum exiting water temperature variation for select foundation depths during heating mode, Phoenix, AZ.

Since Phoenix is a cooling-dominated climate, the minimum number of thermo-active foundation piles is determined by the cooling mode as shown in Table 6-8.

Table 6-8: Minimum number, N, of thermo-active foundation piles for Phoenix, AZ (T_{ground} = 23℃)

	Foundation Depths				
	5m	**10m**	**20m**	**30m**	**40m**
Cooling mode EWT ≤ 30℃	N > 30	N ≥ 20	N ≥ 10	N ≥ 8	N ≥ 6
Heating mode EWT ≥ 2℃	N ≥ 1	N ≥ 1	N ≥ 1	N ≥ 1	N ≥ 1

6.5.7. Number of Thermo-Active Foundations for Tampa, Florida

Tampa is characterized by a humid subtropical climate with hot summer. Based on TMY3 weather data, the average summer and winter temperatures are 25℃ and 15℃, respectively.

Figure 6-16 and Figure 6-17 shows the results of maximum and minimum exiting water temperatures as functions of the number of foundation piles, respectively. As found for all other US climates when the number of thermo-active foundation piles increases, the maximum EWT decreases, and the minimum EWT increases. In addition, deep foundations need fewer piles to achieve reasonable exiting water temperature.

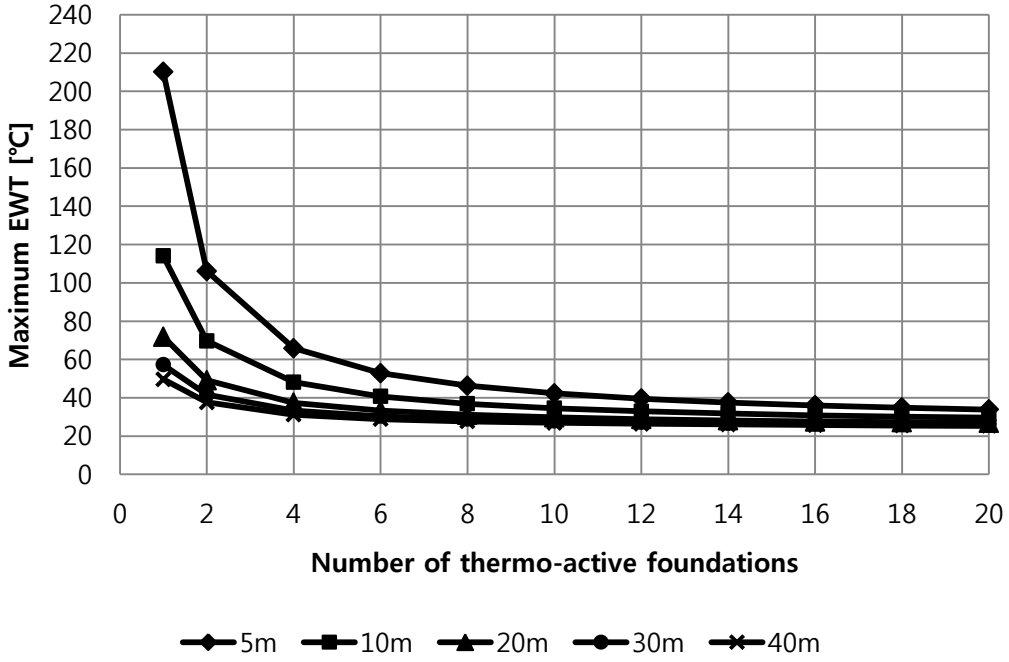

Figure 6-16: Maximum exiting water temperature variation for select foundation depths during cooling mode, Tampa, FL.

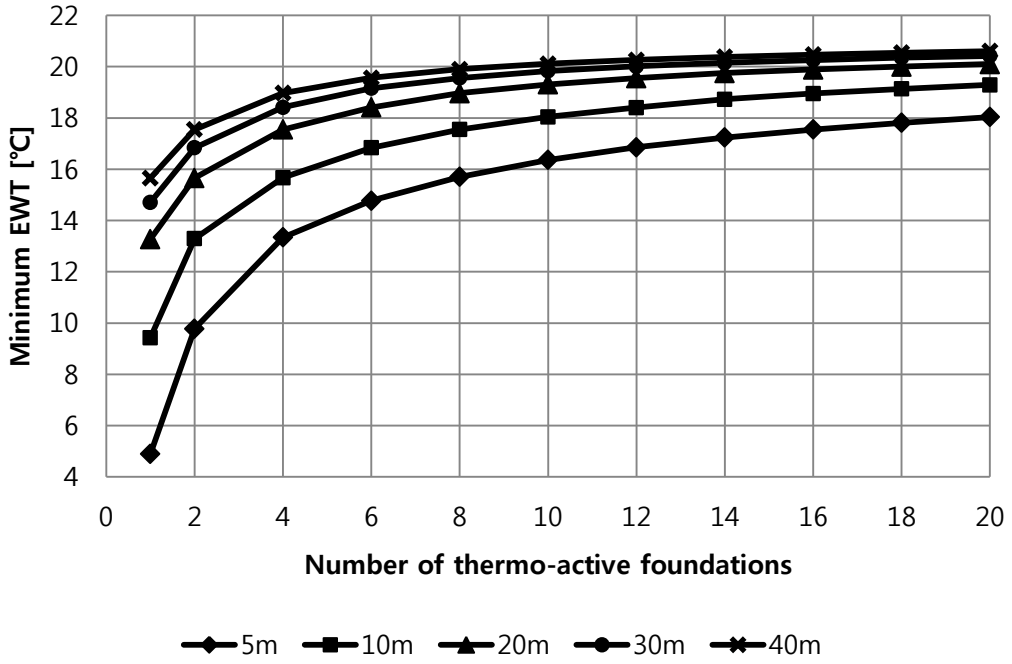

Figure 6-17: Minimum exiting water temperature variation for select foundation depths during heating mode, Tampa, FL.

Table 6-9 lists the required minimum numbers of thermo-active foundation piles for various foundation depths. Similar to the results found for Phoenix, AZ, the minimum number of foundations piles is estimated by the cooling mode in Tampa, FL. .

Table 6-9: Minimum number, N, of thermo-active foundation piles for Tampa, FL (T_{ground} = 22℃)

	Foundation Depths				
	5m	**10m**	**20m**	**30m**	**40m**
Cooling mode EWT ≤ 30℃	N > 30	N ≥ 19	N ≥ 9	N ≥ 7	N ≥ 5
Heating mode EWT ≥ 2℃	N ≥ 1	N ≥ 1	N ≥ 1	N ≥ 1	N ≥ 1

6.6. Impact of Heat Pump Capacity

6.6.1. Introduction

In the previous analysis, the heat pump size is kept fixed for all the cases to estimate the impact of climate on the required number of thermo-active foundation piles, to meet the heating and cooling loads for a prototypical small office building. However, since in practice a geothermal heat pump system designer needs to select a specific to cover all or part of the thermal loads of a building, the is also important to investigate the effect of heat pump size selection on the performance of TAF systems and on the required number of foundation piles. Table 6-10 provides specifications of heat pump systems with a wide range of capacities and efficiencies based on manufacturer ratings. In addition, the analysis is carried out for two climate zones with different characteristics: Chicago and New York.

Table 6-10: Summary of heat pump capacities and efficiencies used on the analysis

Case	Mode	Capacity		Efficiency
		Btu/h	W	
Case 1	Cooling	17,300	5,070.13	EER = 16.6 Btu/h·W
	Heating	14,700	4,308.15	COP =3.0
Case 2	Cooling	24,700	7,238.86	EER = 15.8 Btu/h·W
	Heating	22,000	6,447.57	COP = 3.0
Case 3	Cooling	37,700	11,048.78	EER = 17.5 Btu/h·W
	Heating	30,500	8,938.67	COP = 3.1
Case 4	Cooling	51,500	15,093.17	EER = 16.4 Btu/h·W
	Heating	44,200	12,953.75	COP = 3.1
Case 5	Cooling	58,000	16,998.13	EER = 15.7 Btu/h·W
	Heating	50,100	14,682.87	COP = 3.0
Case 6	Cooling	68,400	20,046.07	EER = 14 Btu/h·W
	Heating	61,500	18,023.88	COP = 2.9
Case 7	Cooling	100,000	29,307.12	EER = 16.8 Btu/h·W
	Heating	82,000	24,031.84	COP = 3.0
Case 8	Cooling	114,000	33,410.12	EER = 16.2 Btu/h·W
	Heating	93,000	27,255.62	COP = 3.0

6.6.2. Discussion of Simulation Results

The performance of TAF systems with the capacities and efficiencies listed in Table 6-10 is evaluated using EnergyPlus for the prototypical office building model described in section 6.1. The results of the simulation analysis are summarized in Table 6-11 and Table 6-12 for Chicago, and Table 6-13 and Table 6-14 for New York.

Generally, the results indicate that few foundation piles for deeper foundations and smaller heat pump capacities. For shallow foundation depths, contact surfaces between the ground and the foundation loops are reduced for the heat exchanger to occur. The reduced heat exchange surfaces or under-sized ground loops can develop imbalance between heat extraction and rejection rates depending on the heat pump size. . This imbalance can cause the working fluid temperature to reach extreme temperatures under both heating and cooling modes, and subsequently inefficient operation of the heat pump system.

As indicated in the simulation results, the minimum number of thermo-active foundation piles is set by the cooling mode in New York and is higher than that needed for Chicago. In other hand, the required of foundation piles under heating mode is lower in New York than that in Chicago. This result is expected since the prototypical office building exhibit higher cooling loads in New York than Chicago. However, the same building has lower heating loads in New York than Chicago.

Table 6-11 through Table 6-14 pinpoints in grey color the cases of heat pump capacities and foundation depths when the required minimum number of piles exceeds the available foundations for the prototypical building (i.e., 12). In these cases, the TAF system is not able to meet all the

thermal loads of the building and an auxiliary system (typically for cooling) is needed to maintain thermal comfort throughout the year.

Table 6-11: Minimum number of thermo-active foundation piles for various heat pump capacities and foundation depths under cooling mode in Chicago, IL.

Number of Foundations		Heat Pump Capacity [W] (Cooling mode)							
		5,070	**7,239**	**11,049**	**15,093**	**16,998**	**20,046**	**29,307**	**33,410**
Foundation Depth [m]	**5**	10	15	26	43	51	72	135	176
	10	6	9	14	22	26	35	65	81
	20	3	6	7	11	13	18	32	39
	30	2	4	6	8	10	12	21	26
	40	2	3	4	7	8	9	16	19
	45	2	2	4	6	7	8	14	17

Table 6-12: Minimum numbers of thermo-active foundation piles for various heat pump capacities and foundation depths under heating mode in Chicago, IL.

Number of Foundations		Heat Pump Capacity [W] (Heating mode)							
		4,308	**6,448**	**8,939**	**12,954**	**14,683**	**18,024**	**24,032**	**27,256**
Foundation Depth [m]	**5**	8	10	16	21	36	35	53	55
	10	5	6	9	11	18	19	27	28
	20	3	3	5	6	10	10	14	15
	30	2	2	4	4	7	7	10	10
	40	2	2	3	3	7	6	7	7
	45	1	2	2	3	5	5	7	7

Table 6-13: Minimum number of thermo-active foundation piles for various heat pump capacities and foundation depths under cooling mode in New York, NY.

Number of Foundations		Heat Pump Capacity [W] (Cooling mode)							
		5,070	7,239	11,049	15,093	16,998	20,046	29,307	33,410
Foundation Depth [m]	5	12	18	32	52	63	89	174	206
	10	7	11	17	27	32	45	82	96
	20	4	6	9	14	16	23	40	46
	30	3	4	7	10	11	15	27	31
	40	2	3	5	7	8	12	20	23
	45	2	3	4	7	8	11	18	20

Table 6-14: Minimum number of thermo-active foundation piles for various heat pump capacities and foundation depths under heating mode in New York, NY.

Number of Foundations		Heat Pump Capacity [W] (Heating mode)							
		4,308	6,448	8,939	12,954	14,683	18,024	24,032	27,256
Foundation Depth [m]	5	6	8	12	14	19	20	25	26
	10	3	4	7	8	10	11	14	14
	20	2	2	4	4	6	6	7	7
	30	2	2	3	3	4	4	5	5
	40	1	1	2	2	3	3	4	4
	45	1	1	2	2	3	3	4	4

Based on the results provided in Table 6-11 through Table 6-14, charts are developed to select the required foundation piles to ensure that a TAF system meets both heating and cooling

load of the prototypical office building for various foundation depths and heat pump capacities as illustrated in Figure 6-18 and Figure 6-19 for Chicago, and Figure 6-20 and Figure 6-21 for New York. Currently, the depth and the number of foundation piles for a building are designed based on the structural loads. The developed charts of Figures 6-18 through 21 would be useful for the designers to take into account the thermal loads to select the proper depth and number of foundation piles.

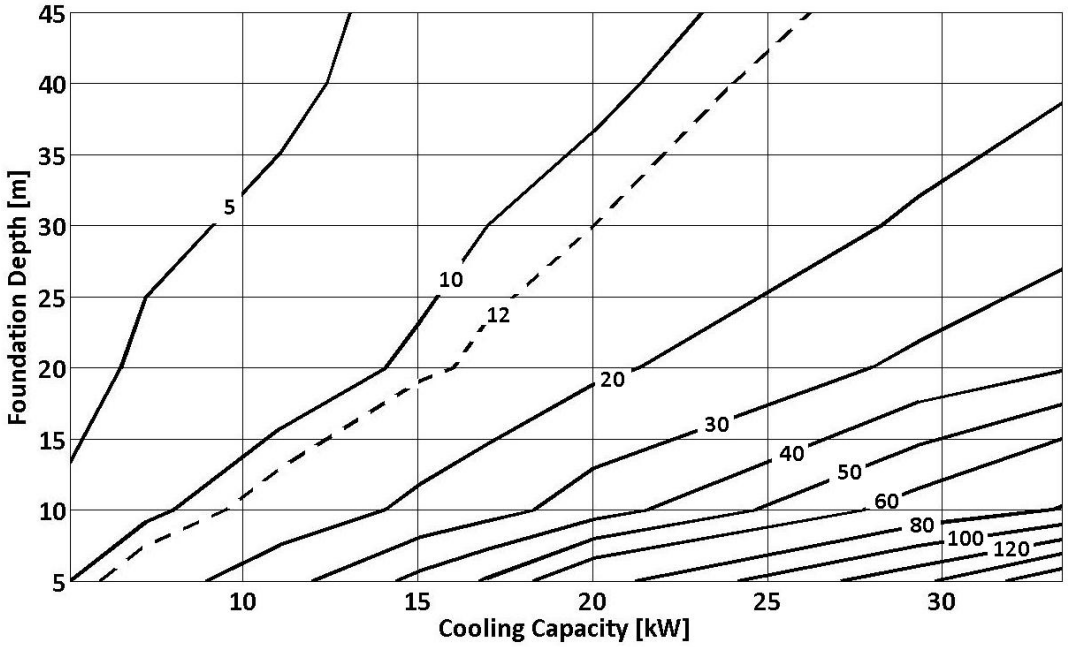

Figure 6-18: Required number of foundation piles as function of foundation depth and heat pump cooling capacity for Chicago, IL

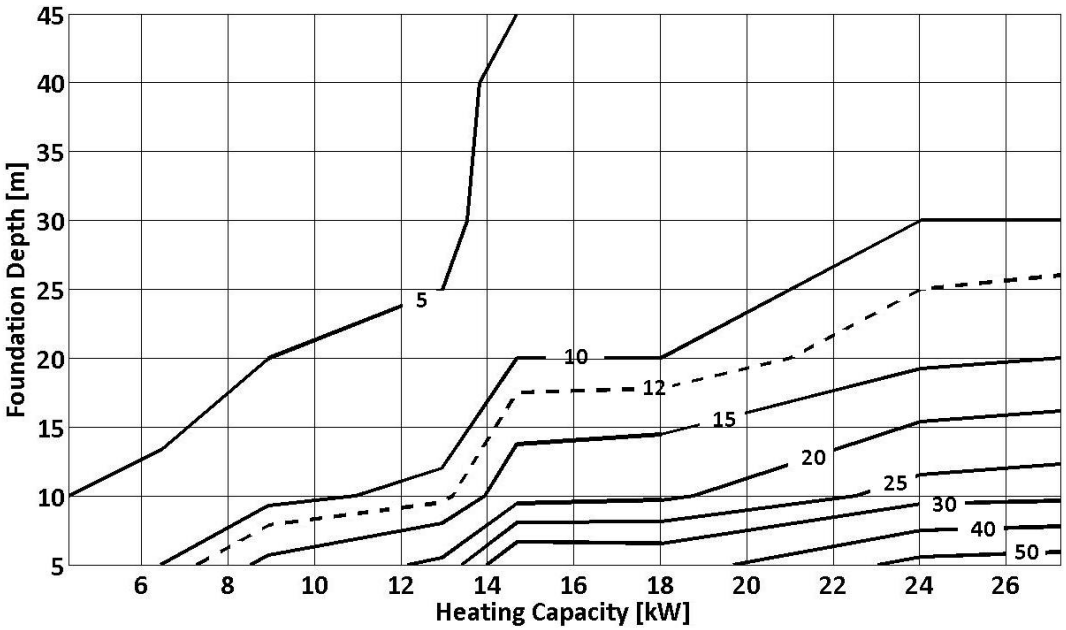

Figure 6-19: Required number of foundation piles as function of foundation depth and heat pump heating capacity for Chicago, IL

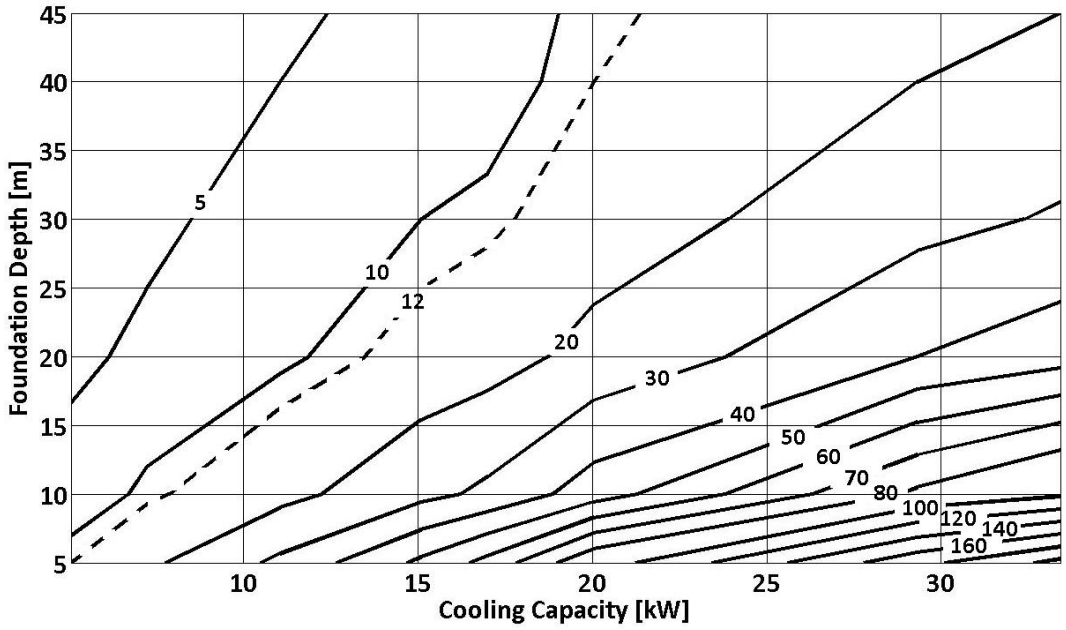

Figure 6-20: Required number of foundation piles as function of foundation depth and heat pump cooling capacity for New York, NY

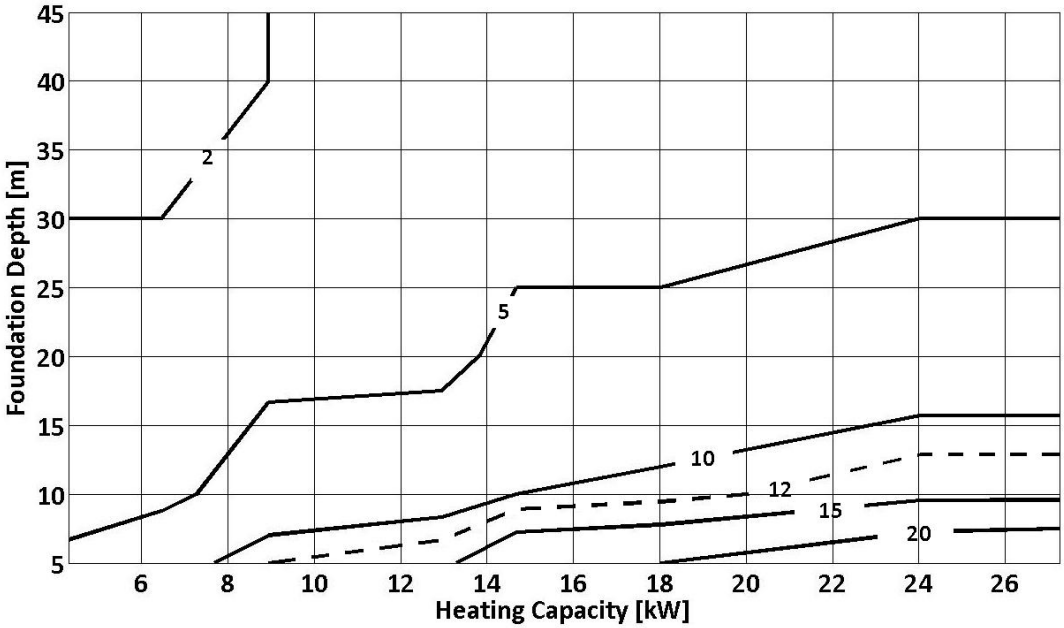

Figure 6-21: Required number of foundation piles as function of foundation depth and heat pump cooling capacity for New York, NY

6.7. Energy Consumption Analysis

6.7.1. Introduction

In the previous section, it is found that the minimum required number of thermo-active foundation piles varies with the heat pump size and the foundation depth for a given climate. The design criteria used are based on design exiting water temperatures for both heating and cooling modes. The exiting water temperature from the ground loop (which is the entering water temperature into a heat pump) is one of the important factors that affect the energy efficiency of a heat pump. Thus, under-sized ground loops can significantly impact the performance of the heat pump system.

In this section, the impact of under-sized ground loops for TAF systems is investigated to evaluate the energy consumption and energy efficiency of the heat pump under various operating conditions. The analysis is carried out using the prototypical office building described in section 6-1.

As a reference, Table 6-15 provides the annual average cooling and heating energy consumptions for baseline building model located in Chicago and New York. The baseline building uses standard VAV system with both boiler and chiller and has no TAF system As shown in Table 6-15, the baseline building model consumes more cooling and heating energy in Chicago than the building model in New York. While the difference in cooling energy is small, there is large difference in heating energy consumption between the two climates.

Table 6-15: Annual average thermal energy consumption of a base case in Chicago and New York

	Cooling Energy [GJ]	Heating Energy [GJ]
Chicago, IL.	77.483	66.543
New York, NY.	77.271	49.549

Table 6-16: Chiller and boiler capacities for a base case

	Chiller: Electric	Boiler: Gas
Capacity [kW]	200.0	90.0
Nominal Efficiency	COP = 3.2	80%

The same office building is modeled with TAF system having various heat pump capacities and foundation depths. The heat pump specifications used in the analysis are outlined in Table 6-17. In the charts developed in the previous section (i.e., Figure 6-18, Figure 6-19, Figure 6-20, and Figure 6-21), it is found that the effect of the ground loop under-sizing is worse for shallow foundation depths due to reduced heat exchange surfaces. In the analysis presented in this

section, the foundation depth is set to 5m for all the cases but the total number of foundation piles is varied.

Table 6-17: Heat pump cooling and heating capacities used in the analysis (Source: WaterFurnace International, 2012)

	Case 1	Case 2	Case 3	Case 4	Case 5	Case 6	Case 7	Case 8
Cooling Capacity [W]	5070.13	7238.86	11048.8	15093.2	16998.1	20046.1	29307.1	33410.1
Heating Capacity [W]	4308.15	6447.57	8938.67	12953.8	14682.9	18023.9	24031.8	27255.6

6.7.2. Discussion of Results

The results are grouped into two categories depending on the number of foundation piles used for the TAF system. In the first group, Group A, the number of foundation piles is allowed to vary to ensure that entering water temperature to the heat pump remains within acceptable limits while in the second group, Group B, the number of piles is fixed to 12. The results for both Group A are summarized in Table 6-18 and Table 6-19 for respectively, Chicago and New York. Based on the results shown in Table 6-18 and Table 6-19, TAF systems of Group B are under-sized, and thus their EWTs reach extreme values under both heating and cooling conditions for all the heat pump capacities except for Case 1. Indeed, the required minimum number of thermo-active foundation piles for Case 1 in Group A for Chicago and New York is 12, the entering water temperatures associated with Case 1 in Group A of Chicago and New York are the same as those in Group B. Moreover, the results of Table 6-18 and Table 6-19 indicate that as the heat pump size increases, the difference in EWTs between Group A and Group B increases.

Table 6-18: Entering water temperatures for GROUP A and GROUP B TAF systems in Chicago, IL

	Group A			Group B		
Case	Number of TAF	Max. EWT	Min. EWT	Number of TAF	Max. EWT	Min. EWT
Case 1	12	26.9	3.6	12	26.9	3.6
Case 2	16	29.6	3.9	12	34.7	2.9
Case 3	28	29.2	4.0	12	48.7	0.9
Case 4	45	29.3	4.5	12	60.9	-0.2
Case 5	55	29.0	3.6	12	65.7	-2.7
Case 6	80	28.8	4.8	12	76.0	-2.4
Case 7	140	29.6	5.1	12	96.6	-7.6
Case 8	180	29.8	5.5	12	110.4	-6.6

Table 6-19: Entering water temperatures GROUP A and GROUP B TAF systems in New York, NY

	Group A			Group B		
Case	Number of TAF	Max. EWT	Min. EWT	Number of TAF	Max. EWT	Min. EWT
Case 1	12	29.0	5.3	12	29.0	5.3
Case 2	20	28.7	6.2	12	37.0	4.3
Case 3	32	29.8	6.1	12	51.9	2.3
Case 4	55	29.3	7.0	12	64.8	1.4
Case 5	70	28.8	6.8	12	70.0	-0.5
Case 6	90	29.8	7.7	12	80.4	0.2
Case 7	180	29.8	8.2	12	101.3	-3.3
Case 8	210	29.9	8.4	12	112.0	-2.8

Figure 6-22 through Figure 6-25 illustrates graphically the variations in cooling and heating energy end-uses for all TAF systems (Group A and Group B) for both Chicago and New York. The results clearly indicate that Group A TAF systems operate more efficiently and use less energy for both heating and cooling that Group B TAF systems. Furthermore, as illustrated in Figure 6-22 through Figure 6-25, the difference in energy consumptions between Group A and Group B increases as the heat pump size increases. Thus, it can be concluded that the impact of ground loop under-sizing for TAF systems can be significant on its energy efficiency and can be more severe when the heat pump are oversized.

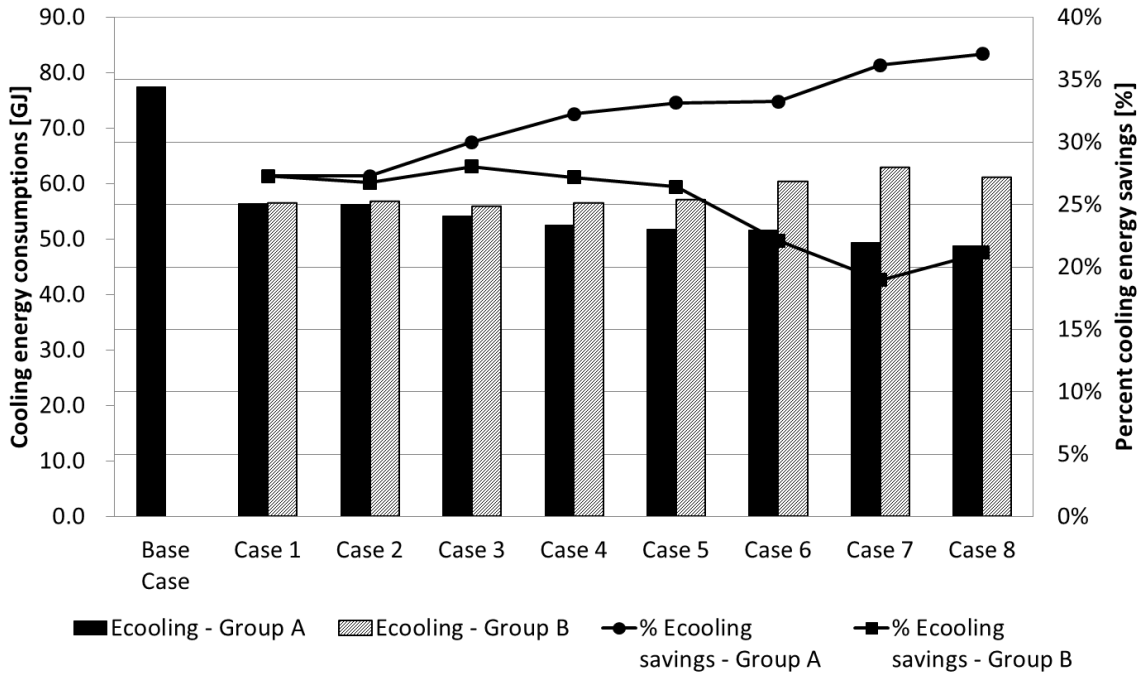

Figure 6-22: Cooling energy consumption and percent savings in Chicago, for a TAF system with a foundation depth = 5m

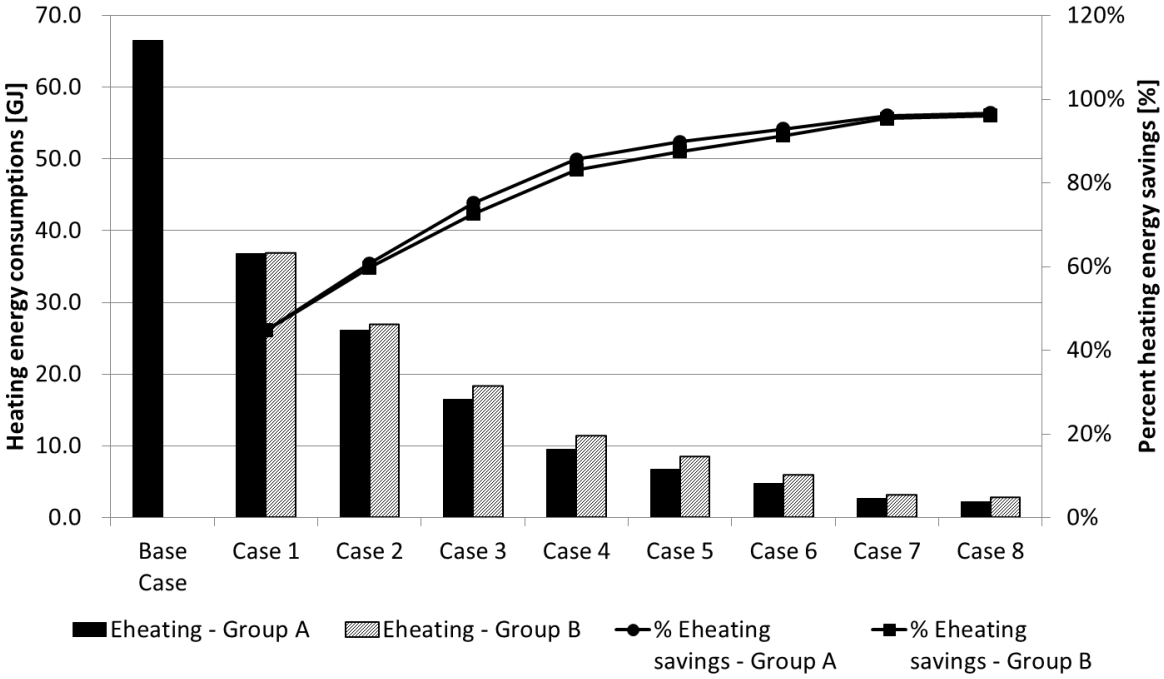

Figure 6-23: Heating energy consumption and percent savings in Chicago, for a TAF system with a foundation depth = 5m

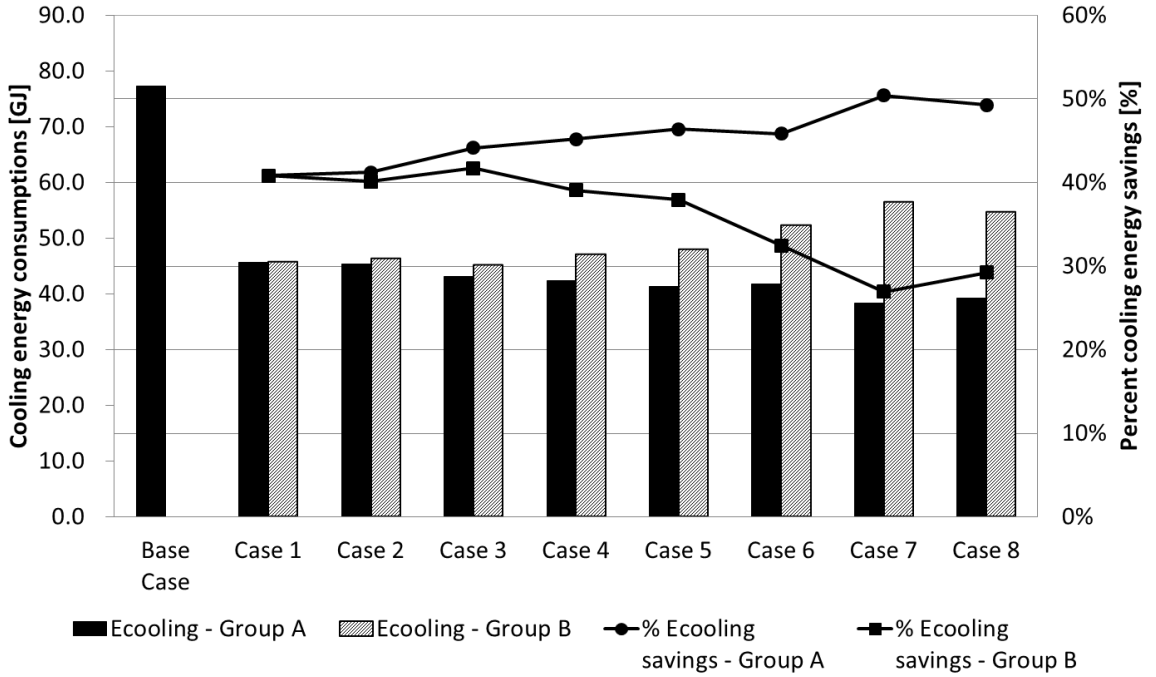

Figure 6-24: Cooling energy consumption and percent savings in New York, for a TAF system with a foundation depth = 5m

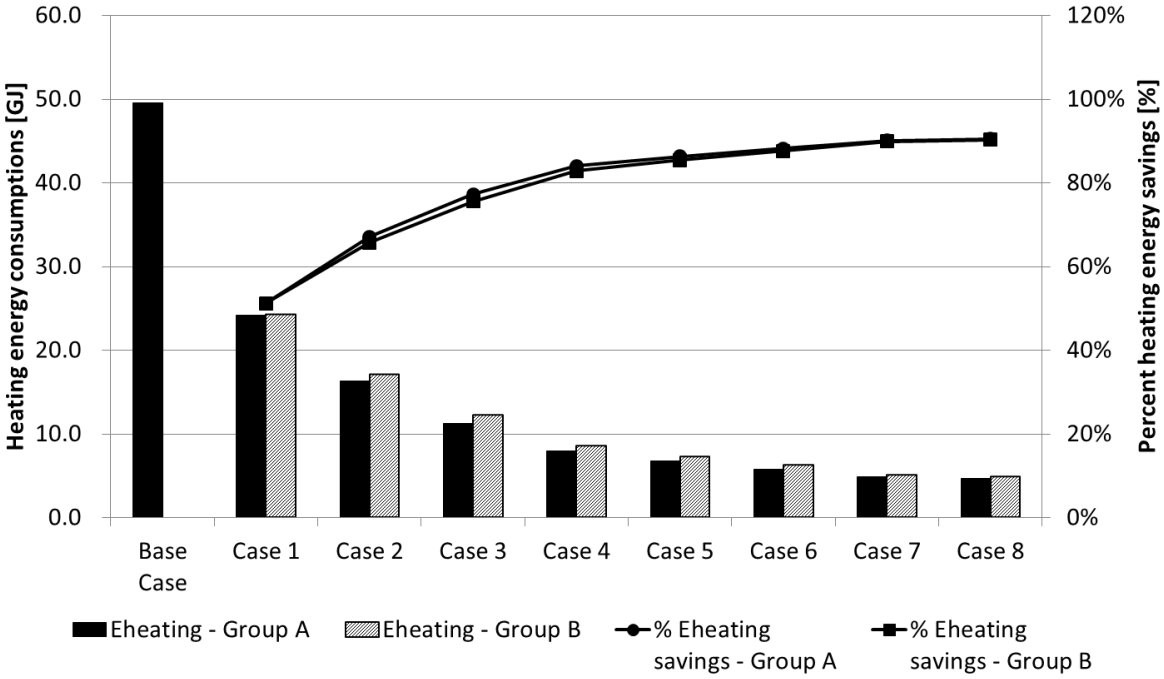

Figure 6-25: Heating energy consumption and percent savings in New York, for a TAF system with a foundation depth = 5m

6.8. Summary and conclusions

This chapter investigated the impact of climate conditions on the minimum number of foundation piles required for TAF systems. It also estimated the proper size of the heat pump based on the foundation design. The selection criteria of the number of foundation piles is based on threshold limits of acceptable exiting fluid temperature from the ground loops, and entering water temperatures to the heat pump under both heating and cooling modes. These threshold limits consist of a maximum EWT of 30℃ and a minimum EWT of 2℃.

The first analysis investigated the impact of climate zones on the required numbers of thermo-active foundation piles to meet the thermal loads of a prototypical office building. The required numbers of thermo-active foundations are summarized in Table 6-20 and Table 6-21 for

both cooling and heating mode, respectively. For this analysis, the same size of heat pump was used for all the climate zones.

Table 6-20: Minimum number, N, of thermo-active foundation piles operating under cooling mode with a design EWT ≤ 30℃

Region	T_{ground}	Foundation Depth [m]				
		5m	10m	20m	30m	40m
Cheyenne, WY	7℃ (44.6°F)	N ≥ 8	N ≥ 5	N ≥ 3	N ≥ 2	N ≥ 2
Chicago, IL	10℃ (50.0°F)	N ≥ 10	N ≥ 6	N ≥ 3	N ≥ 2	N ≥ 2
Denver, CO	10℃ (50.0°F)	N ≥ 10	N ≥ 6	N ≥ 3	N ≥ 2	N ≥ 2
New York, NY	12℃ (53.6°F)	N ≥ 12	N ≥ 7	N ≥ 3	N ≥ 3	N ≥ 2
Phoenix, AZ	23℃ (73.4°F)	N > 30	N ≥ 20	N ≥ 10	N ≥ 8	N ≥ 6
Tampa, FL	22℃ (71.6°F)	N > 30	N ≥ 19	N ≥ 9	N ≥ 7	N ≥ 5

Table 6-21: Minimum number, N, of thermo-active foundation piles operating under heating mode with a design EWT ≥ 2℃,

Region	T_{ground}	Foundation Depth [m]				
		5m	10m	20m	30m	40m
Cheyenne, WY	7℃ (44.6°F)	N ≥ 13	N ≥ 7	N ≥ 4	N ≥ 3	N ≥ 2
Chicago, IL	10℃ (50.0°F)	N ≥ 8	N ≥ 5	N ≥ 3	N ≥ 2	N ≥ 2
Denver, CO	10℃ (50.0°F)	N ≥ 8	N ≥ 5	N ≥ 3	N ≥ 2	N ≥ 2
New York, NY	12℃ (53.6°F)	N ≥ 6	N ≥ 4	N ≥ 2	N ≥ 2	N ≥ 1
Phoenix, AZ	23℃ (73.4°F)	N ≥ 1	N ≥ 1	N ≥ 1	N ≥ 1	N ≥ 1
Tampa, FL	22℃ (71.6°F)	N ≥ 1	N ≥ 1	N ≥ 1	N ≥ 1	N ≥ 1

As described in the Tables 6-20 and 6-21, shallower foundation depths need more ground loops to maintain acceptable exiting water temperatures throughout the year. In addition, it is observed that the minimum number of thermo-active foundation piles is significantly influenced by

climate conditions. For the heating-dominated regions, such as Cheyenne, the required number of thermo-active foundation piles is based on the heating mode. However, for the cooling-dominated regions, such as Phoenix and Tampa, the number of thermo-active foundation piles is based on cooling mode.

Since, building foundations are designed based on a structural load analysis. Charts have been developed to aid architects and engineers in selecting the proper depth and number of foundation piles based on thermal load analysis. Specifically, these charts allow users to determine the minimum required number of foundation piles as a function of both heat pump capacity and the foundation depth. These charts indicate that large thermal loads and thus larger heat pumps require more thermo-active foundation piles for all foundation depths. Moreover, the impact of the heat pump capacity is found to be more influential for shallower foundation depths. The charts are provided in Figure 6-18 and Figure 6-19 for Chicago, and Figure 6-20 and Figure 6-21 for New York.

The effect of under-sized ground loops on the energy efficiency of thermo-active foundations was investigated for two climates, Chicago and New York. It is found that when the number of foundation piles is properly determined to maintain many enough reasonable EWTs, larger heat pumps can save energy use for both cooling and heating. However, if the number of piles are not sufficient for a specific heat pump size (i.e. undersized ground loop system), the energy efficiency of TAF systems is significantly reduced.

CHAPTER 7. CONCLUSION AND FUTURE WORK

7.1. SUMMARY AND CONCLUSION

The study presented in this thesis have three main purposes: (i) to develop a three-dimensional numerical model to estimate the thermal performance of thermo-active foundation (TAF) systems, (ii) to generate thermal response factors using g-function calculation approach to model TAF systems in detailed building energy simulation tools, and (iii) to provide a design guidelines for properly design TAF systems including selecting heat pump capacity and the minimum number of foundation piles.

For the numerical analysis, a three-dimensional cylindrical finite difference model was developed as described in Chapter 3. The three-dimensional numerical model was validated by measured data obtained from a laboratory experimental set-up performed by the Centrifuge Lab of the Geotechnical Engineering and Geo-mechanics, the University of Colorado at Boulder. It was found that predictions from the three-dimensional numerical model agree well with the empirical data, and the numerical model was able to model accurately ground-coupled heat transfer between a thermo-active foundation heat exchanger loops and the ground. After the validation analysis, the impact of several design and operating parameters on thermal performance of TAF systems is evaluated. The results of the parametric analysis indicated that:

- The deeper the foundation is, the more heat is exchanged by the TAF system. The faster the fluid is flowing through the foundation loops, the more heat is exchanged by the TAF system with a sudden increase of heat transfer when the fluid flow shifted from laminar flow to turbulent regime.

- As the distance between the U-tube legs (shank space) is smaller, the more heat interactions occur resulting in less heat transfer exchanged by the TAF system.
- If the foundation pile is wide enough to hold several U-tube legs, more heat is exchanged by the TAF system.

The second achieved goal of the study was to generate thermal response factors to model TAF systems as discussed in Chapter 4. In particular, existing g-function modeling approaches for ground-source heat pumps (GSHP) developed by Eskilson (1987) and Yavuzturk (1999), were employed in to develop new g-functions specific to TAF systems. Since the existing g-function model for conventional vertical GSHPs was based on a two-dimensional model, the boundary conditions of the three-dimensional model developed for this study were modified to validate the calculation procedure. The g-function model developed in Chapter 4 was successfully verified and agreed well that developed by Eskilson's for long-time steps and by Yavuzturk's for short-time steps.

Then, a series of sensitivity analyses is carried out to assess the impact of several parameters on the calculation of the TAF g-functions. The results of this sensitivity analyses in Chapter 5 are summarized below:

- Deeper foundations have higher thermal response factors.
- Wider shank space results in higher short-time step thermal response factors.
- Volumetric flow rate has no significant impact on the calculation of thermal response factors

- Higher concrete thermal conductivity results in higher short-time step thermal response factors.
- Lower soil thermal conductivity gives higher short-time thermal response factors. However, soil thermal conductivity does not affect the long-time step thermal response factors.

In order to model TAF systems in whole-building energy simulation tool, the thermal response factors generated in Chapter 5 were implemented in EnergyPlus, using vertical ground-coupled heat exchanger model of EnergyPlus. Then, a simulation analysis is carried to evaluate of effectiveness of TAF systems in heating and cooling a prototypical small office building located in Chicago. The simulation analysis included the effects on building heating and cooling end-uses of design and operating parameters such as foundation depth, shank space, soil and foundation, and volumetric fluid flow rate. The simulation energy analysis indicated that:

- As the foundation depth increases, heating and cooling energy use is reduced.
- As the shank space increases, heating and cooling energy use is reduced due to reduced thermal interactions between the U-tube loops.
- As the soil thermal conductivity increases, heating and cooling energy use is reduced due higher heat transfer between the foundation loops and the ground.
- As the concrete thermal conductivity increases, heating and cooling use is energy reduced due to lower thermal resistance to heat transfer between the foundation loops and ground.

- As the volumetric fluid flow rate increases, heating and cooling energy use is reduced due to higher convective heat transfer coefficients within the foundation loops.

In Chapter 6, design guidelines were developed to select the minimum number of thermo-active foundation piles for a given heat pump capacity and for a given foundation depth. The design guidelines account for the impact of climate conditions and the relationship between the heat pump capacity, the foundation depth, and the minimum number of thermo-active foundations. The design guidelines would be useful when designing TAF systems so both thermal loads and structural loads can be accounted for when specifying building foundations.

To select a proper number of thermo-active foundation piles, s the ground loop should be properly sized. If the ground loop is undersized, the exiting fluid temperature (EWT) can reach extreme temperatures, and can cause heat pumps to operate at lower energy efficiencies. For this study, design range of EWT was set to be above 2℃ (heating mode) and below 30℃ (cooling mode).

Based on the EnergyPlus simulation analysis, it is found that for hot climates, more foundation piles were required to meet cooling loads of a prototypical small office building. For heating-dominated climates, the minimum number of foundation piles is determined by the heating mode. In addition, it is found that TAF systems with shallower foundation depths, more piles were needed to maintain a reasonable exiting water temperature and ensure energy efficient operation for the heat pump. Moreover, it is found that larger heat pump required more foundation piles. Based on the simulation analysis results, design guidelines charts were developed to help architects and engineers design TAF systems.

7.2. FUTURE WORK

The ultimate goal of the study presented in this thesis is to develop a comprehensive design guideline as well as a simulation tool suitable to design and evaluate the performance of for thermo-active foundation systems under various climatic and operating conditions. While the work presented in the thesis has set the stage to achieve this ultimate goal, additional tasks need to be completed in order to develop design and analysis tools for TAF systems as briefly described below:

- A more detailed TAF system model needs to be developed to account and assess the impact of thermal interactions of neighboring loops within the same foundation pile. The detailed TAF system model can also determine the interactions between the foundation piles and the heat transfer between the ground medium and the building foundation elements. This heat transfer can affect the heating and cooling loads of the buildings air-conditioned by the TAF systems.

- The estimation of the g-functions for TAF systems can then be improved using the detailed heat transfer model described above. The validation of the energy simulation results predicted from these g-functions can be carried out from measurements obtained from an actual building heated and/or cooled by a TAF system.

- The development of design guidelines and/or design tool can then be based on the validated simulation analysis tool for various climate zones, foundation designs, building types, and operating conditions.

REFERENCES

ASHRAE Research ASHRAE Handbook: HVAC Applications - Chapter 32 [Book]. - 2007.

ASHRAE Research ASHRAE Handbook: HVAC Systems and Equipments - Chapter 26 [Book]. - 2008.

Cenk Yavuzturk, Jeffrey D. Spitler A Short Time Step Response Factor Model for Vertical Ground Loop Heat Exchangers [Journal]. - [s.l.] : ASHRAE Transactions, 1999. - Part 2, pp.465-474 : Vol. 105.

Cenk Yavuzturk, Jeffrey D. Spitler, Simon J. Rees A Transient Two-Dimensional Finite Volume Model for the Simulation of Vertical U-Tube Ground Heat Exchangers [Journal]. - [s.l.] : ASHRAE Transactions, 1999. - Part 2, pp.475-485 : Vol. 105.

Christian Kaltreider Heat Transfer Analysis of Thermo-active Foundations [Journal]. - 2011.

D. Adam, R. Markiewicz Energy from earth-coupled structures, foundations, tunnels and sewers [Journal]. - [s.l.] : Geotechnique, 2009. - No 3, pp.229-236 : Vol. 59.

ENERGYPLUS TM EnergyPlus Engineering Reference - pp.768-777. - 2010.

Frank Kreith, Mark S. Bohn Principles of Heat Transfer, Sixth Edition - Chapter 3, Chapter 4 [Book].

G. Phetteplace Geothermal Heat Pumps [Journal]. - [s.l.] : ASEC, 2007. - 1(32), pp.32-38 : Vol. 133.

H. Brandl Energy foundations and other thermo-active ground structures [Journal]. - [s.l.] : Geotechnique, 2006. - No. 2, pp.81-122 : Vol. 56.

James J. Hirsch DOE-2.2 - Building Energy Use and Cost Analysis Program: Dictionary - pp.299-305. - [s.l.] : E. O. Lawrence Berkeley National Laboratory, 2009. - Vol. 2.

Jeffrey D. Spitler GLHEPRO – A DESIGN TOOL FOR COMMERCIAL BUILDING GROUND LOOP HEAT EXCHANGERS [Conference] // 4th International Conference on Heat Pumps in Cold Climate. - Aylmer, Quebec : [s.n.], 2000.

John A. Shonder, Patrick J. Hughes Increasing confidence in geothermal heat pump design methods [Conference] // Proc. 2nd Stockton Geothermal Conference. - 1998.

John S. McCartney Centrifuge Modeling of Soil-Structure Interaction in Geothermal Foundations [Report]. - 2010.

Jonathan J. Giardina Evaluation of ground coupled heat pumps for the state of Wisconsin [Conference]. - 1995.

Jun Gao, Xu Zhang, Jun Liu, Kuishan Li, Jie Yang Numerical and experimental assessment of thermal performance of vertical energy piles: An application [Journal]. - [s.l.] : Applied Energy, 2008. - Issue 10, pp.901-910 : Vol. 85.

Moncef Krarti Energy Audit of Building Systems: An Engineering Approach, Second Edition - Chapter 9 [Book]. - [s.l.] : Francis and Taylor, CRC Press, Boca Raton, Florida, 2010.

P.J. Bourne-Webb, B. Amatya, K. Soga, T. Amis, C. Davidson, P. Payne Energy pile test at Lambeth College, London: geotechnical and thermodynamic aspects of pile response to heat cycles [Journal]. - [s.l.] : Geotechnique, 2009. - Issue 3, pp.237-248 : Vol. 59.

S. P. Rottmayer, W. A. Beckman, and J. W. Mitchell Simulation of a Single Vertical U-Tube Ground Heat Exchanger in an Infinite Medium [Journal]. - [s.l.] : ASHRAE Transactions, 1997. - Part 2, pp.651-659 : Vol. 103.

Steve Kavanaugh An Instruction Guide for Using a Design Tool for Vertical Ground-Coupled, Groundwater and Surface Water Heat Pumps Systems - Ground Source Heat Pump System Designer, GshpCalc Version 5.0. - 2010.

Steve Kavanaugh, K. Rafferty Ground source heat pumps - Design of Geothermal Systems for Commercial and Institutional Buildings [Book]. - [s.l.] : ASHRAE, 1997.

T. Kusuda, P. R. Achenbach Earth temperature and Thermal Diffusivity at Selected Stations in the United States [Journal]. - [s.l.] : ASHRAE Transactions, 1965. - Part 1 : Vol. 71.

Thomas Ray Young Development, Verification, and Design Analysis of the Borehole Fluid Thermal Mass Model for Approximating Short Term Borehole Thermal Response // MS Thesis. - [s.l.] : Oklahoma State University, 2001.

U.S. Department of Energy Geothermal Technologies Program: Geothermal Basics [Online]. - Retrieved 2011-03-30. - http://www1.eere.energy.gov/geothermal/geothermal_basics.html.

WaterFurnace Inc. Heat Pump Product Catalog - Hydronic NSW, Hydronic NDW [Online]. - 2012. - http://www.waterfurnace.com/literature/envision/SC1007WN.pdf.

Yunus A. Cengel, Michael A. Boles Thermodynamics And Engineering Approach, 5th Edition - Chapter 11 [Book]. - [s.l.] : McGraw-Hill Book Company, 2005.

APPENDIX

APPENDIX A – COMPLETE RESULTS OF VALIDATION ANALYSIS IN CHAPTER 5

APPENDIX-A. VALIDATION ANALYSIS RESULTS

A-1. PROBE COLUMN #1

Table A-1: Experimental measurements of ground temperatures for probe column #1 (in ^{o}C)

Time [sec]	PROBE1-1	PROBE1-2	PROBE1-3	PROBE1-4	PROBE1-5	PROBE1-6
3600	19.69	20.13	20.10	19.45	19.62	19.35
7200	20.34	20.76	20.77	20.14	20.15	19.94
10800	19.97	20.33	20.68	20.18	19.75	19.65
14400	19.80	20.15	20.69	19.65	19.57	19.54
18000	19.74	20.03	20.16	19.72	19.43	19.40

Table A-2: Model predictions of ground temperatures for probe column #1 (in ^{o}C)

Time [sec]	PROBE1-1	PROBE1-2	PROBE1-3	PROBE1-4	PROBE1-5	PROBE1-6
3600	19.85	19.98	19.98	19.95	19.92	19.89
7200	20.31	20.35	20.37	20.35	20.31	20.26
10800	20.14	20.18	20.18	20.15	20.11	20.07
14400	19.84	19.87	19.87	19.85	19.82	19.79
18000	19.68	19.70	19.70	19.69	19.66	19.64

Table A-3: The temperature difference between measurements and model predictions for probe column #1 (in ^{o}C)

Time [sec]	PROBE1-1	PROBE1-2	PROBE1-3	PROBE1-4	PROBE1-5	PROBE1-6
3600	0.16	0.15	0.12	0.50	0.30	0.53
7200	0.03	0.40	0.40	0.21	0.15	0.32
10800	0.17	0.15	0.51	0.03	0.36	0.42
14400	0.04	0.28	0.82	0.20	0.25	0.24
18000	0.05	0.33	0.46	0.03	0.23	0.24

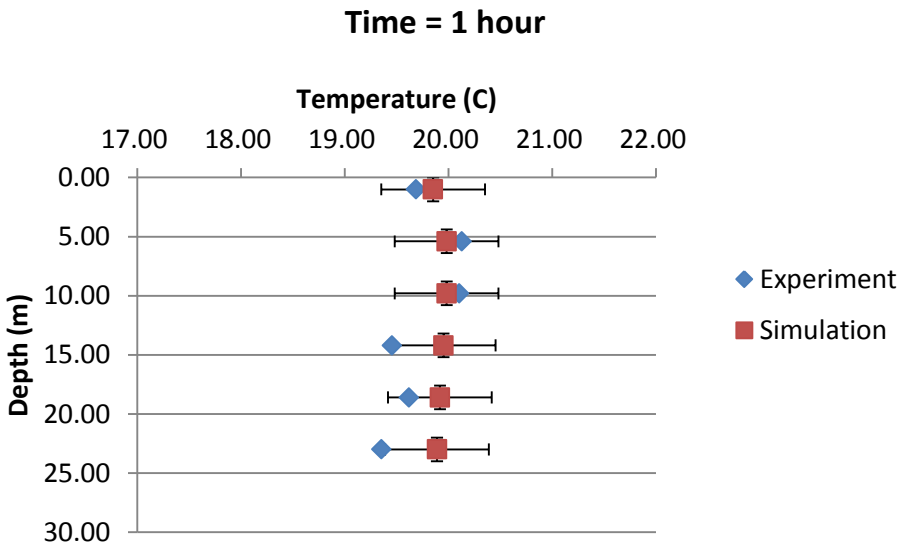

Figure A-1: Vertical ground temperature profile for probe column #1 at 3600 seconds (after 1 hour)

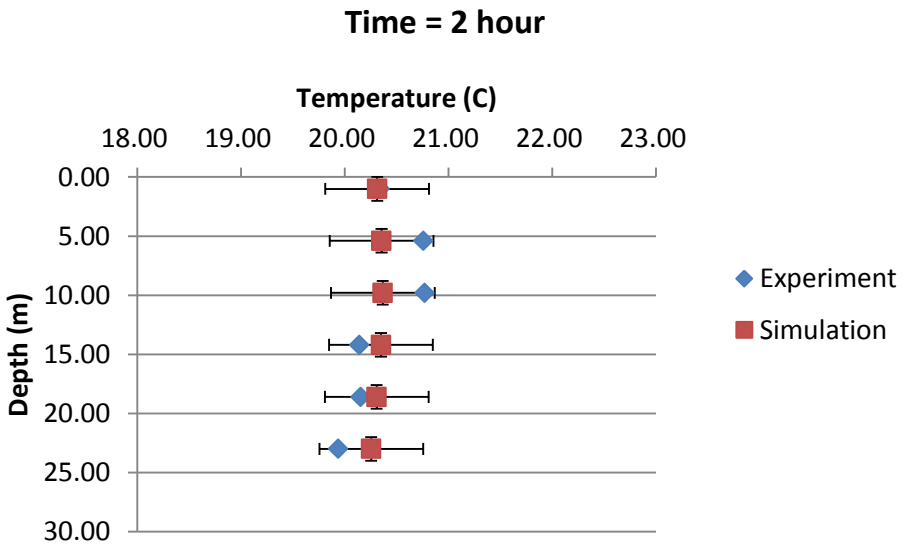

Figure A-2: Vertical ground temperature profile for probe column #1 at 7200 seconds (after 2 hours)

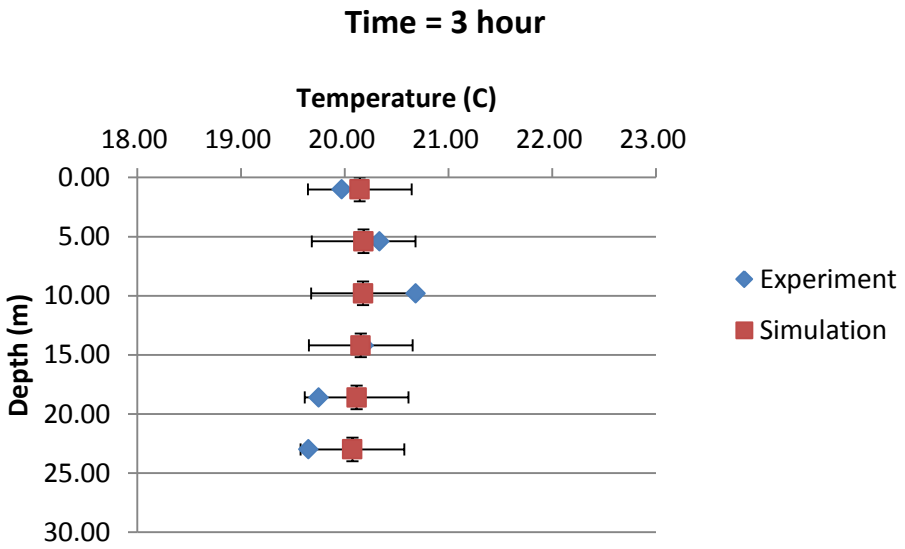

Figure A-3: Vertical ground temperature profile for probe column #1 at 10800 seconds (after 3 hours)

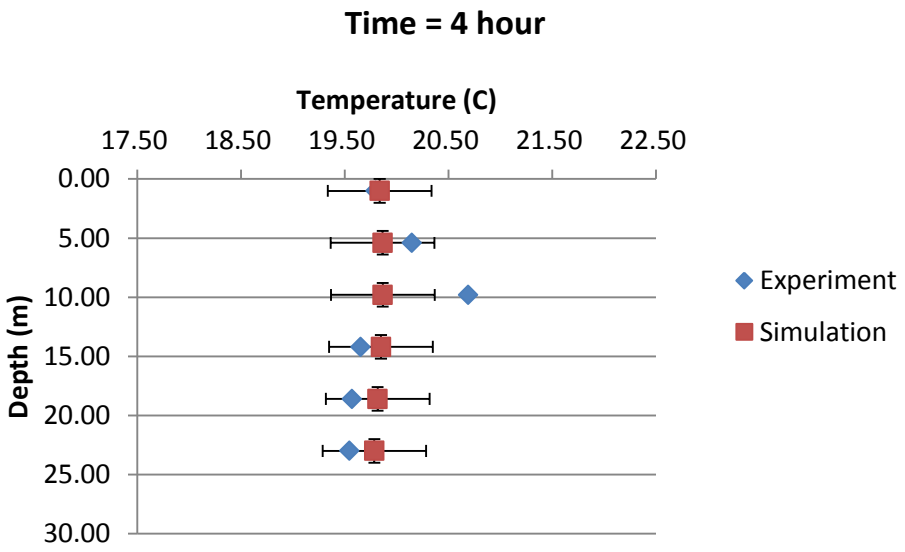

Figure A-4: Vertical ground temperature profile for probe column #1 at 14400 seconds (after 4 hours)

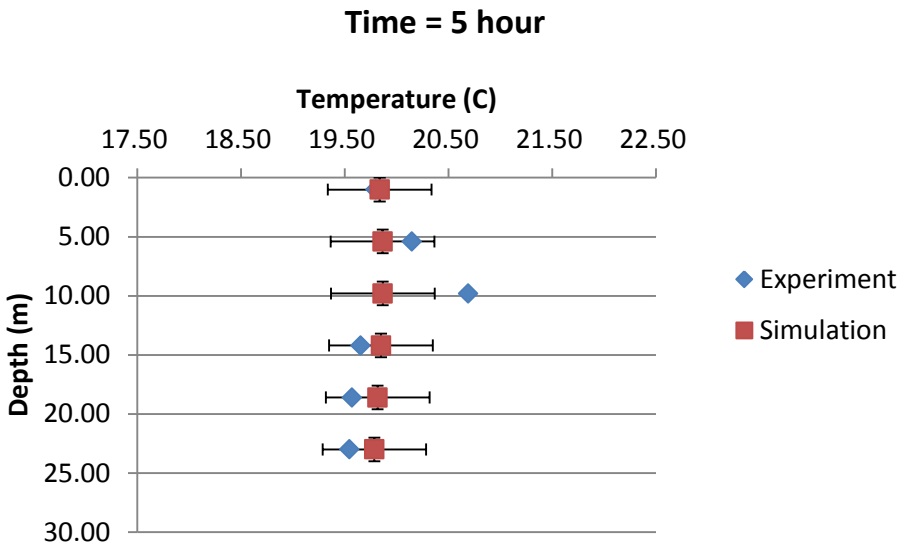

Figure A-5: Vertical ground temperature profile for probe column #1 at 18000 seconds (after 5 hours)

A-2. PROBE COLUMN #2

Table A-4: Experimental measurements of ground temperatures for probe column #1 (in ^{o}C)

Time [sec]	PROBE2-1	PROBE2-2	PROBE2-3	PROBE2-4	PROBE2-5	PROBE2-6
3600	18.92	18.87	18.72	19.18	18.56	19.30
7200	19.41	19.32	19.23	19.70	19.04	19.75
10800	19.54	19.53	19.40	19.75	19.07	19.82
14400	19.62	19.52	19.43	19.81	19.25	19.75
18000	19.68	19.67	19.41	19.87	19.25	19.81

Table A-5: Model predictions of ground temperatures for probe column #1 (in ^{o}C)

Time [sec]	PROBE2-1	PROBE2-2	PROBE2-3	PROBE2-4	PROBE2-5	PROBE2-6
3600	18.99	18.92	18.88	18.86	18.85	18.85
7200	19.58	19.53	19.49	19.46	19.42	19.38
10800	19.86	19.86	19.83	19.79	19.74	19.70
14400	19.71	19.72	19.70	19.68	19.64	19.60
18000	19.62	19.63	19.62	19.60	19.57	19.54

Table A-6: The temperature difference between measurements and model predictions for probe column #1 (in ^{o}C)

Time [sec]	PROBE2-1	PROBE2-2	PROBE2-3	PROBE2-4	PROBE2-5	PROBE2-6
3600	0.07	0.05	0.16	0.32	0.29	0.46
7200	0.16	0.21	0.26	0.25	0.38	0.37
10800	0.32	0.33	0.43	0.04	0.67	0.12
14400	0.09	0.20	0.28	0.13	0.38	0.16
18000	0.06	0.04	0.21	0.26	0.32	0.26

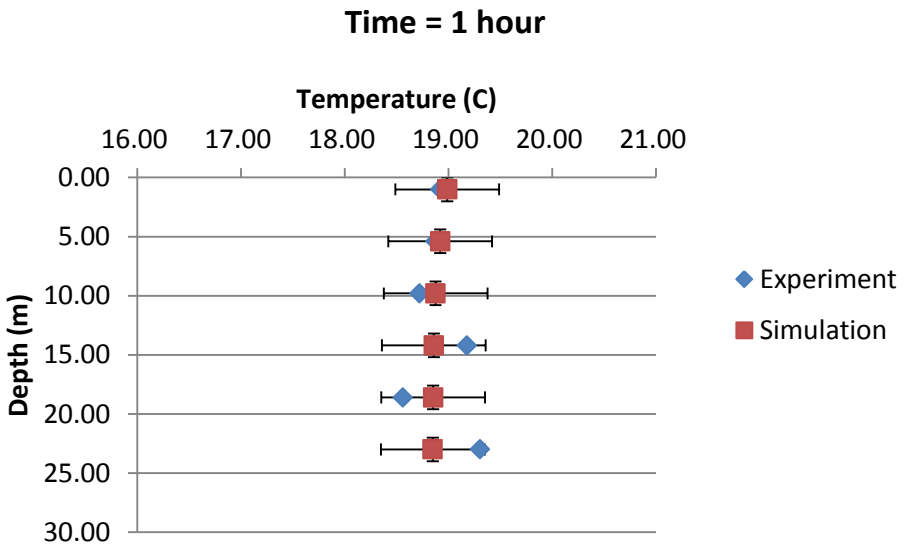

Figure A-6: Vertical ground temperature profile for probe column #2 at 3600 seconds (after 1 hour)

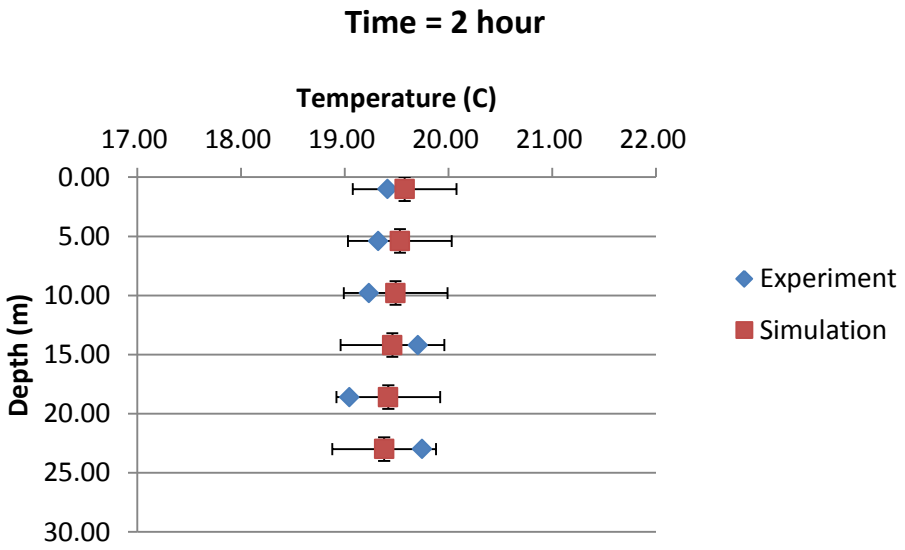

Figure A-7: Vertical ground temperature profile for probe column #2 at 7200 seconds (after 2hours)

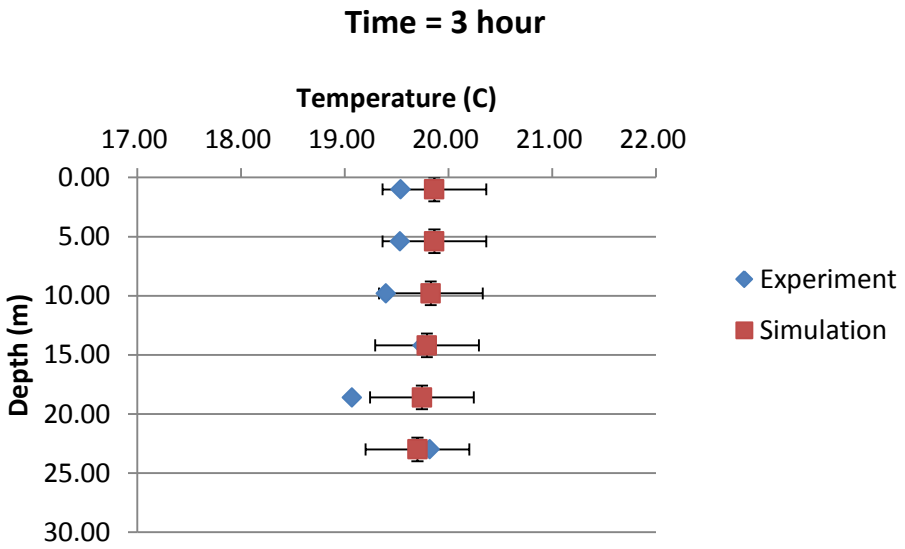

Figure A-8: Vertical ground temperature profile for probe column #2 at 10800 seconds (after 3 hours)

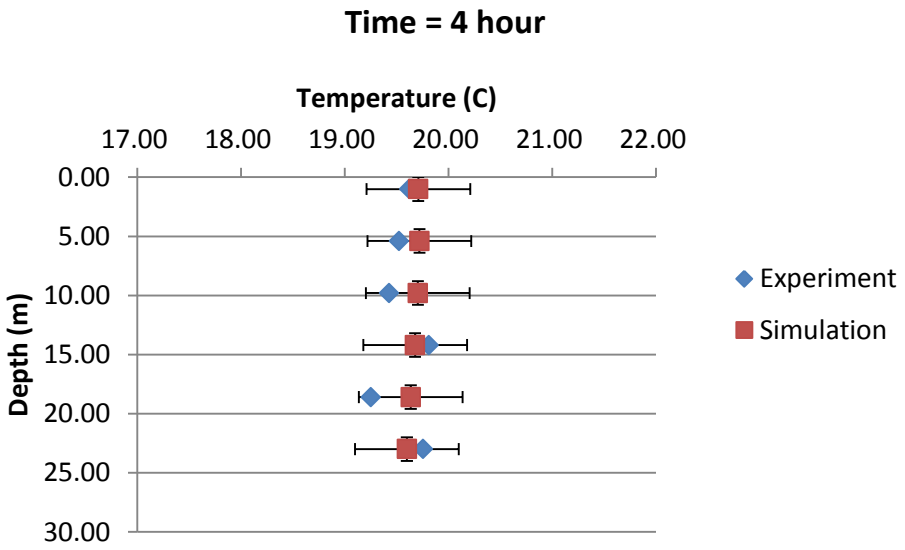

Figure A-9: Vertical ground temperature profile for probe column #2 at 14400 seconds (after 4 hours)

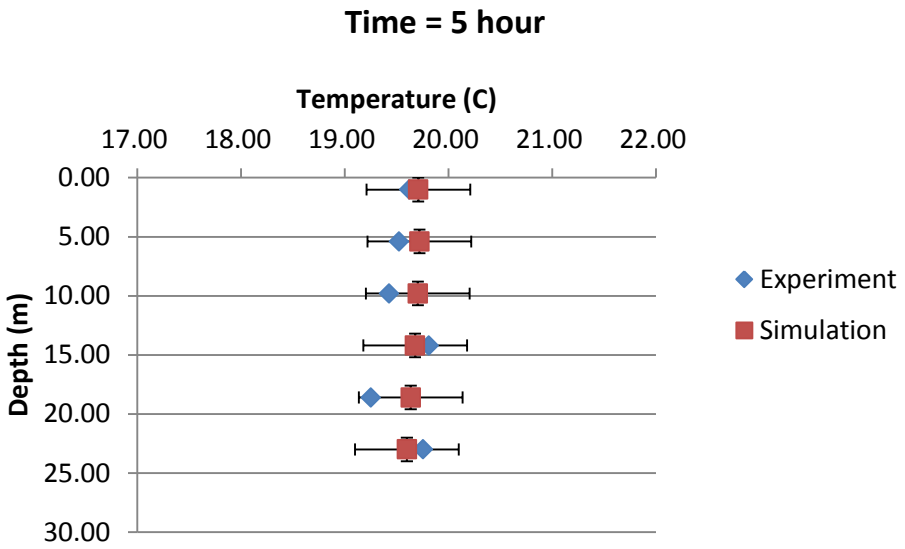

Figure A-10: Vertical ground temperature profile for probe column #2 at 18000 seconds (after 5 hours)

A-3. PROBE COLUMN #3

Table A-7: Experimental measurements of ground temperatures for probe column #1 (in ^{o}C)

Time [sec]	PROBE3-1	PROBE3-2	PROBE3-3	PROBE3-4	PROBE3-5	PROBE3-6
3600	19.21	18.98	18.73	19.11	19.01	18.74
7200	19.43	19.26	18.78	19.13	19.20	18.89
10800	19.55	19.55	19.15	19.41	19.53	19.07
14400	19.78	19.49	19.37	19.46	19.58	19.22
18000	19.87	19.84	19.48	19.67	19.80	19.55

Table A-8: Model predictions of ground temperatures for probe column #1 (in ^{o}C)

Time [sec]	PROBE3-1	PROBE3-2	PROBE3-3	PROBE3-4	PROBE3-5	PROBE3-6
3600	18.90	18.77	18.69	18.67	18.67	18.66
7200	19.45	19.33	19.24	19.20	19.16	19.14
10800	19.57	19.53	19.47	19.42	19.37	19.34
14400	19.56	19.55	19.52	19.49	19.44	19.41
18000	19.54	19.54	19.52	19.50	19.47	19.44

Table A-9: The temperature difference between measurements and model predictions for probe column #1 (in ^{o}C)

Time [sec]	PROBE3-1	PROBE3-2	PROBE3-3	PROBE3-4	PROBE3-5	PROBE3-6
3600	0.31	0.21	0.04	0.44	0.34	0.08
7200	0.02	0.07	0.46	0.06	0.04	0.25
10800	0.02	0.01	0.32	0.01	0.16	0.26
14400	0.22	0.06	0.16	0.03	0.14	0.19
18000	0.33	0.30	0.04	0.17	0.33	0.11

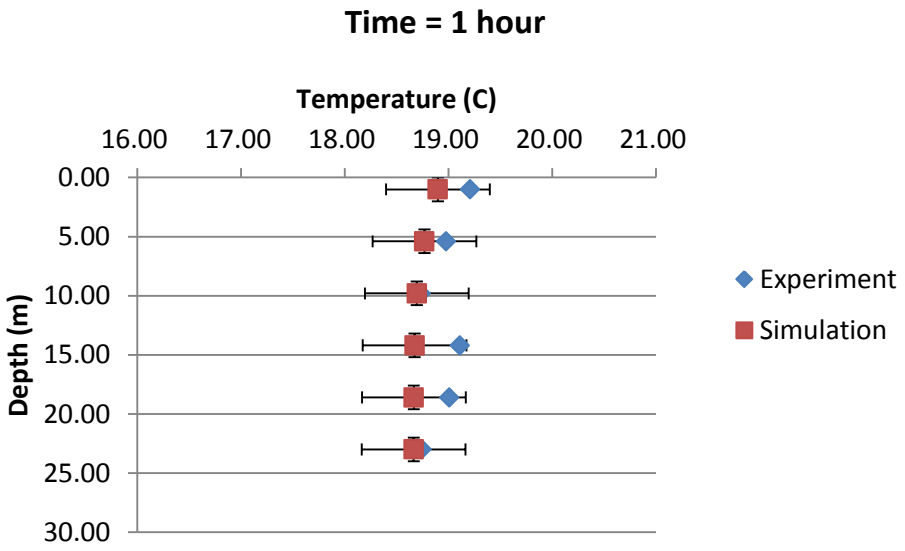

Figure A-11: Vertical ground temperature profile for probe column #3 at 3600 seconds (after 1 hour)

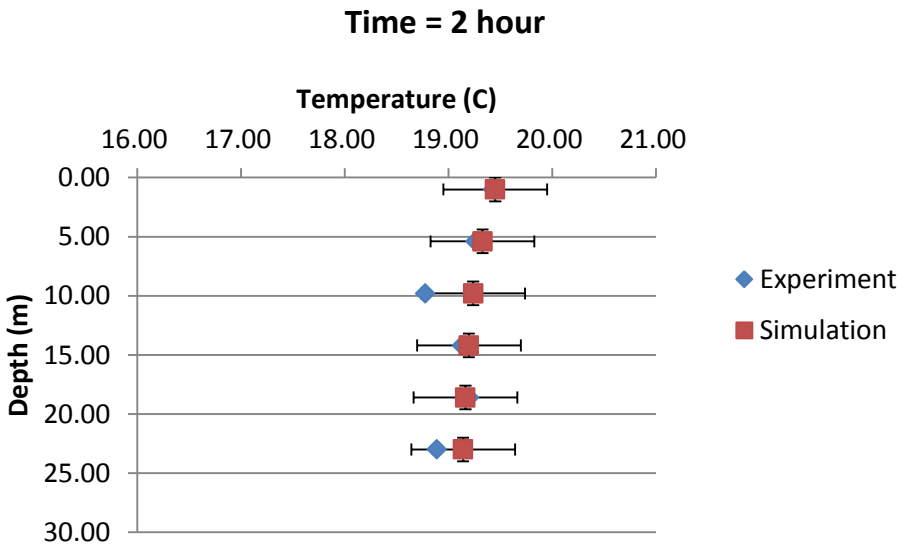

Figure A-12: Vertical ground temperature profile for probe column #3 at 7200 seconds (after 2 hours)

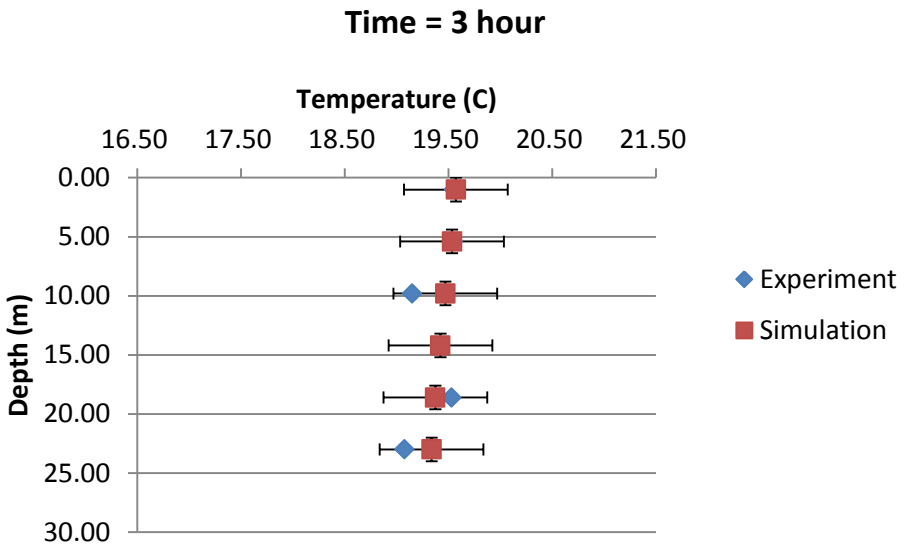

Figure A-13: Vertical ground temperature profile for probe column #3 at 10800 seconds (after 3 hours)

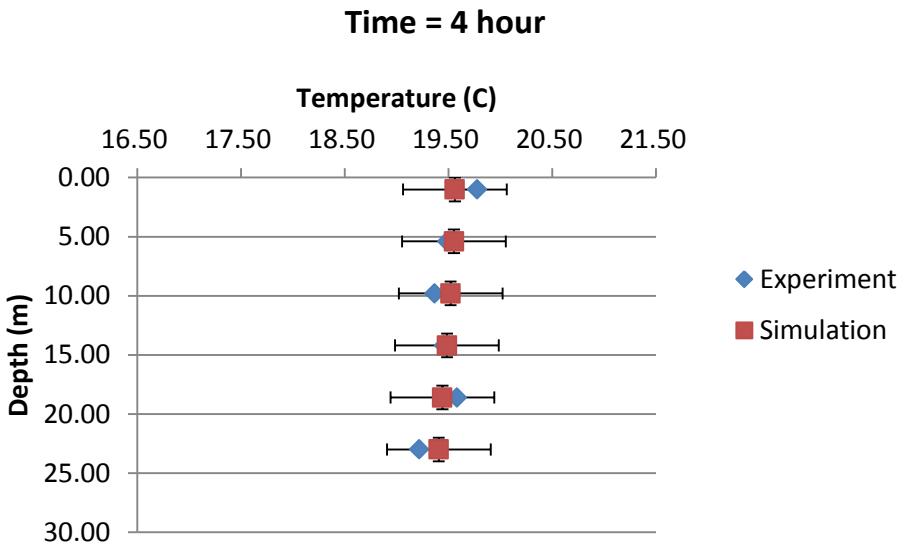

Figure A-14: Vertical ground temperature profile for probe column #3 at 14400 seconds (after 4 hours)

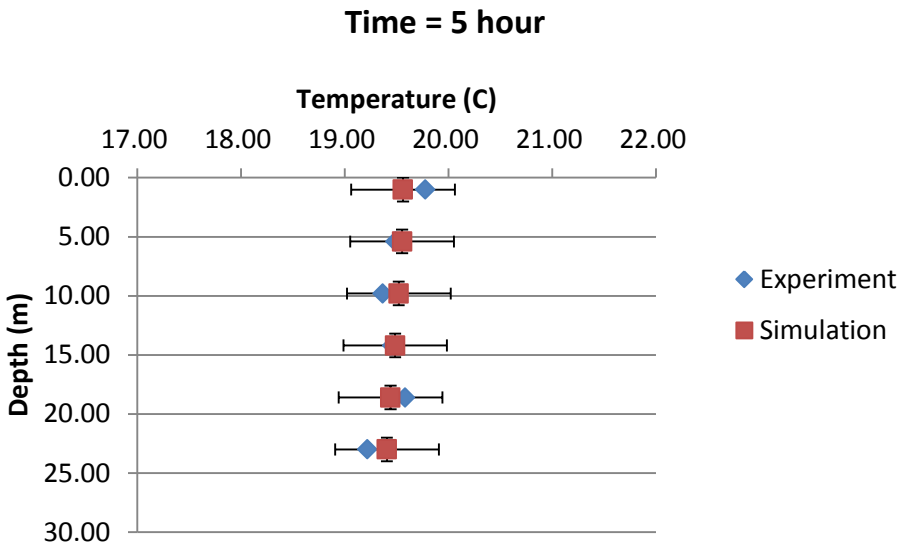

Figure A-15: Vertical ground temperature profile for probe column #3 at 18000 seconds (after 5 hours)

A-4. PROBE COLUMN #4

Table A-10: Experimental measurements of ground temperatures for probe column #1 (in ^{o}C)

Time [sec]	PROBE4-1	PROBE4-2	PROBE4-3	PROBE4-4	PROBE4-5	PROBE4-6
3600	19.09	NA	18.75	18.70	18.80	18.74
7200	19.55	NA	18.98	18.95	18.95	18.89
10800	19.69	NA	19.39	19.25	19.39	19.07
14400	19.81	NA	19.43	19.12	19.14	19.22
18000	19.88	NA	19.51	19.40	19.63	19.55

Table A-11: Model predictions of ground temperatures for probe column #1 (in ^{o}C)

Time [sec]	PROBE4-1	PROBE4-2	PROBE4-3	PROBE4-4	PROBE4-5	PROBE4-6
3600	18.84	18.70	18.63	18.60	18.60	18.59
7200	19.22	19.08	18.97	18.92	18.89	18.88
10800	19.41	19.35	19.28	19.22	19.18	19.15
14400	19.46	19.44	19.40	19.37	19.32	19.29
18000	19.49	19.48	19.46	19.43	19.40	19.37

Table A-12: The temperature difference between measurements and model predictions for probe column #1 (in ^{o}C)

Time [sec]	PROBE4-1	PROBE4-2	PROBE4-3	PROBE4-4	PROBE4-5	PROBE4-6
3600	0.25	NA	0.12	0.09	0.20	0.15
7200	0.33	NA	0.01	0.02	0.06	0.01
10800	0.28	NA	0.12	0.03	0.21	0.08
14400	0.35	NA	0.03	0.25	0.18	0.07
18000	0.39	NA	0.05	0.03	0.24	0.18

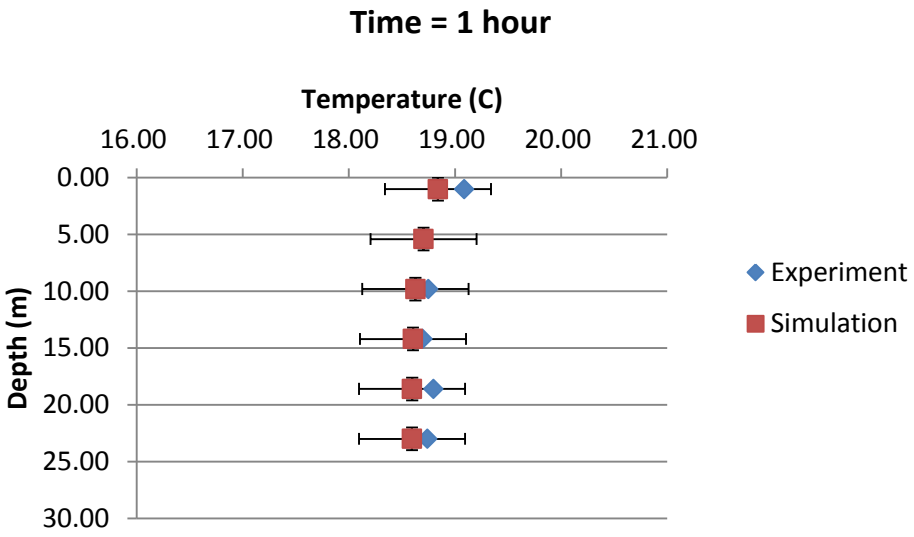

Figure A-16: Vertical ground temperature profile for probe column #4 at 3600 seconds (after 1 hour)

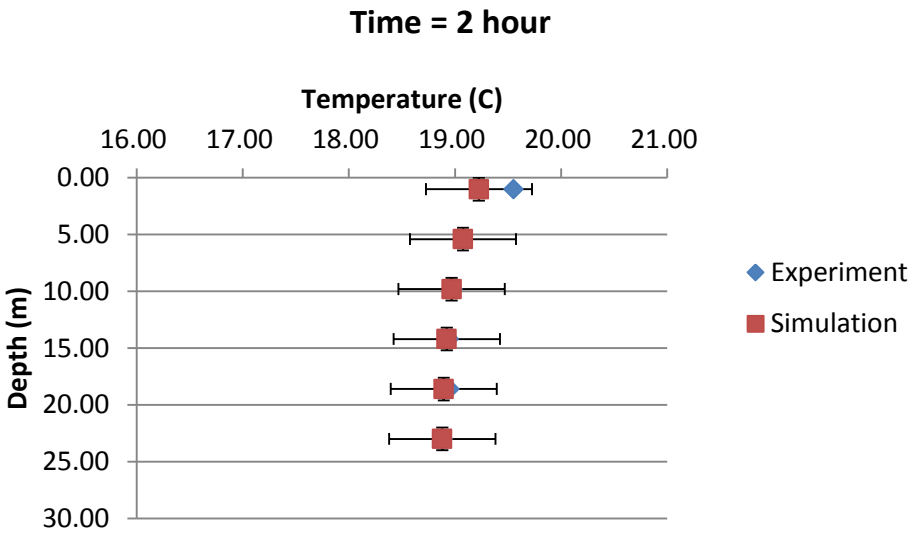

Figure A-17: Vertical ground temperature profile for probe column #4 at 7200 seconds (after 2 hours)

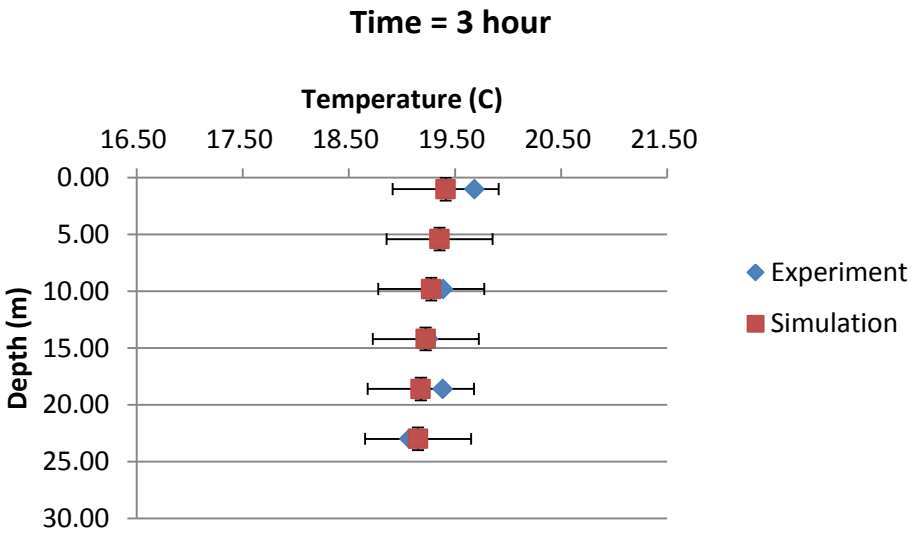

Figure A-18: Vertical ground temperature profile for probe column #4 at 10800 seconds (after 3 hours)

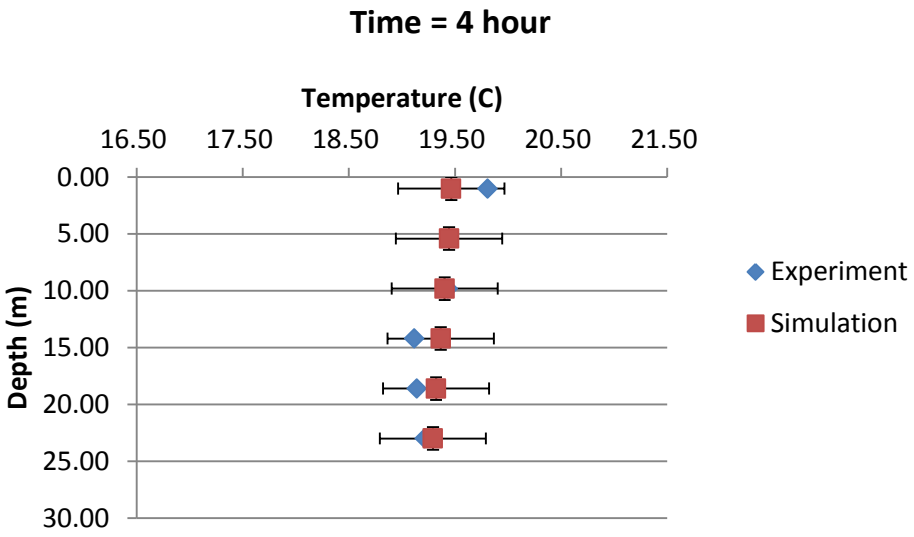

Figure A-19: Vertical ground temperature profile for probe column #4 at 14400 seconds (after 4 hours)

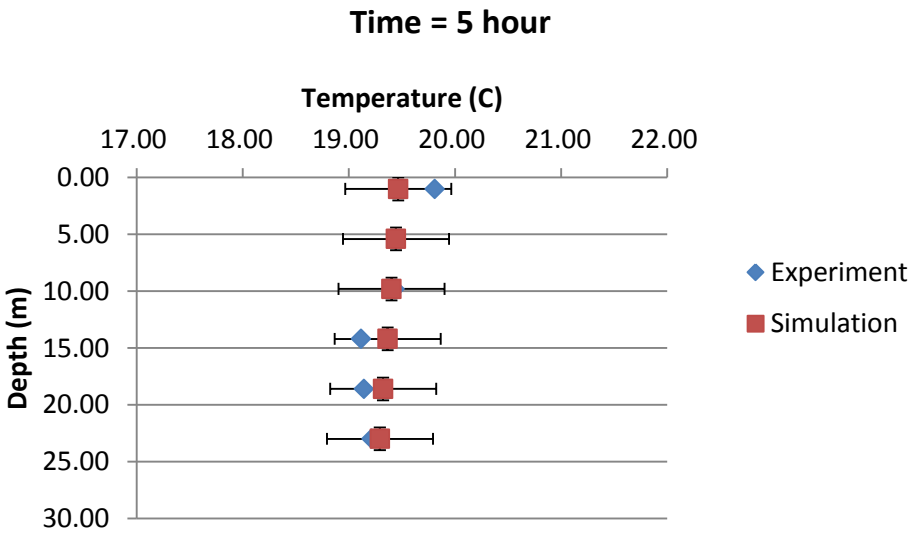

Figure A-20: Vertical ground temperature profile for probe column #4 at 18000 seconds (after 5 hours)